THE UNIVERSITY OF MANITOBA

AN INVESTIGATION AND REVIEW OF OEDOMETER AND TRIAXIAL TESTS ON WINNIPEG CLAYS

by

PETER GORDON SAMUEL TRAINOR

A THESIS
SUBMITTED TO THE FACULTY OF GRADUATE STUDIES
IN PARTIAL FULFILLMENT OF THE REQUIREMENTS FOR THE DEGREE OF
MASTER OF SCIENCE

DEPARTMENT OF CIVIL ENGINEERING

WINNIPEG, MANITOBA

AUGUST 1982

AN INVESTIGATION AND REVIEW OF OEDOMETER AND TRIAXIAL TESTS ON WINNIPEG CLAYS

BY

PETER GORDON SAMUEL TRAINOR

A thesis submitted to the Faculty of Graduate Studies of the University of Manitoba in partial fulfillment of the requirements of the degree of

MASTER OF SCIENCE

ABSTRACT

An extensive laboratory program of small diameter CIŪ triaxial tests and oedometer tests on undisturbed Winnipeg clay has been executed. Blocks of clay from depths of 5.5 m, 9.0 m and 11.5 m depth were chosen for the study to substantiate and augment previous research. Significant new insights have been gained into the behaviour of the clay, and explanations have been offered for previous apparent anomalies. The traditional semi-logarithmic plot of the compression versus the logarithm of the effective stress in an oedometer test is inappropriate for Winnipeg clay. Arithmetic scale plots of compression versus effective stress are much more useful. The latter show that in the recompression range the relationship is linear, but the compressibility is unusually high. After recompression a yield occurs at the preconsolidation pressure, p'_c, but the higher p'_c, the lesser the amount of yield. The value of p'_c decreases with depth so that at 5.5 m the yield is barely noticable, whereas at 11.5 m the yield is very sharp. To increase the definition of the yield and also to complement the arithmetic scale plotting method, many of the oedometer samples were loaded with small equal increments. The more usual method is to load samples using a constant increment ratio, which suits logarithmic plotting.

In triaxial compression the Winnipeg clay behaves as a lightly to moderately overconsolidated deposit, with A_f values ranging from 0.0 to 1.1. The effective-stress strength envelopes are, however, unusual in shape. At low effective pressures, the envelopes are curved and appear to have zero cohesion intercept. It is demonstrated that this curvature at low pressures is likely caused by a general softening of

the microstructure, rather than by failure along fissures. At higher pressures there is apparently no abrupt transition between normally consolidated and overconsolidated envelopes, even though normally consolidated and overconsolidated failure modes were distinctly different. A possible explanation for both the curvature and the lack of a transition is a high content of the swelling clay mineral calcium montmorillonite or of a similar mineral. Both normally consolidated and overconsolidated strength envelopes for this mineral are curved, and the behaviour of the natural Winnipeg clay may be similar. Although the author's envelopes are unusual in shape, the test results are highly compatible with the results of previous research. The unusual shape is in fact an explanation for the widely conflicting c' and ϕ' parameters previously quoted for normally consolidated and overconsolidated envelopes.

ACKNOWLEDGEMENTS

I wish to extend my gratitude to my supervisor, Professor A. Baracos for his guidance; his interest in the Lake Agassiz clays spans many years.

Research into the properties of Winnipeg clays was concurrently being carried out by Dr. J. Graham. His willingness, and that of his postgraduate students to discuss findings and hypotheses was invaluable. I would also especially like to thank Mr. Ananthan Suppiah for the exchanges of ideas which took place during our friendship.

Appreciation is also extended to Mr. N. Piamsalee, soils lab. technician, and to Mr. John Clark, machinist. Mrs. Jessamine Lew did an excellent and timely job of typing the thesis, and I am also very grateful to Mrs. V. Ring for the loan of a typewriter.

Finally, the author wishes to thank the University of Manitoba for financial assistance in the form of a postgraduate fellowship, and Louise Chudy for her understanding and moral support.

TABLE OF CONTENTS

CHAPTER PAGE

LIST OF SYMBOLS AND ABBREVIATIONS

a'	-	intercept of q_f versus p'_f
a_v	-	coefficient of compressibility in oedometer test
a_{vo}	-	average value of a_v in the recompression range
$a_{v(iso)}$	-	average value of compressibility = $\Delta e/\Delta\sigma'_c$ in isotropic consolidation
A, B	-	porewater pressure parameters
A_f	-	value of A at failure
c'	-	effective cohesion intercept
C_α	-	coefficient of secondary compression
C_c	-	compression index
C_v	-	coefficient of consolidation
C.I.$\bar{U}$	-	isotropically consolidated undrained triaxial compression test
e	-	voids ratio
$e_{n/c}$	-	voids ratio in a normally consolidated state at given stress
e_o	-	initial voids ratio
E_{50}	-	elastic modulus to 50% of failure stress
H	-	height, thickness
k	-	coefficient of permeability
K_o	-	coefficient of earth pressure at rest
L.I.R.	-	load increment ratio; = final stress/initial stress
n/c	-	normally consolidated
o/c	-	overconsolidated
p'	-	average normal stress; = $(\sigma'_1 + \sigma'_3)/2$
p'_f	-	p' at failure

p'_c - effective vertical preconsolidation pressure in oedometer test

$p'_{c(iso)}$ - effect preconsolidation pressure in an isotropic (triaxial) consolidation test

p'_i - initial vertical equilibrium pressure under no-swell conditions

p'_o - in-situ vertical effective overburden pressure

p'_s - low vertical pressure causing sample to swell ($p'_s < p'_i$)

q - shear stress; $(\sigma_1-\sigma_3)/2$

q_f - q at failure

t - time

t_f - time to failure

u - porewater pressure

$\bar{u}$ - excess porewater pressure

v - volume

z - depth, vertical axis direction

α' - slope of q_f versus p'_f

γ - unit weight

γ_w - unit weight of water

Δ - change, e.g., Δe

Δh - layer thickness

ΔT - loading period

ε_1 - major principal strain (i.e axial strain in a triaxial compression test)

p - settlement

σ - normal stress

σ_3 - minor total principal stress = cell pressure

σ'_1, σ'_3 - major and minor effective principal stresses, i.e vertical and horizontal stresses in triaxial compression

σ'_c - applied consolidation stress; vertical stress in an oedometer test, spherical stress in triaxial tests

σ'_{ff} - effective normal stress on the theoretical failure plane at failure

σ'_{oct} - effective octahedral normal stress

σ'_r - correction to $(\sigma_1-\sigma_3)$ due to the strength of membranes and filter drains

τ - shear stress

τ_{ff} - shear stress on the theoretical failure plane at failure

ϕ' - effective angle of shearing resistance

$\phi'_{n/c}$ - effective angle of shearing resistance for soil in the normally consolidated state

LIST OF TABLES

LIST OF FIGURES

CHAPTER 1

INTRODUCTION

1.1 GENERAL INTRODUCTION

In any construction involving soil, an estimate is required of the deformations at the boundaries of a bulk of soil due to the internal stress changes caused by construction loads. These loads may be imposed through structural foundations, from the addition or removal of a large volume of soil, or from a change in groundwater conditions.

The deformations may be due to either a widespread compression, expansion,or shearing, of the soil particles in the loaded area,or due to shear strains concentrated in a highly localized set of rupture zones. If the shear stresses in the soil are low, the deformation rates will generally decrease with time and a settlement or heave analysis can be based on the compressibility of the soil. If the shear stresses approach the shear strength of the soil particles, an increase in deformations followed by a sudden collapse may follow a period of apparent stability. In the latter case a stability analysis is usually based on an assumption of rigid-plastic behaviour, using an estimation of the shear strength of the soil.

The general aim of this thesis was to improve the state of knowledge of the basic material properties of undisturbed Winnipeg clay, properties which may be used in simple settlement and stability analyses. Specifically,the laboratory work involved two testing programs:

(a) A series of oedometer tests, primarily to measure the

drained compressibility, a_v, in the in-situ vertical direction.

(b) A series of consolidated-undrained triaxial compression tests with pore-pressure measurement, (CIŪ), primarily to measure the variation of peak shear strength with effective normal stress.

More complex analyses, require an evaluation of the anisotropic nature of the soil, and the degree to which this affects both compressibility and shear strength. However, an attempt to account for anisotropy inevitably requires a number of more complicated tests. Because the structure of a natural deposit can easily be disturbed, some of the required tests are difficult to perform, and the measured parameters may be inaccurate. Further, no great progress can be made in the evaluation of anisotropy unless simple parameters can be measured with accuracy and repeatability. It is to this end that this thesis is addressed. A review of previous research on undisturbed Winnipeg clay revealed some conflicting results and uncertain conclusions about the behaviour in the oedometer and CIŪ triaxial tests. A general review of these results and an outline of the current research is contained in Section 1.4.

1.2 DISCUSSION OF SETTLEMENT AND STABILITY ANALYSES

1.2.1 Analysis of Settlements

The design of a vertically loaded structural foundation on a horizontal stratum is almost always governed by settlement criteria. For a typical design safety factor of 2.5, the maximum design load is

only governed by stability considerations in the case of small footings on soils with a limited range of intermediate plasticity or on soils which are hard and brittle (Burland, 1977). In the classical settlement analysis, a one-dimensional approximation is obtained by using linear elastic theory to predict average vertical stress increases in n horizontal layers. The one-dimensional compressibility, a_v, is then used to compute the final compression in each layer. The final settlement is then given by:

$$\rho_{final} = \sum_{1}^{n} \frac{a_v}{(1+e_o)} \cdot \Delta\sigma \cdot \Delta h \qquad (1.1)$$

The inherent assumptions that the axes of principal stress and strain remain coincident and vertical beneath the loaded area, and the use of a single coefficient of compressibility for a material as complex and non-linear as a natural clay, have often been questioned by engineers. However, studies which have compared the above classical analysis to more exact analytical or numerical solutions which take account of non-linearity, anisotropy, non-homogeneity, and rotation of the axes of principal stress, have somewhat allayed these concerns. These studies, e.g Gibson (1974), Burland (1977) show that:-

(a) The vertical stress distribution is not greatly affected by the likely range of non-linearity or non-homogeneity for a typical soil, except where a stiff layer overlies a soft layer.

(b) Rotations from the vertical, of principal stress increments are minor in regions where major strains occur.

The results of simple one-dimensional analyses compare very

favourably with more sophisticated methods, and errors are usually small compared to those that can be attributed to sampling and testing of the soil. Settlement is dependent upon the mean values of the soil compressibility in the profile. An accurate determination of a_v from a series of oedometer tests at different depths is more likely to improve the settlement estimate than a sophisticated analysis.

1.2.2 Rates of Settlement

Prediction of settlement rates is much less reliable than prediction of the settlement magnitude. The bulk in-situ permeability, the controlling factor, is dependent on extreme values of permeability occuring locally in fissures, horizontal beds, or varves, which linked together form a secondary permeability system. Estimates of field rates of settlement are likely to be gross underestimates if based on laboratory tests on small samples, in which the effective permeability is close to that of the intact clay. Another cause of error is that the compressibility of a clay has been shown to be strain-rate dependent. As a result laboratory values of the coefficient of consolidation, c_v, are a function of load increment ratio, and sample height, in deviation from Terzaghi's Consolidation theory. Since field rates of strain may be many thousands of times slower than rates in laboratory oedometer tests (Crawford, 1964(b)), the "final" strain in the laboratory differs from that in the field. This is discussed in Chapter 3.

1.2.3 Analysis of Stability

Failure of a natural slope or a foundation on a natural soil

is dependent upon weak "links" in the profile, rather than average soil conditions. Examples of weak links are; previous shear planes, fissures, natural beds of weak materials, and tension cracks. The probability of failure, is almost impossible to estimate, being dependent upon the statistics of extreme values (De Mello, 1977). Design is then based on the correlation of an acceptable factor of safety with local or general experience. The factors of safety have to be recognised as being purely nominal. Two ideal slopes, each composed of a different homogeneous material, may be shown to have equal factors of safety, but widely different probabilities of failure (De Mello, 1977).

Since the strength of a soil is dependent upon the effective stress conditions, and the pore-pressure, u, has a dominant influence on most failures, it would seem prudent to use only effective stress analysis. However an accurate prediction of the most unfavorable distribution of pore-water pressures is extremely difficult. In contrast, accumulation of local experience may lead to an good estimation of the range of undrained strengths likely to exist at failure, in which case total stress analysis can be justified.

In an effective stress analysis of an overconsolidated clay deposit, the results of laboratory peak strengths over some middle range of normal stresses may be approximated by the linear relationship; $\tau_{ff} = c' + \sigma'_{ff} \tan\phi'$. The c' and ϕ' values from curve fitting do not represent true angles of friction or true cohesion between particles. In particular, use of the c' and ϕ' relationship for a range of field stresses outside the range tested in the laboratory can lead to a gross overestimate of the in-situ strength.

1.3 STABILITY PROBLEMS - LOCAL EXPERIENCE

Since Winnipeg is topographically flat, the most troublesome soil instability problems have occured on the banks of the Red and Assiniboine Rivers, although there have also been failures of man-made fills, excavations, and foundations. Although most of the brown clay and blue clay deposits are of a medium-stiff constituency, riverbank slides have been common even at slopes flatter than 9:1. The difficulties in reliable analysis, and reasons for such poor and erratic stability have been discussed by Baracos and Graham (1980), and Freeman and Sutherland (1974), and are summarized below:

(a) Residual strengths are very low, ($\phi'_r \simeq 7\text{-}9^o$, $c'_r \simeq 0$), and are considerably less than peak strength values due to the high smectite content of the clay. The existence of old failure surfaces will considerably reduce stability.

(b) The brown clay has been observed to contain numerous slickenslides and fissures, and a nuggety structure can be seen when the soil is allowed to swell. Triaxial tests on the brown clay have shown a wide scatter in peak effective strengths from $c' = 42$ kPa, $\phi' = 19^o$ to $c' = 3.5$ kPa, $\phi' = 14.5^o$.

(c) Actual slides have often involved large components of horizontal movement. Since peak effective strength has been shown to be reduced for shear along clay laminations, analyses should include the possibility of non-circular slip surfaces with long flat horizontal portions.

(d) A considerable reduction in strength appears to occur

when the clay is allowed to swell under low confining pressures. Thus strength at the toe of a slope may be very low.

1.4 OBJECTIVES OF THE LABORATORY TESTING PROGRAM

1.4.1 General

This work was undertaken as a part of an ongoing research program into the mechanical properties of undisturbed Winnipeg clay at the University of Manitoba. Completed studies by Pietrzak (1979), Noonan (1980), and Lew (1981), have all made use of clay samples taken from an undeveloped university site, situated opposite the present physical education building (Figure 1.1). All studies made use of an excellent block sampler, (Domaschuk, 1977), to recover undisturbed blocks of clay. For the present study blocks were taken from depths of 5.5 m, 9.0 m and 11.5 m.

1.4.2 Oedometer Testing Program

A review of previous oedometer testing of Winnipeg blue clay, Crawford (1964), Noonan (1980), and Martin (1961), revealed the following characteristics of the void ratio versus log. effective-stress relationship:

(a) A highly curved section at stresses below the preconsolidation pressure.

(b) A very steep initial "virgin compression" section with C_c values ranging from 0.6 to 1.0.

(c) Distinct curvature of the "virgin compression" section

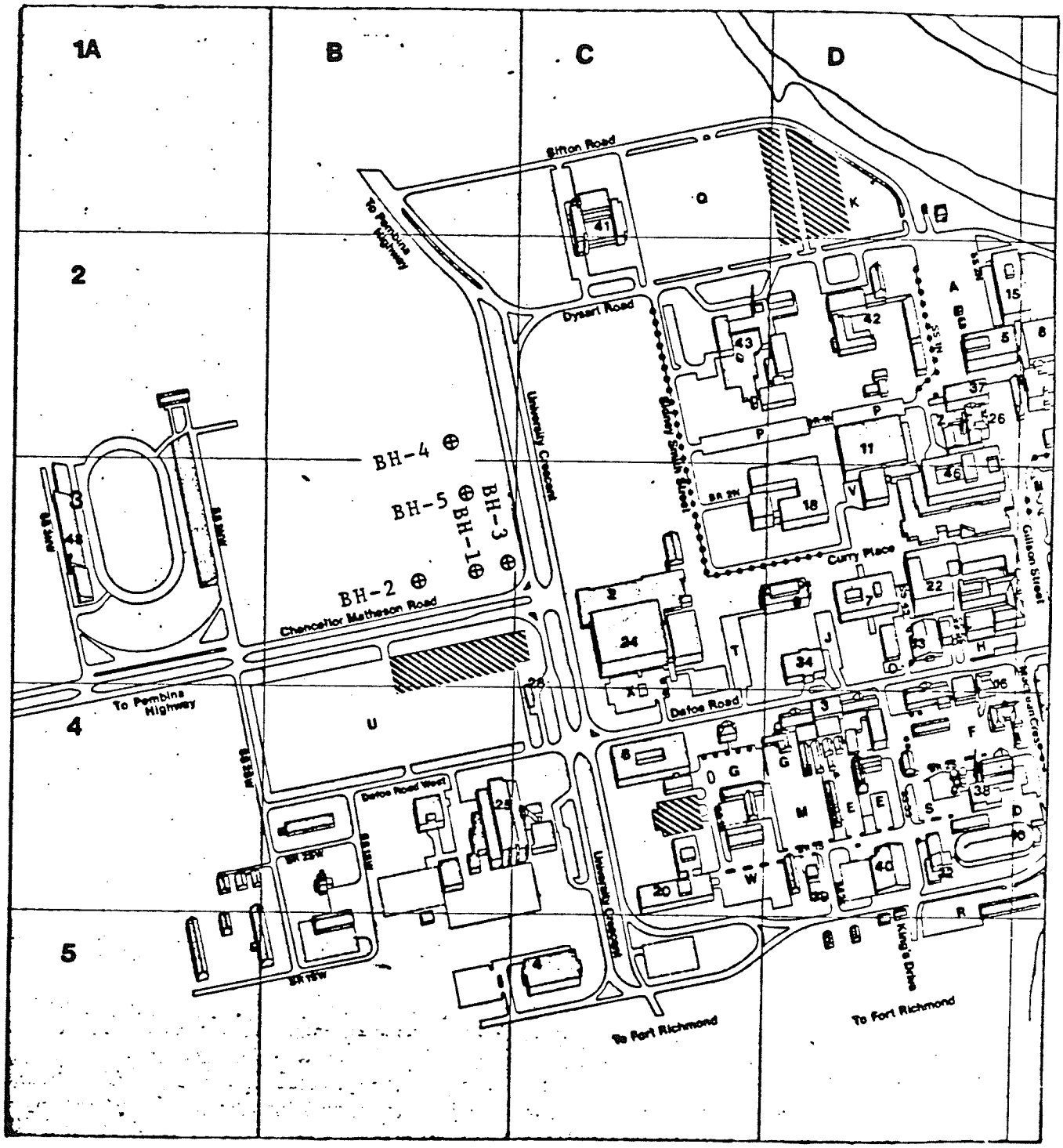

Figure 1.1 Site Plan and Location of Boreholes

at high stresses, (concave upward).

The pronounced curvature at low stresses causes difficulty in estimation of p'_c by the Casagrande Method, and has been attributed to disturbance caused by allowing samples to swell, (Baracos et. al., 1980), or to other disturbance during sampling or preparation.

The initial aim of the author's research was to see if the determination of the value of p'_c could be improved by careful trimming procedures and by eliminating the initial swelling. The first samples were loaded using a load increment ratio (L.I.R.) of 1.6, and showed an apparent yield point in the void ratio versus (arithmetic) stress relationship. It was concluded that the arithmetic scale plot gave a better understanding of behaviour than the traditional semi-logarithmic plot. Because of the method of loading,however, the data points become spaced further and further apart. To produce equally spaced data points in an arithmetic plot, the loading sequence was altered to make all the loads small and equal.

In the above "constant load increment" test,however, the load increment ratio is reduced at each increment and deviations from Terzaghi Theory occur at low load increment ratios (Leonards, 1961). As a result after a few constant increments of load, the standard S-shaped consolidation curves were no longer produced. Although "primary" and "secondary" consolidation can no longer be distinguished without direct pore-pressure measurement, the test still gives a valid estimation of compressibility. The interesting results obtained from the first constant increment test led to the decision to undertake further tests at depths of 5.5 m, 9.0 m and 11.5 m. The expanded objectives of the testing program are summarized below:

(a) To achieve a more accurate determination of p'_c by altering the loading sequence and the plotting techniques.

(b) To estimate average values of p'_c and coefficient of compressibility, a_v, for each of the studied depths, 5.5 m (brown clay) and 9.0 m and 11.5 m (blue clay).

(c) To study the effect of initial swelling on the void ratio versus effective stress curve, in particular the effect on the initial compressibility and the preconsolidation pressure.

(d) To study the effect of load increment and interval of loading on the void ratio versus effective stress curve.

(e) To study the effect of load increment on the shape of the consolidation-time curves, and evaluate the coefficient of consolidation, C_v, and the coefficient of secondary compression, C_α.

1.4.3 Consolidated Undrained Triaxial Testing Program

Previous determinations of the peak effective stress failure envelopes for Winnipeg clay have been reported by Mishtak (1964), Crawford (1964(a)), Freeman and Sutherland (1974), and Pietrzak (1979). An important conclusion from Pietrzak's study was that the effective strength envelope for Winnipeg blue clay was approximately independent of depth, and could be approximated by three linear sections, (Baracos et. al., 1980), as follows:

(a) A low stress section in which strength is believed to be controlled by fissures or the nuggety structure of the clay

$p' < 60$ kPa $\qquad c' = 6$ kPa, $\quad \phi' = 32^{o}$

(b) An overconsolidated section:

60 kPa $< p' <$ 200 kPa $\qquad c' = 33$ kPa, $\quad \phi' = 13^{o}$

(c) A normally consolidated section:

200 kPa $< p'$ $\qquad c' = 3$ kPa, $\quad \phi' = 22.5^{o}$

The three stage hypothesis helps explain discrepancies in the c' and ϕ' parameters cited by the previous authors, in an attempt to fit a single straight line to their data. The problem is partially recognised in these publications. Crawford, noted a substantial reduction in strength in two drained tests on samples which had been allowed to swell, and urged further research into this effect. Freeman, suggested that his lower c' values were due to testing at a lower range of effective stresses; a visual inspection of the grouping of his test data for the blue clay gives support to the hypothesis of a low strength envelope.

A review of Pietrzak's data,however,showed that only four samples out of seventeen had actually been tested in the low-stress range. In the light of this,further research was needed and the aims of the present program were primarily:

(a) To evaluate the peak strength failure envelope for Winnipeg clay at depths of 5.5 m (brown clay), and 9.0 m and 11.5 m (blue clay), using CIŪ triaxial tests.

(b) To perform sufficient tests at each depth to accurately define the above envelopes over a wide range of stresses. Of particular interest was the envelope for the brown clay (5.5 m) which had not been tested by Pietrzak.

Also, the moisture content at 11.5 m depth was higher than that at 9.0 m depth, (Chapter 2), and it was suspected that the envelopes for the two strata of blue clay might differ.

(c) To examine the modes of failure occuring in each sample and identify any changes with consolidation stress or with depth.

(d) To measure the compressibility in isotropic compression, and compare results with those from oedometer tests.

CHAPTER 2

SOIL RECOVERY AND DESCRIPTION, WITH RELATION TO THE GENERAL STATIGRAPHY IN THE WINNIPEG AREA

2.1 SEDIMENTATION HISTORY, MINERALOGY, AND STRUCTURE OF DEPOSITS

The soils in the Winnipeg area are largely lacustrine deposits formed in Glacial Lake Agassiz, which drained into Hudson's Bay about 7,000 years ago. A chronicle of the major phases of the lake has been provided by Elson (1961, 1967). Lake sediments have been found over an area of 200,000 square miles, although waters probably did not cover more than 60,000 square miles simultaneously. Winnipeg lies in a former major sedimentation basin,which follows the present day Red River from Lake Winnipeg, 400 miles south into Minnesota and North Dakota, and covers approximately 14,000 square miles. Depths of clay in the Winnipeg area vary from about 3 m in the north-west to as much as 18 m in the east (Render, 1970).

A typical borehole log for the site from which samples for this study were taken is shown in Figure 2.1 (Baracos et al., 1980). Overlying the Ordovician Dolomitic Limestone bedrock is a deposit of grey till, (Keewatin Drift), which varies in thickness from 0.3 to 6 m (Wicks, 1965). The till contains sand and gravel, with a silt-clay matrix, and is generally well compacted near the bedrock surface, but poorly compacted in its upper layers. Different systems of classification have been used to separate the overlying clay beds. Teller (1976), and Last (1974), identified three units in the Red River basin, based

on texture, abundance of clasts and mineralogy, but found that the intermediate unit may not be identifiable in the central offshore basin, which includes the Winnipeg area.

The division of sediments into two units, Lake Agassiz I, and Lake Agassiz II, (Elson, 1961; Wicks, 1965), seems more appropriate in the Winnipeg area. The Lake Agassiz II unit is a surface layer 2.5 m to 4.5 m thick containing silty clay and a layer of tan silt. The major clay unit however, is the underlying Lake Agassiz I unit from which all the samples for this study were taken. A summary of the typical features of this unit is given below. More detailed information is contained in the following references; Elson (1961, 1967), Wicks (1965), Last (1974), Teller (1976) and Baracos (1977).

2.2 FEATURES OF THE LAKE AGASSIZ I CLAY UNIT

This unit includes all of the clay between the till and the tan silt layer (Figure 2.1). The color generally progresses from a light brown to a chocolate brown, and then changes to a blue-grey which becomes darker with depth. The transition between the brown, and the blue (or grey) clay is marked by a mottled zone, which is usually less than 0.5 m thick, but has sometimes been reported to extend for several metres. The color change is likely due to oxidation as there is no significant change in mineralogy through the deposit. Principal clay minerals are montmorillonite and illite in roughly equal amounts, plus a minor amount of kaolinite. The exchangable cation associated with the montmorillonite is mainly calcium. Some researchers have identified mixed layer illite-montmorillonite minerals, Wicks (1965), Baracos (1977),

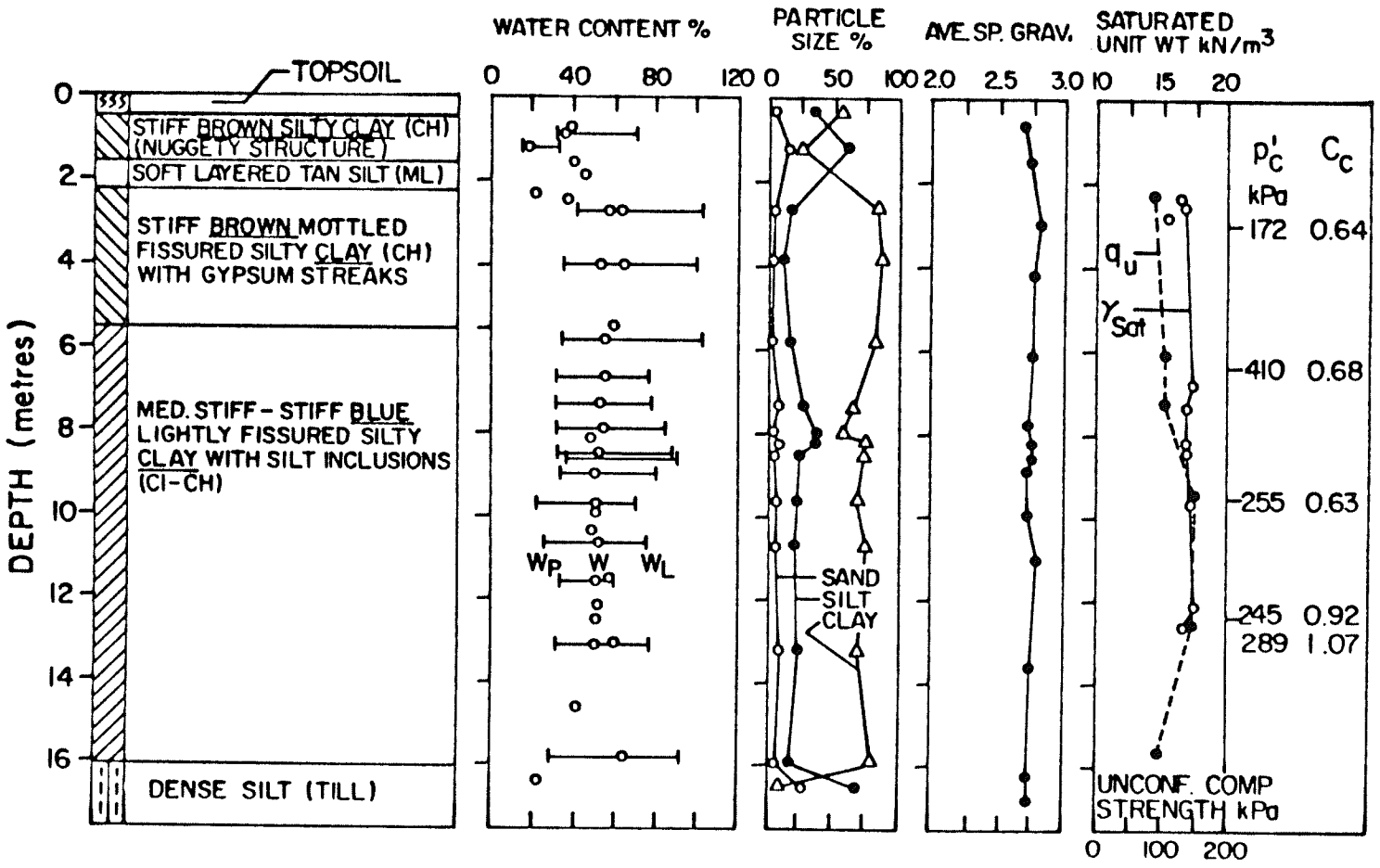

Figure 2.1 Average Borehole Log. Information, University of Manitoba Campus (After Baracos et. al., 1980)

and this suggests that the sediments derive from the Cretaceous shales of similar mineralogy which outcrop to the south and west.

Whereas the mineralogy does not change, variations in the environment of the lake during deposition of the Lake Agassiz I unit are indicated by the structure of the deposit. Clasts, which may be calcareous silt, limestone pebbles, or granite pebbles, are very abundant close to the till, but steadily decrease in frequency throughout unit I. A retreat of the glacier front would explain this decrease as the clasts were probably ice-rafted. Descriptions of the prominence and extent of varves occuring in unit I vary in the literature. Wicks (1965) describes the upper part as characterised by very fine varves, 15 per cm, whereas the lower part has a massive structure. However Baracos (1977) shows that there is a considerable marbling effect in the brown clay, and some in the blue clay; this effect is attributed to the mechanical mixing of banded slurries,which would otherwise have been consolidated to form distinct varves. A likely cause of this action is scour by large ice-bergs, the tracks of which are visible on aerial photographs of the region (A. Baracos, personal communication, 1981).

2.3 TYPICAL SAMPLE DESCRIPTION

2.3.1 Introduction

Undisturbed blocks of clay, approximately 250 mm x 250 mm x 450 mm deep were recovered from 900 mm diameter boreholes using a special tool devised by Domaschuk (1977). Samples were recovered from borehole 4 (July, 1980) and borehole 5 (January, 1981) at depths of 5.5 m, 9.0 m, and 11.5 m. A few 100 mm diameter piston samples were also recovered

from borehole 4 at the 5.5 m and 9.0 m depths. All samples were carefully wrapped in thin plastic film and sealed with wax reinforced with a layer of cheesecloth. Storage was in a humidity-controlled room. In addition the samples from borehole 4 were stored at a constant temperature of 4^{o} to 6^{o} Celcius, to simulate field conditions. Unfortunately an equipment malfunction in November 1980 caused the samples to freeze, necessitating the recovery of further samples from borehole 5 in january 1981.

The following descriptions refer specifically to soil samples used in this study.

2.3.2 Brown Clay, 5.5 m Depth

Samples were medium stiff to stiff and contained occasional fissures, some of which were slickenslided. Heavy marbling was evident, with dark and light brown layers twisted into irregular swirls. There were often patches of a crumbly, rust-brown colored material which contained black specks and streaks, and had poorly defined boundaries. Occasional vertical streaks of a soft, light-grey material, were believed to be the remains of deep root systems.

2.3.3 Blue Clay at 9.0 m Depth

The blue clay samples were medium-stiff, and appeared to be intact. Only two fissures were discovered during dissection of the clay blocks, and these were highlighted by an olive-brown hue, which penetrated the clay for three to four millimeters on each side of the fissures. Small pebbles and silt clasts were numerous, but the surrounding clay

matrix appeared massive. Upon drying the clay, very faint color differences were visible, but a marbling effect was not distinct as in the brown clay.

2.3.4 Blue Clay 11.5 m

Samples were similar to those taken from 9.0 m depth, except that the clay was softer, slightly darker in color, and contained more silt clasts. The latter were studded in thin horizontal bands rather than being randomly spaced. Test samples were trimmed to avoid these bands as the author was interested in the properties of the clay. Small fragments of granite or limestone were common, and a 100 mm well-rounded granite cobble was discovered in one block sample.

2.4 STANDARD CLASSIFICATION TESTS

The variation with depth of the Atterberg limits, moisture contents, average specific gravity, and grain size distribution is shown in Figure 2.1, (Baracos et. al., 1980), which was compiled using data from boreholes 1, 2 and 3 (Figure 2.1). Hydrometer and specific gravity tests were not repeated for boreholes 4 and 5, but the moisture contents and Atterberg limits shown in Table 1.1 are similar to the previous values. The average moisture content of the blue clay at 11.5 m was about 60%, as compared to 50% at 9.0 m, a difference which was significant enough to justify the expectation that the oedometer and triaxial test results for the two depths might be different.

The entire unit I deposit has a liquid limit greater than 50% and can be classified as highly plastic (CH). A slightly higher silt

content in the upper 4-5 m of the blue clay causes comparitively lower Atterberg limits. For this reason the sequence brown clay, grey clay, and grey plastic clay has been used to describe the deposit, Freeman and Sutherland (1974), Baracos (1977).

Sensitivity values were evaluated by the author, using a Swedish Fall-Cone apparatus, and were found to range from 2.5 to 3.0 at the three depths studied.

2.5 IN-SITU PERMEABILITY AND FISSURING OF THE CLAY

The (CH) classification of the Lake Agassiz I clay suggests that intact material should be virtually impermeable. However in most clays a secondary permeability system exists due to the presence of fissures and varves. It has been reported by Day (1977), that from an examination of clay surfaces in many excavations and tunnel projects, fissuring appears to be a feature of the natural clay. Estimates of the in-situ permeability from the response of wells to pumping tests have also been given by Day (1977). Single well response tests on wells installed in the Lake Agassiz II and upper Lake Agassiz I deposits indicate bulk permeabilities of 1.8×10^{-6} mm/sec. Similar tests on the deeper portions of the Lake Agassiz I unit indicate permeabilities which are significantly lower, with a mean of 3.8×10^{-7} mm/sec. Also well hydrographs indicate that 90% of the hydraulic head in the underlying carbonate aquifer is dissipated in the lower part of unit I. The conclusion is that fissures are much less abundant at greater depths.

Moisture Contents

Depth Metres	Bore Hole Number	Type	Moisture Content % Mean	No.	Std. Dev.
5.5	4	3" ϕ Piston	53.2	7	3.1
5.5	5	Block	54.0	112	3.4
9.0	4	Block	48.6	22	2.0
9.0	4	3" ϕ Piston	50.7	34	1.8
9.0	5	Block	50.7	15	1.8
11.5	4	Block	59.2	10	1.7
11.5	5	Block	62.0	52	2.7

Note: Bore hole #4 drilled in July, 1980.

Bore hole #5 drilled in January, 1981.

Atterberg Limits

Depth Metres	Liquid Limit %	Plastic Limit %	Plasticity Index %
5.5	93	31	62
9.0	70	26	44
11.5	86	34	52

Table 2.1 Atterberg Limits and Moisture Contents of Samples Used in Test Programs

CHAPTER 3

CONSOLIDATION THEORY AND APPLICATION

3.1 INTRODUCTION

The experimental work of this thesis includes a program of twenty oedometer tests which were performed primarily to evaluate the compressibility of Winnipeg clay. Compression of a saturated fine grained soil such as a clay, however, is a time dependent process. Volume change cannot take place without the expulsion of water from the microscopic interparticle voids, and this process is known as consolidation. The practical use of a consolidation theory is to provide a scaling law, so that results of tests on thin laboratory samples may be used to predict the behaviour of thick field strata. The classical Terzaghi theory, is very convenient for use in engineering practice for two reasons:

(a) It predicts a simple scaling law for the effect of thickness on consolidation strain rate.

(b) It predicts that there is a "final" strain or settlement which is reached when excess pore-pressures become small. This "primary" strain is independent of sample thickness.

However, discrepancies between predicted and observed behaviour occur at low rates of strain or low rates of loading in laboratory tests. Also considerable "secondary" strains may occur after the excess pore-pressures are essentially dissipated, and these are not accounted for by Terzaghi theory.

In the author's research, many of the oedometer tests were

conducted at a slow rates of loading, and as a result deviations from Terzaghi theory were large. In many cases primary and secondary consolidation could not be distinguished, although the compressibilities calculated from void ratio versus effective stress curves are still valid in the prediction of field settlements. This chapter provides an introduction to the reasons for the deviation from Terzaghi theory, and a discussion of alternative theories and concepts, and their practical significance.

The accuracy of the use of Terzaghi "primary" strains as a method of estimating the long term settlement of a thick layer is a matter of some dispute. Various modifications to Terzaghi theory attempt to account for strain rate effects in laboratory tests. The predicted behaviour of thick samples based on these theories is compared with the limited amount of direct experimental evidence on the one-dimensional consolidation of thick samples. Chapter three concludes with a discussion of the possible upper and lower bounds to the strains in a thick layer, based on the results of an oedometer test on a thin sample.

3.2 TERZAGHI THEORY, AND APPLICATION TO LABORATORY TEST RESULTS

Consolidation is the process of volume reduction of a mass of fine grained soil due to a decrease in the size of the interparticle voids. This thesis considers only fully saturated soils, for which the rate of volume reduction is equal to the rate of expulsion of pore water. The basic equation of one dimensional consolidation, assuming conservation of mass, and Darcy's law is:

$$\frac{\partial e}{\partial t} = \frac{k(1+e_o)}{\gamma_w} \frac{\partial^2 \bar{u}}{\partial z^2} \qquad (3.1)$$

Before introducing the further assumptions adopted in the Terzaghi Theory, typical consolidation versus time and consolidation versus log. time curves, from oedometer tests on Winnipeg clay, are considered, (Figure 3.1). The following two characteristics of these curves are typical of all clays.

(a) The consolidation process does not cease after a finite time, nor does displacement approach a final value asymptotically.

(b) When the load increment ratio, (L.I.R = final stress/ initial stress), is large, the semi-log. curve shows a definite reversal in curvature. When the L.I.R is small there is no such reversal.

The Terzaghi Theory does not account for (a) or (b) above. It assumes a linear time-independent constitutive equation.

$$\frac{de}{d\sigma'} = - a_v \tag{3.2}$$

Assuming also the validity of Terzaghi's Theory of effective stress, ($\sigma' = \sigma - u$), then $d\sigma' = - d\bar{u}$ and,

$$\frac{\partial e}{\partial t} = a_v \frac{\partial \bar{u}}{\partial t} \tag{3.3}$$

thus from equation 3.1

$$\frac{\partial \bar{u}}{\partial t} = c_v \frac{\partial^2 u}{\partial z^2} \tag{3.4}$$

where c_v is the coefficient of consolidation, a constant for the Terzaghi solution $= \dfrac{K(1+e_o)}{a_v \gamma_w}$

Solutions to equation 3.4 are available in many soil mechanics

texts, eg. Leonards (1962). It is clear, however, that from the assumption of equation 3.2, that consolidation "finishes" after a strain, Δe, equal to $a_v.\Delta\sigma'$. Thus the theoretical consolidation curve must approach a "final" displacement or strain asymptotically, as pore-pressure dissipates. Although this contradicts (a), above, the application of Terzaghi theory is not a major problem if the experimental consolidation versus log. time curve is similar to Figure 3.1(a), produced by use of a large L.I.R. The pore-pressures can reliably be assumed to almost completely dissipate in the vicinity of the "heel" of the curve, (point A). An experimental value of c_v can then be estimated, so that the Terzaghi theoretical curve approximates the portion of the experimental curve which precedes point A, (Figures 3.1(a) and (b)). In other words the theoretical curve approximates the "primary" consolidation, during which $\Delta\bar{u}$ is measurable.

The Terzaghi theory embraces the basic factors affecting the dissipation of excess pore-pressures caused by an increase in total stress. These factors are; permeability, compressibility of the soil particle structure, and drainage path length. It predicts the simple scaling law; rate of consolidation is inversely proportional to the square of the drainage thickness. Since field strata are usually many times thicker than oedometer samples, the rates of consolidation strain in the field may be thousands of times slower than in the laboratory, and excess pore-pressures may take many years to dissipate. The Terzaghi theory, however, assumes that this large difference in strain rates has no effect on the consolidation process, and that the value of the "primary" strain is a constant. As is shown later these assumptions are erroneous.

All modifications to Terzaghi theory are essentially an attempt

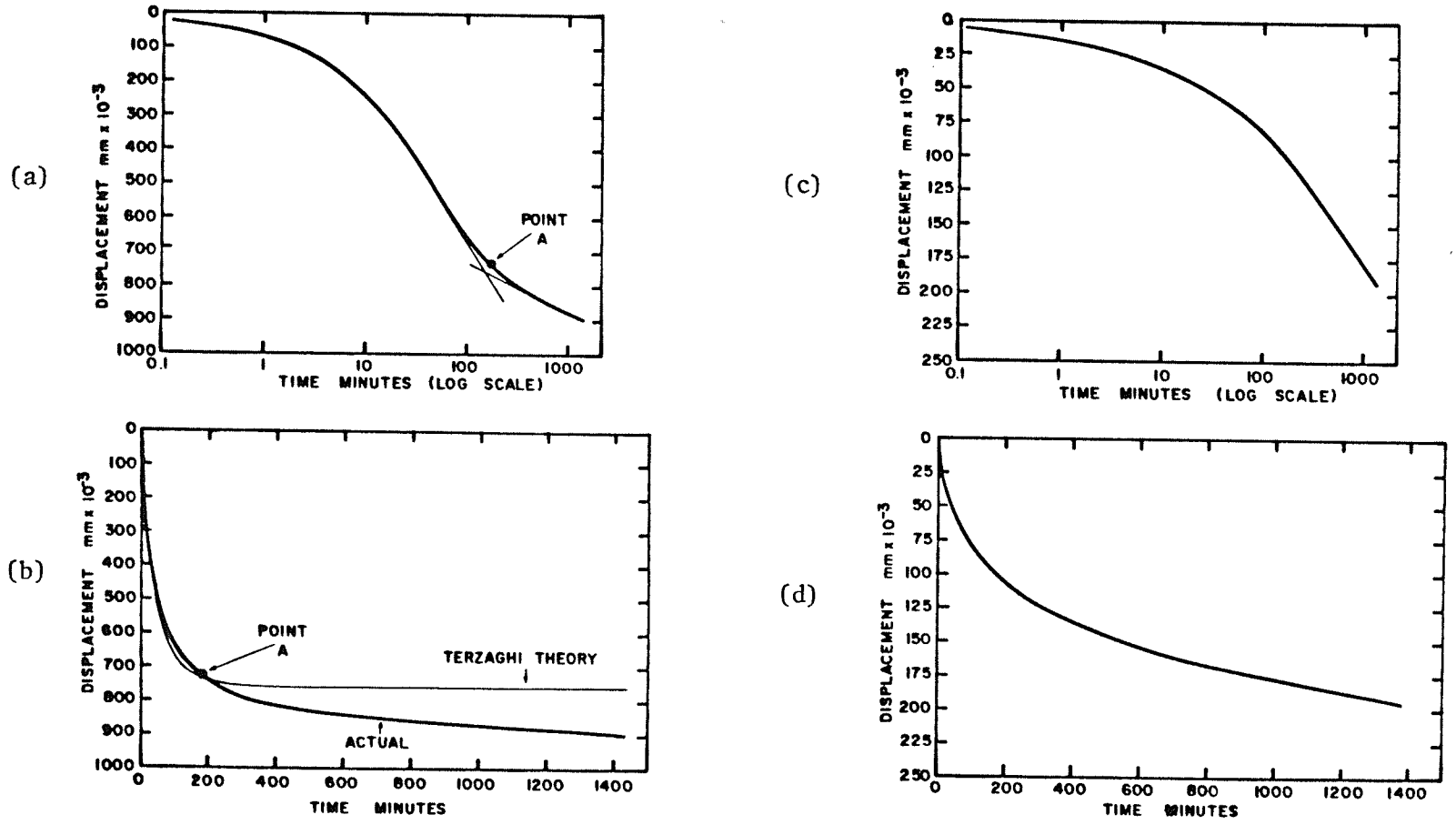

Figure 3.1 Typical Oedometer Displacement versus Time Curves (Winnipeg Clay, 9.0 m)
(a) and (b) L.I.R = 1.6 - (730 kPa to 1160 kPa): (c) and (d) L.I.R = 1.1 - (407 kPa to 435 kPa)

to evaluate the effect of strain rate or loading rate on the consolidation process. The main purpose of modified theories is to produce a better model for the consolidation of thick layers.

3.3 PROBLEMS IN THE DEFINITION OF "PRIMARY" AND "SECONDARY" CONSOLIDATION

There is no doubt that the compressibility of the soil particle structure is dependent upon time as well as effective stress. It was shown earlier, (Figure 3.1), that compression continues indefinitely past the theoretical limit of Terzaghi "primary" consolidation. This "secondary" compression or consolidation, usually proceeds at an approximately linear rate, (with log. time), and is described by the coefficient of secondary compression, C_α, = $\Delta e/\Delta \log. t$. The use of the term "creep", to describe secondary effects in the oedometer test is confusing, because of an often assumed similarity with the creep at constant stress which occurs in single-phase solids and is independent of thickness, (Hawley and Borin, 1973). In a saturated soil, (a two phase solid), there is no reason to assume that the basic flow equilibrium equation, (equation 3.1), does not operate just because $\Delta\bar{U}$ becomes immeasurably small. The above authors point out that it is the curvature of the isochrone, $\partial^2 u/\partial z^2$, (equation 3.1), that governs the consolidation process, not the magnitude of $\Delta\bar{u}$ per se. The magnitude of $\partial^2 u/\partial z^2$ is always very small in a thick field stratum, and an element of soil within the stratum undergoing "primary" consolidation, may be directly compared to an element of soil within a thin laboratory sample undergoing "secondary" consolidation. With the magnitudes of $\partial^2 u/\partial z^2$ comparable, the only difference is an all round pressure, $\Delta\bar{u}$. This can have no influence

on the effective interparticle forces, and on the microscopic processes causing strains in the soil particle structure.

From oedometer tests on the highly compressible Mexico city clay, three types of consolidation curve were produced; the shape depends on the magnitude of the load increment ratio, (Figure 3.2), (After Leonards and Girault, 1961). For type II and type III curves produced by small load increment ratios or by a pressure increment spanning the preconsolidation pressure, the "primary" and "secondary" stages could only be defined by direct measurement of pore-pressures. The amount of "primary" consolidation strain per unit stress increase was not constant, and the ratio of "primary" to "secondary" consolidation was extremely sensitive to the load increment ratio. The above authors noted that type II and type III curves had been found to occur for a very wide range of fine grained soil types. Their testing program involved careful monitoring of side friction, which they concluded was not a cause of the change in shape of the consolidation curves.

Despite the conceptual and experimental difficulties in distinguishing between primary and secondary consolidation, the coefficient of secondary compression, C_α, is often considered as a soil property. Wahls (1962) presented experimental evidence to support the contention that C_α is a function of void ratio, and independent of load increment or load increment ratio; for a given soil, recompression behaviour varies with the degree of preconsolidation, but once P_c' is exceeded, there is a common "Virgin Secondary Compression - Void Ratio Curve".

Mesri (1977), discussed reasons for a "time-and stress - compressibility interelationship", and presented data which showed that C_α varied linearly with C_c, (where $C_c = \Delta e / \log \sigma'$ for each increment,

and is calculated at the end of primary consolidation). Data were presented for a number of different soils, and for a given soil, the linearity held true in the recompression as well as the virgin compression range. The range of C_α/C_c for inorganic soils was found to be 0.025 to 0.060. Previous work by Walker and Raymond (1968) had shown the correlation between C_α and C_c in tests on a Leda clay. The arguments supporting a relationship between the rate of change of deformation,with stress increase, and with time,are interesting. The formulation of the relationship in terms of log. stress and log. time, and also the calculation of C_c from the end of "primary" consolidation are rather unsatisfactory.

3.4 THE COMPRESSION OF A PARTICLE SYSTEM CONSIDERED AS A SERIES OF EVENTS

In a particulate system, the average strains which occur in the soil skeleton are due to a vast number of small movements of small particles, or displacement "events". These events can be:

(a) First "events", occurring at weakest or most unstable particle contacts due to an average increase in effective stress.

(b) First"events"at the same weakest contacts due to prolonged time.

(c) A chain reaction of "events"following the first events above.

At present there is no mathematical model to represent this type of system. Equation 3.2 has no experimental background, but is merely the simplest constitutive equation. It describes the "resistance"

of the soil structure to compression as linear and time independent. By a series of oedometer tests on a Leda clay, performed at slow constant rates of strain, Crawford (1965), showed that this "resistance" decreased markedly as the strain rate was reduced. This is consistent with what might be intuitively expected from the description of the compression process as a series of "events" (see above)

3.5 BJERRUM'S CONCEPTS OF INSTANT AND DELAYED COMPRESSION

The concepts of "instant" and "delayed" compression as an advance on the terms "primary" and "secondary" consolidation, were proposed by Bjerrum (1967), and are illustrated by Figure 3.3. The dashed curve defines the new terms, which describe the reaction of the soil skeleton to a suddenly applied load increment, assuming that the pore water in the voids is incapable of retarding compression. It thus represents the theoretical "free-response" of the soil skeleton, or the response of a very thin sample. The fully drawn curve is the actual consolidation curve, resulting from a retardation of both "instant" and "delayed" compression by hydrodynamic effects.

Although Bjerrum's ideas were a conceptual coup, it is not possible in Figure 3.3 to predict the shape of the actual consolidation curve directly from the shape of the "free-response" curve. The resistance of the soil skeleton to compression must first be formulated by a constitutive equation consistent with the complete "free-response", in the same manner that equation 3.2 describes an "instant" linear compression.

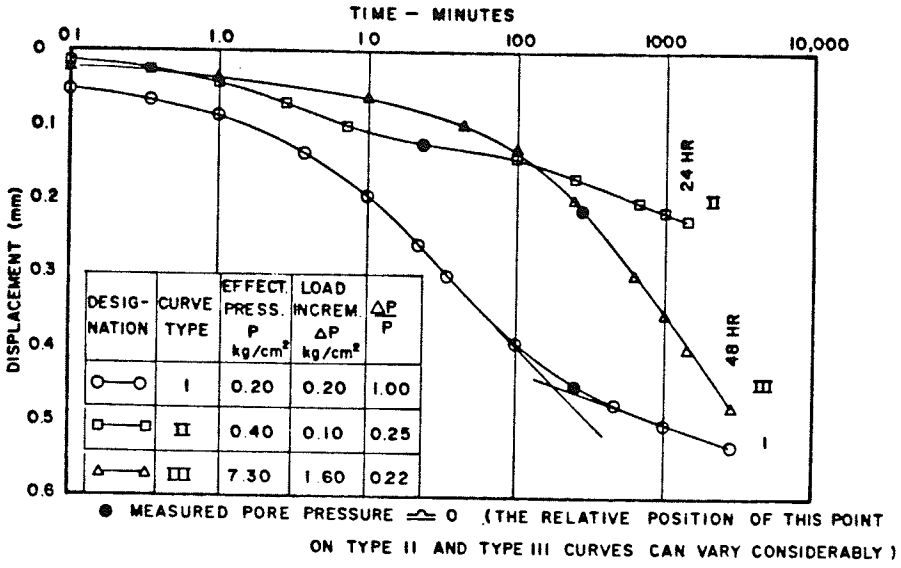

Figure 3.2 Effect of L.I.R. on Consolidation versus Log. Time Curves (Mexico City Clay, After Leonards and Girault, 1961)

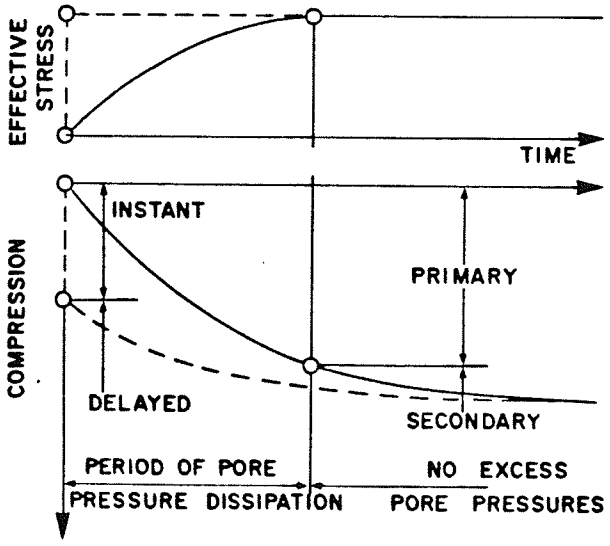

Figure 3.3 The Concepts of "Instant" and "Delayed" Compression (After Bjerrum, 1967, Fig. 15)

3.6 CONSOLIDATION THEORIES WHICH ACCOUNT FOR DELAYED EFFECTS

A solution consistent with Bjerrum's ideas has been presented by Garlanger (1972), who proposed the following modification to equation 3.3 to take account of delayed effects.

$$\frac{\partial e}{\partial t} = \frac{\partial e}{\partial \sigma'} \frac{\partial \bar{u}}{\partial t} + \left(\frac{\partial e}{\partial t}\right)_c \qquad (3.5)$$

where the rate of delayed compression $\left(\frac{\partial e}{\partial t}\right)_c$ and $\frac{\partial e}{\partial \sigma'}$, (a_v) are both functions of pressure and void ratio.

In equation 3.5 it is assumed that "instant" and "delayed" compression are independent processes. When a sample of clay is allowed to consolidate for several days in "secondary" (ie. almost entirely delayed) compression, it develops an increased resistance to further loading. This is known as the quasi-preconsolidation effect, (Leonards and Altschaeffl, 1964; Bjerrum, 1967). Using Bjerrum's and Garlanger's concepts, this decrease in observed compressibility is due solely to a decrease in delayed compression, $(\partial e/\partial t)_c$, whereas $\partial e/\partial \sigma'(a_v)$ remains constant. This assumption can be challenged. Returning to the idea of compression events discussed earlier, it would seem likely that the stabilization occurring during "secondary" consolidation would also decrease the "instant" compressibility under a small stress increase.

Garlanger's Theory is an example of a modification to the Terzaghi Theory, which attempts to account for increased compressibility at lowered rates of strain. Other examples of such theories are:

(a) Solutions based on rheological models of soil skeleton compressibility; eg. Gibson and Lo (1961) - linear spring in series with Kelvin body; Barden (1965) - linear spring

in series with non-linear dashpot.

(b) Isotache theories (Sulkje, 1969), and the "Unified Theory", a modification by Hawley and Borin (1973).

3.7 EFFECT OF THICKNESS ON CONSOLIDATION STRAINS ACCORDING TO MODIFIED CONSOLIDATION THEORIES

The above theories, including Garlanger's, have been used in an attempt to model the experimental rate of dissipation of pore-pressures, and the effect of load increment ratio, with varying success. Unfortunately most solutions which have been presented are numerical rather than analytical, so that direct equations for the effect of scale were not given. All the solutions, however, predict that strains occurring during the "primary" phase should increase with sample thickness. From Terzaghi Theory all consolidation strain versus time curves essentially merge as soon as pore-pressures become small, regardless of thickness. Curves based on the above theories may merge as soon as pore-pressures become small, or at a later stage, depending upon the magnitude of parameters selected to describe the time dependent compression of the soil skeleton.

The suggestion that the primary strains in an oedometer test underestimate the strains occurring in a field stratum, has not found any general acceptance by practising engineers, and is refuted by some researchers, eg. Leonards (1977). In an earlier publication, (Leonards and Altschaeffl, 1964), the latter author presented data from artificial sedimentation of a clay at extremely slow rates of loading, (1 kPa/day to 10^{-2} kPa/day), and no measurable excess pore-pressures were developed. It was found that in this range of loading rates, compressibility actually

decreased very significantly as the rate of loading decreased. This suggests an aging or thixotropic effect not accounted for in the above theories.

3.8 RESULTS OF EXPERIMENTAL ATTEMPTS TO DETERMINE THE EFFECT OF THICKNESS ON CONSOLIDATION

Unfortunately there have been very few controlled experiments on the effect of sample thickness on one-dimensional consolidation. Research problems include:

(a) The time of consolidation of a thick sample may be several years, and samples need to be monitored for a considerable time after pore-water pressures become small.

(b) Side friction may be more significant in thick samples.

(c) To compare results, all samples must be uniformly consolidated to an equal initial void ratio and pressure, before application of the stress increment.

The results of a study conducted on an artificially sedimented marine clay from Hiroshima Bay were presented by Aboshi (1973), and are shown in Figure 3.4. The consolidation strain versus time curves do not merge after "primary" consolidation, but become approximately parallel in secondary compression. Thus the coefficient C_α can be used to describe consolidation after long times, regardess of thickness. The strains at "end of primary" increased, but only slightly. These results compare well with the trends apparent in a study by Berre and Iverson (1972), on undisturbed samples of a normally consolidated marine clay. Unfortunately, at the time of publication of the latter results, the oedometer tests had not been continued long enough to show whether the

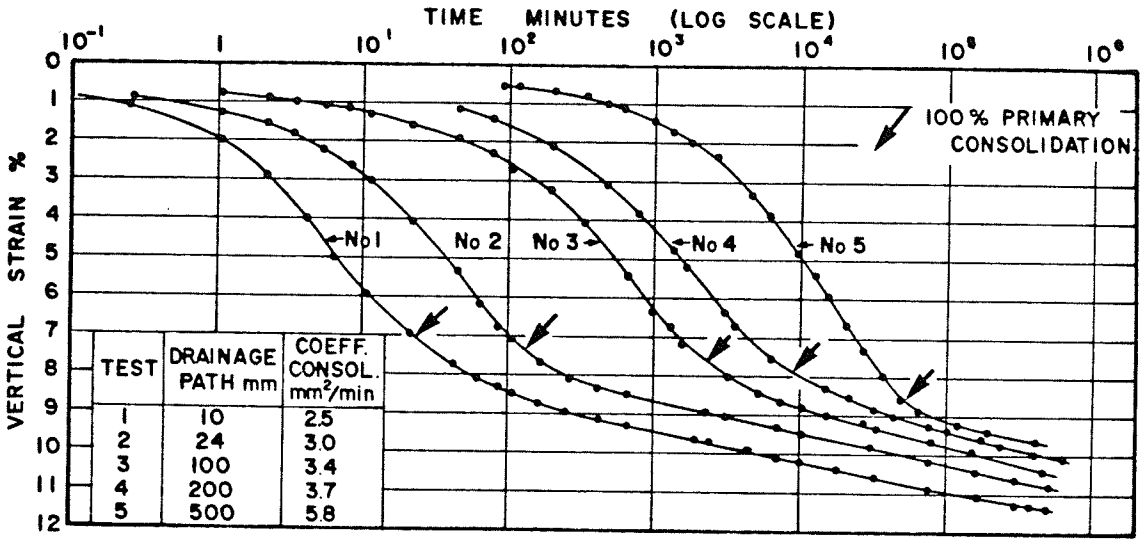

Figure 3.4 The Effect of Thickness on Consolidation versus Log. Time Curves for Artificially Sedimented Samples of a Marine Clay from Hiroshima Bay (After Aboshi, 1973)

curves do become parallel in "secondary" compression. Much more experimental data is needed before the suggested trends can be established.

3.9 UPPER AND LOWER BOUND PREDICTIONS OF LONG TERM SETTLEMENT BASED ON OEDOMETER TESTS

Based on the discussion of Sections 3.6 and 3.7, three different estimates of the long term strain, (Δe), and thus settlement, of a thick layer of clay are illustrated in Figure 3.5. It is assumed that the laboratory curve S1, from an oedometer sample of thickness H_1, merges with a hyporthetical "free-response" curve, S0, soon after the end of "primary" consolidation. Curves S1 and S0 can thereafter be defined by $C_\alpha = 22 \times 10^{-3}$. Curves S2, S3 and S4 are possible curves for a layer of identical material with thickness H_2, where $H_2 = 100\ H_1$.

Curve S2 may be justified by the contention of Leonards (1977), that primary consolidation strain in an oedometer test does not underestimate primary strain in the field. The curve was developed by assuming that primary consolidation follows the Terzaghi model, and is then followed by secondary consolidation, $C_\alpha = C_\alpha$ (oedometer). Curve S4 is constructed with the assumption that consolidation strain versus time curves eventually merge regardless of thickness. This follows from consolidation theories which attempt to account for Bjerrum's "delayed" compression, or for strain rate effects, eg. Garlanger (1972). Curve S3 is intermediate between curves S2 and S4 and is based on the experimental work of Aboshi (1973). The long term strain versus time curve is parallel, but not coincident with, the laboratory curve S1.

The equations for long term strain from the above curves are:

Curve S2 $$\Delta e(S2) = \Delta e(\text{primary}) + C_\alpha \log. \frac{t}{t_2} \qquad (3.6)$$

where $t > t_2$

and $t_2 = t_1\left(\frac{H_2}{H_1}\right)^2$ from Terzaghi Theory

Curve S4 $$\Delta e(S4) = \Delta e(\text{primary}) + C_\alpha \log. \frac{t}{t_1} \qquad (3.7)$$

where $t > t_2$ (approximately)

and t_1 = Duration of primary consolidation in the laboratory test

Curve S3 $$\Delta e(S3) = \Delta e(\text{primary}) + C_\alpha \log. \frac{t}{t_3} \qquad (3.8)$$

where $t > t_2$ (approximately)

and t_3 is an arbitary time between t_1 and t_2

Notes:

(a) The difference between the above predictions increases as C_α increases.

(b) The value of $\Delta e(S3)$ from equation 3.8 appears to need the input of an arbitary time t_3. However the "primary" strain may be taken from the e versus σ'_c curve for 24 hours consolidation, and this includes some "secondary" consolidation. If the strain rate after time t_2 is then assumed to be given by C_α, this is equivalent to the assumption that $t_3 = t_2 - (24 \text{ hours} - t_1)$. This may be deduced from Figure 3.5.

(c) In the curves of Figure 3.5 no account is taken of the fact that the bulk in-situ permeability is likely to be much greater than that of a laboratory sample. All predicted curves would as a result be shifted to the left. The long term strain prediction of equation 3.7 (curve S4) would be unaffected by this.

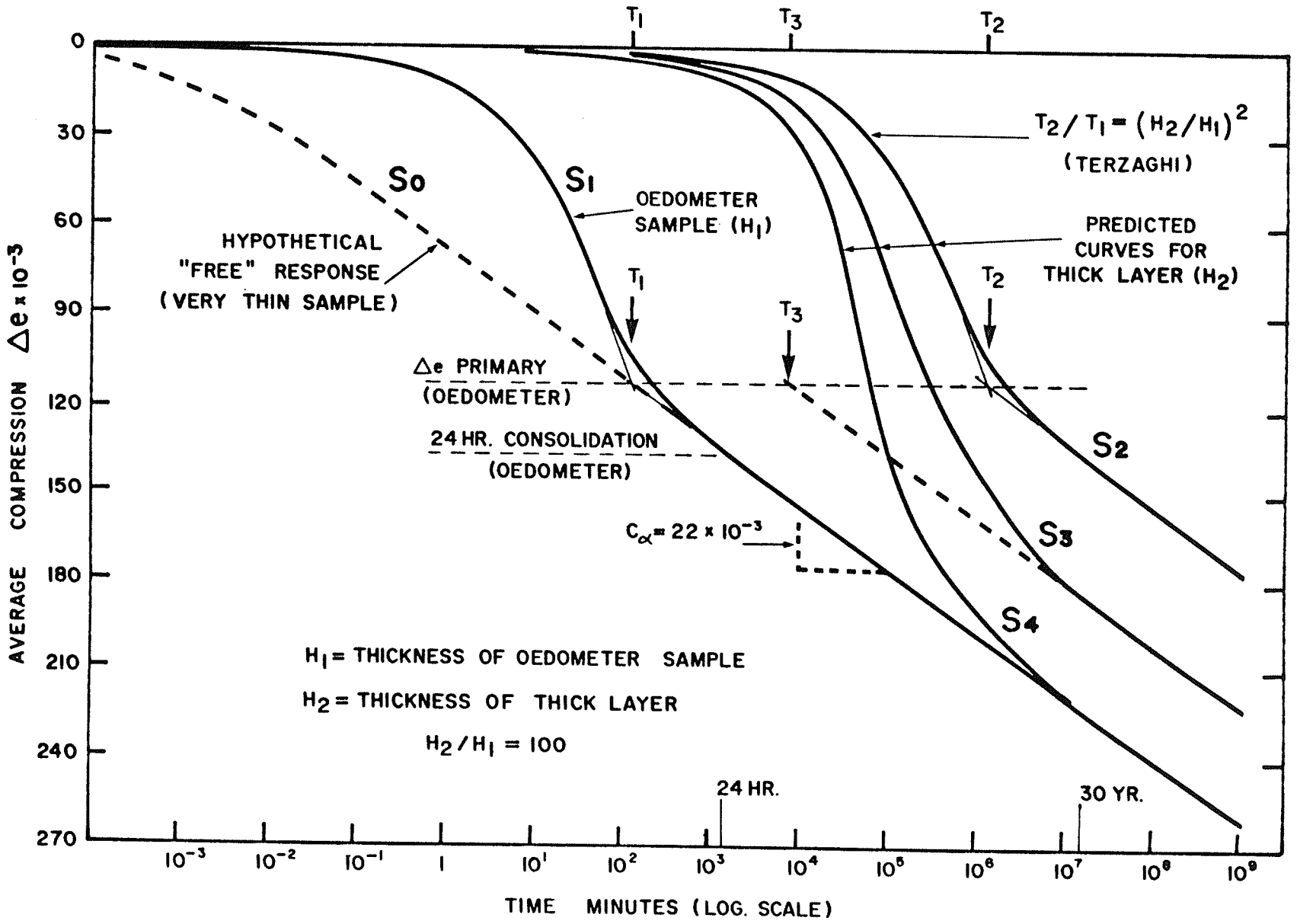

Figure 3.5 Upper and Lower Bounds to Settlement of a Thick Layer, Based on the Results of an Oedometer Test

CHAPTER 4

OEDOMETER TESTING

PROCEDURES, RESULTS AND DISCUSSION

4.1 TESTING PROGRAM AND PROCEDURES

A total of twenty stress-controlled tests were performed using fixed-ring, double drainage oedoemters. The samples were nominally 18 mm thick by 63.5 mm diameter, and loads were applied using a 10.21 to 1 level-ratio press. Disturbance was minimized during the trimming process by the lubrication of the consolidation rings with silicon oil, the maintenance of sharp cutting edges, and by the use of the equipment shown in Figure 4.1. Lubrication of the rings also helped reduce side friction during the actual tests.

All samples were initially prevented from swelling; distilled water was added after the porous stones had been seated with a small stress of about 5 kPa, and then the vertical strain was kept at zero or a slight compressive value by the gradual addition of stress. The magnitude of this initial swell-compensating stress varied from 50 to 83 kPa, and samples were left for from 12 to 24 hours before the start of actual test loading. The loading sequence and loading period, ΔT, for each test are given in Table 4.1; loads were applied in a series of constant increments, ΔP, or using a constant L.I.R. equal to 1.6. In some cases the sample was initially unloaded to a stress, p'_s, and allowed to swell.

Precautions were taken to separate effects on consolidation characteristics due to test procedures, from those which might be due to local soil differences. Tests were run in control groups of 2 or 3

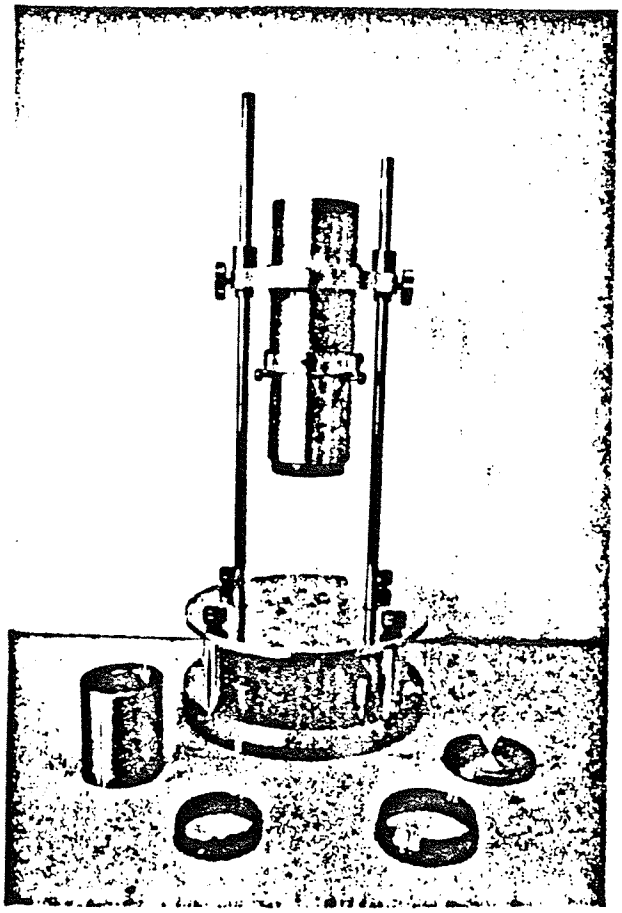

Figure 4.1 Trimming Equipment for
Oedometer Samples

samples trimmed from immediately adjacent positions in a block.

Because of the very low strain rates which occur at the end of a long loading period, 48 hours was considered a practical maximum period, ΔT, without the use of precise temperature control to stabilize both the measuring equipment and the sample. The measurement of vertical displacement was accomplished using an L.V.D. Transducer sensitive to 1 μm, and values were recorded by an automatic data logger.

4.2 PRESENTATION OF RESULTS

4.2.1 General Introduction

As shown in Table 4.1, the testing program consisted of 10 oedometer tests from a depth of 9.0 m (blue clay), 4 tests from 11.5 m (blue clay), and 6 tests from 5.5 m (brown clay). The primary goal of this research was to determine the undisturbed consolidation - compression characteristics at each of the above depths, with particular focus on the compressibility, and the preconsolidation pressure. A general discussion based on the results of all tests will be presented later in this chapter. The topics of discussion include the repeatability of tests, the degree of local variation in properties, the differences between depths, and the effects of the different loading procedures on behaviour. As a prelude to this discussion, Sections 4.2.2 to 4.2.5 describe in detail the results of four specific tests, as follows:

(a) Test C, 9.0 m, Blue Clay, (Section 4.2.2). Constant Increment Ratio Test, L.I.R = 1.60, ΔT = 24 hours.

(b) Test U, 9.0 m, Blue Clay, (Section 4.2.3). Constant Increment Test, $\Delta\sigma$ = 48.5 kPa, ΔT = 24 hours.

(c) Test I, 11.5 m, Blue Clay, (Section 4.2.4). Constant Increment Test, $\Delta\sigma$ = 43.0 kPa, ΔT = 8 hours.

(d) Test T, 5.5 m, Brown Clay, (Section 4.2.5). Constant Increment Test, $\Delta\sigma$ = 162 kPa, ΔT = 24 hours.

Test C serves as a good introduction to the consolidation behaviour of Winnipeg clay in a constant load increment ratio, (standard), test. Test U, at the same depth, 9.0 m, is an example of a constant load increment test, a type of test used extensively in this study. Tests I and T are also constant increment tests, presented as typical of tests at the 11.5 m and 5.5 m depths.

4.2.2 Test C, 9.0 m Blue Clay

Constant Increment Ratio Test, L.I.R = 1.60, ΔT = 24 hours

Test C is presented as typical for the constant L.I.R tests at this depth. Figure 4.2 shows two facets of the experimental void-ratio versus consolidation stress relationship. The traditional semi-logarithmic presentation is shown in Figure 4.2(a), whereas in Figure 4.2(b) both axes are scaled arithmetically. From the semi-logarithmic plot the preconsolidation pressure, P'_c, is estimated as 410 kPa by use of the Casagrande construction; the overconsolidation ratio for this depth is thus about 5*. The initially steep virgin compression branch, ($C_{c\ max}$ = 0.90), at stresses higher than P'_c, and the well-rounded recompression branch at stresses less than P'_c, are typical for the Winnipeg

---

*In-situ vertical effective stresses are difficult to estimate accurately, but assuming that the saturation zone lies 1 to 3 m below surface, then $P'_o \simeq$ 70 to 100 kPa.

Test No	Bore Hole and Sampling Method	Initial Void Ratio, e_o	Typical Loading Sequence L.I.R.	(kPa)	Loading Period (Hrs)	Initial Stress p'_i (kPa)	Initial Loading if Diff. from Typical
			Brown Clay 5.5 m				
[M]	BH4-Piston	1.38	1.6	-	24	62	
[N]	BH4-Piston	1.53	1.6	-	24	63	
[O]	BH5-Block	1.54	-	48.3	8	83	
[P]	BH5-Block	1.54		48.5	24	66	
[S]	BH5-Block	1.54		162.0	24	83	83 kPa to 164 kPa
[T]	BH5-Block	1.57		162.3	24	83	83 kPa to 18 kPa to 164 kPa
			Blue Clay 9.0 m				
[C]	BH4-Block	1.35	1.6	-	24	60	
[D]	BH4-Block	1.33	1.6	-	24	70	
[E]	BH4-Block	1.26	1.6	-	12	66	
[F]	BH4-Block	1.26	1.6	-	12	73	
[G]	BH4-Block	1.30	1.6	-	48	60	
[J]	BH4-Piston	1.41	1.6	-	24	67	
[K]	BH4-Piston	1.33	1.6	-	48	67	
[L]	BH4-Piston	1.41	-	42.9	8	67	
Q	BH5-Block	1.35		48.2	24	66	
U	BH5-Block	1.35		48.5	24	67	67 kPa to 18 kPa to 67 kPa
			BLUE CLAY 11.5 m				
[H]	BH4-BLOCK	1.63	1.6	-	24	66	
[I]	BH4-BLOCK	1.59	-	43.0	8	66	
R	BH5-BLOCK	1.62	-	48.3	24	50	
V	BH5-BLOCK	1.75	-	45.8	24	50	

Notes: (a) BH4 Drilled July, 1980, BH5 Drilled January, 1981, see Figure 1.1.

(b) [C D] Indicates control group, ie samples C and D cut from adjacent soil.

Table 4.1 Schedule of Consolidation Tests

clay. Winnipeg clays contain a high proportion of expansive clay minerals, e.g. Baracos (1977). It has been suggested that the rounded recompression curve might be due to a combination of sampling and trimming disturbance, and excessive swelling strains occuring as a result of the common practice of initial consolidation to a stress much less than p'_o (Baracos et. al., 1981). Test C, however, was not allowed to swell, and the trimming techniques were more than adequate considering that the sensitivity of the clay is only about 3, (Chapter 2). In addition the test was commenced only one day after soil drilling, to eliminate any disturbance due to storage.

It is the author's opinion that arithmetic scale plotting of the void ratio versus consolidation stress relationship leads to a much better understanding of the recompression behaviour, the significance of p'_c, and the virgin compression behaviour. Figure 4.2(b) shows that the recompression is approximately linear and is followed by a distinct yield at p'_c, and then strain stiffening in the virgin compression range. The value of p'_c can easily be defined by the intersection of the dashed lines, which are extrapolations of pre-, and post-yield curves. The resulting value, p'_c = 410 kPa is close, (in this case equal), to that given by the more complicated Casagrande construction. A distinct yield is an indication of undisturbed behaviour. Figure 4.2(b) suggests that field settlement calculations could be based on the single linear relationship $\Delta_e = a_{vo}.\Delta\sigma'$ provided p'_c is not exceeded, ($a_{vo} = 3.7\text{x}10^{-4}\text{kPa}^{-1}$).

The consolidation versus logarithmic time curves produced by each load increment are shown in Figure 4.3. All curves were type I curves (Chapter 3), and it was therefore possible to calculate both the coefficient of secondary compression, C_α, and the coefficient of

consolidation, C_v, for all eight load increments. Figure 4.4 shows that C_v decreased by one order of magnitude in the recompression range, from about 78 x 10^{-3} mm^2/sec to about 6 x 10^{-3} mm^2/sec, and remained approximately constant at stresses above P'_c. C_α peaks in the vicinity of P'_c, but because of the limited number of data points, it is not clear whether the peak occurs at or after the preconsolidation pressure. It has been suggested that the C_α versus void ratio curve (Figure 4.5) is independent of pressure increment (Wahls, 1962). The initial behaviour varies with the degree of preconsolidation, but the "virgin secondary compression - void ratio curve", should be unique for all tests. The complete set of C_α versus e curves are examined in Section 4.2.9.

The compression index, C_c is often used to denote the average slope of the e versus log σ'_c curve in the virgin compression region. It can also be defined as a test variable, $C_c = \Delta e/\log.\sigma'_c$ for each stress increment, in the recompression as well as in the virgin compression range. The relationship between C_α and C_c is remarkably linear, (Figure 4.6), and the value of $C_\alpha/C_c \simeq 0.035$ is within the range of 0.025 to 0.60 for inorganic soils (Mesri, 1977). Mesri recommends that C_c be calculated from the value of Δe at the end of "primary" consolidation. However this was not possible when type III consolidation curves were produced (From constant increment tests see next section). To be consistent C_c was calculated from Δe at the end of the loading period.

4.2.3 Test U, 9.0 m Blue Clay

Constant Increment Test, $\Delta\sigma$ = 48.5 kPa, ΔT = 24 hours

Oedometer test U was conducted using small constant load increments, $\Delta\sigma$ = 48.5 kPa applied every 24 hours. After initial consolida-

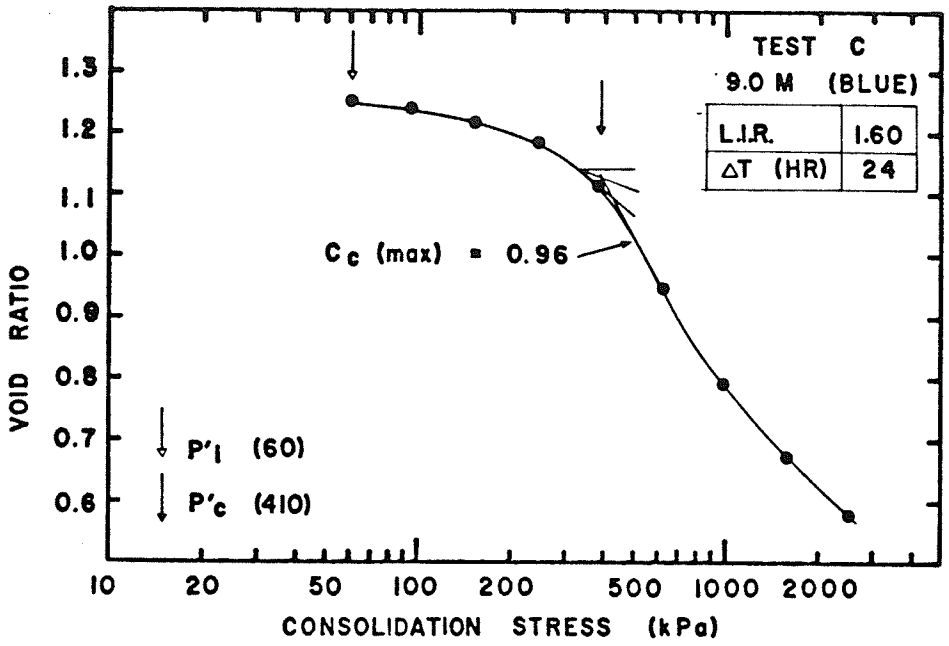

(a)

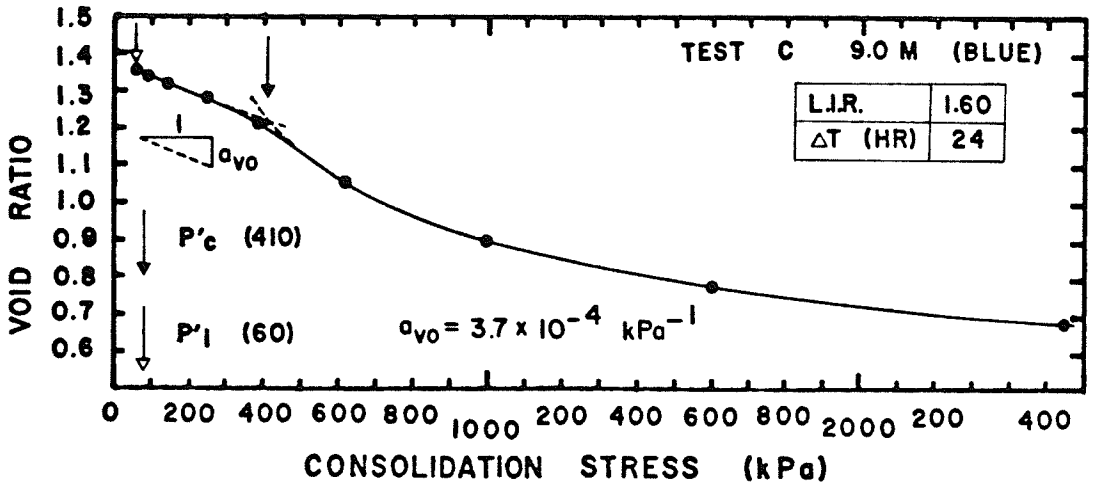

(b)

Figure 4.2 Oedometer Test C, Blue Clay from 9.0 m
Void Ratio versus Consolidation Stress

(a) The Traditional Semi-logarithmic Plot

(b) Arithmetic Scales

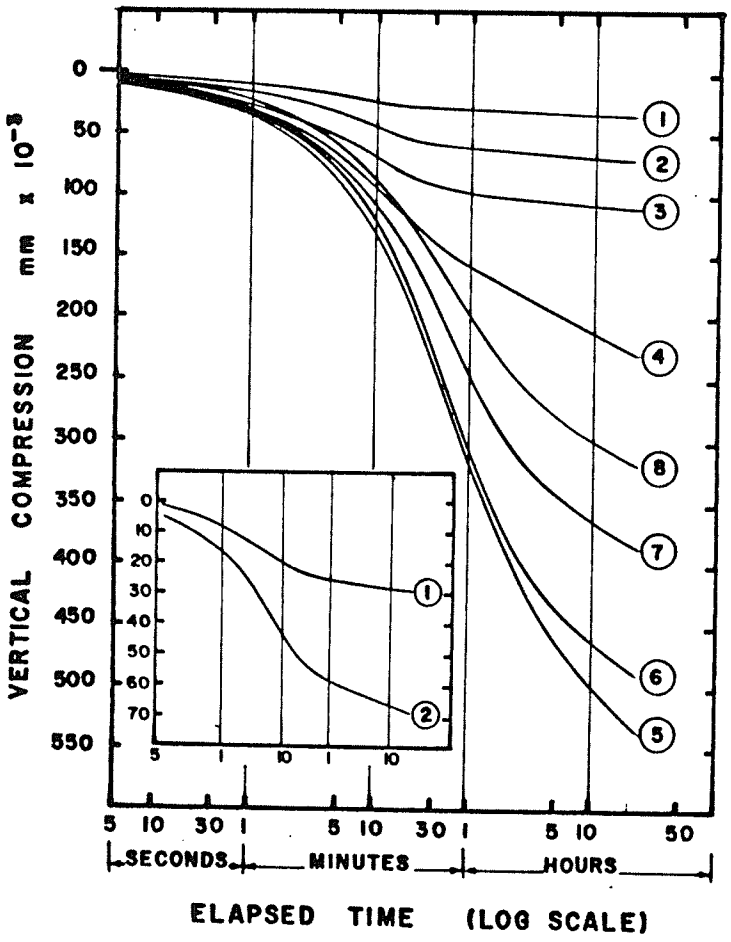

Figure 4.3 Oedometer Test C, 9.0 m Depth. Consolidation versus Time Curves in order of Loading

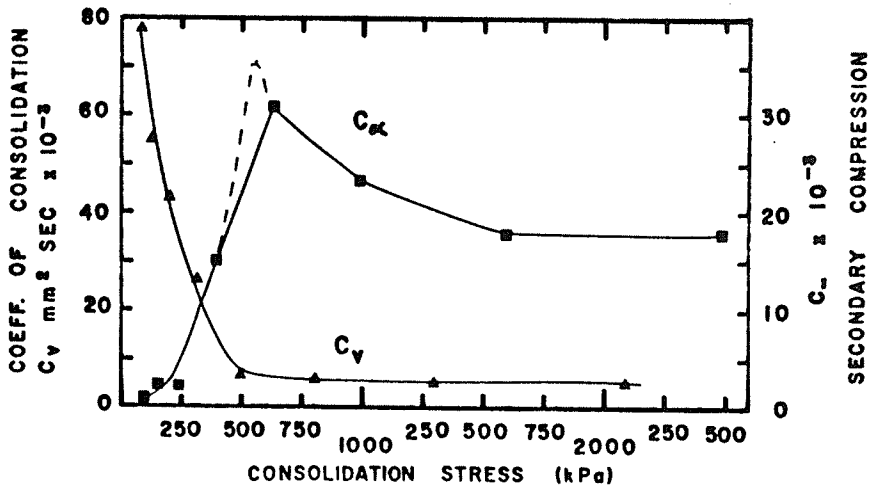

Figure 4.4 Oedometer Test C, 9.0 m Depth. Coefficients of Secondary Compression, and Consolidation, versus Consolidation Stress

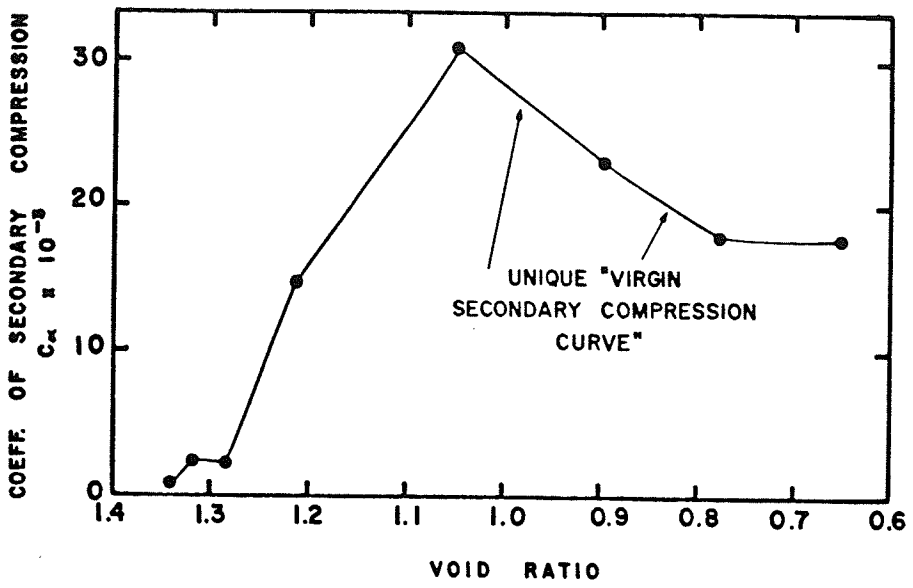

Figure 4.5 Oedometer Test C, 9.0 m Depth. Coefficient of Secondary Compression versus Void Ratio

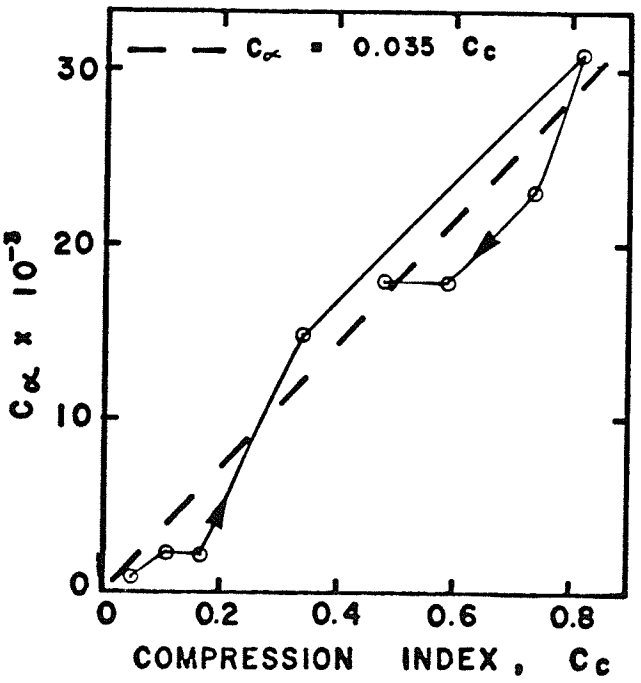

Figure 4.6 Oedometer Test C, 9.0 m Depth. Relationship Between C_α and C_c

tion to P'_c = 67 kPa, the first increment was an unloading to P'_s = 18.5 kPa, so that swelling occurred. The e versus σ'_c curve, (Figure 4.7), has a yield at a preconsolidation pressure of 410 kPa, and a linear recompression stage, $a'_{vo} = 3.5 \times 10^{-4}$ kPa^{-1}. Neither the use of a small load increment, nor the swelling strains, have affected the curve significantly (compare with test C above, Figure 4.2). Also shown in Figure 4.7 are the coefficients of compressibility, a_v, and secondary compression, C_α, for each stress increment; a_v is simply the local slope between data points on the e versus σ'_c curve, and a small increase in compressibility occurs for the second load increment. In the initial cycle from 67 kPa to 18.5 kPa and back to 67 kPa there is a slight increase in void ratio. During the next increment from 67 to 115 kPa it appears that the sample loses this hysteresis, showing increased compressibility for just one load increment. In contrast there is no corresponding early peak in C_α, which increases consistently; slowly until yield and then rapidly to a peak at 550 kPa.

Note that the peak values of C_α and C_c for test U, (Figures 4.7 and 4.8), are lower in comparison with test C. As discussed in Section 4.2.7 it is likely that this is due to a variation in soil properties rather than the differences in loading procedure.

The consolidation versus logarithmic time curves for each increment are shown in Figure 4.9. Type I curves occur for the first 4 increments, but curves 5 through 20 have no inflection point and are thus type III. The type III curves do not indicate that excess porepressures have not dissipated in the time period, ΔT^*. They are merely

*In fact there is evidence that when small load ratios are used the rate of dissipation increases (Leonards and Girault, 1961; Bjerrun, 1967).

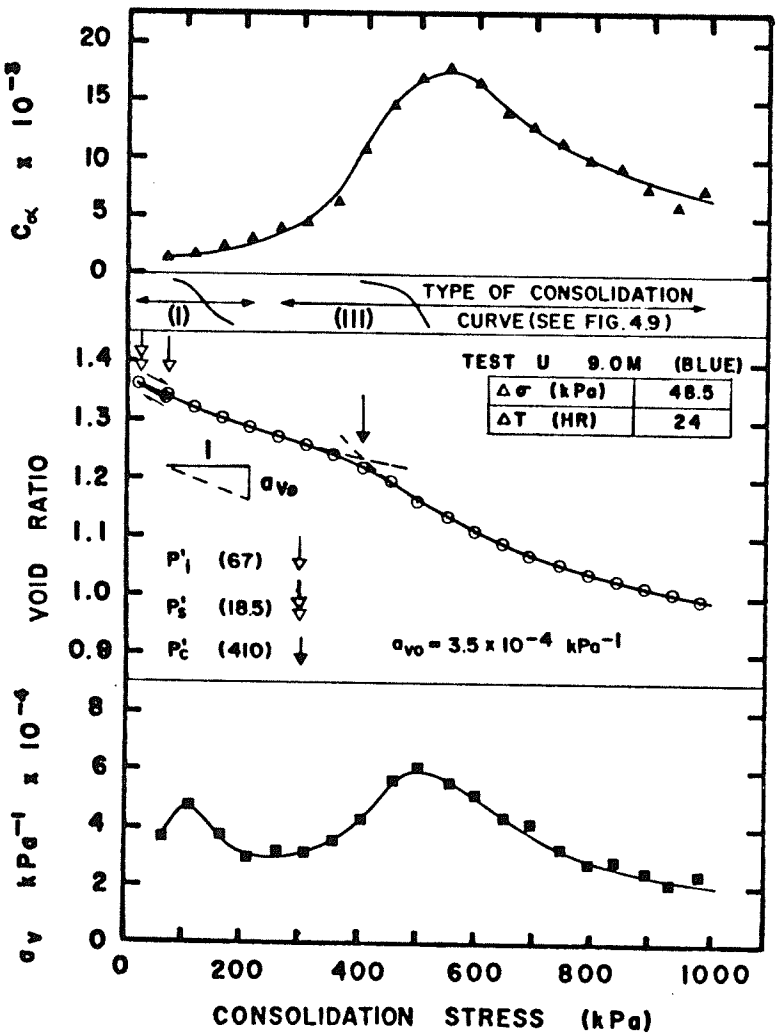

Figure 4.7 Oedometer Test U, 9.0 m Depth. Void Ratio versus Consolidation Stress, with Coefficients C_α and a_v

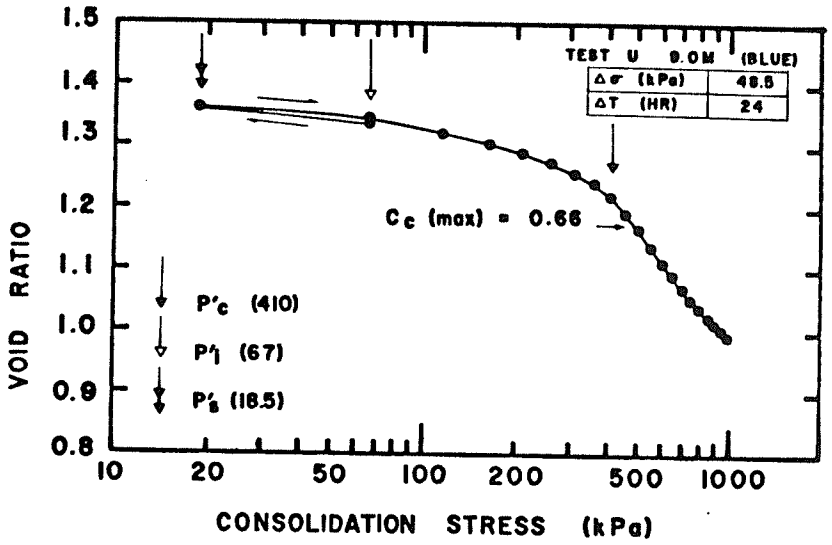

Figure 4.8 Oedometer Test U, 9.0 m Depth. Void Ratio versus Log. Consolidation Stress.

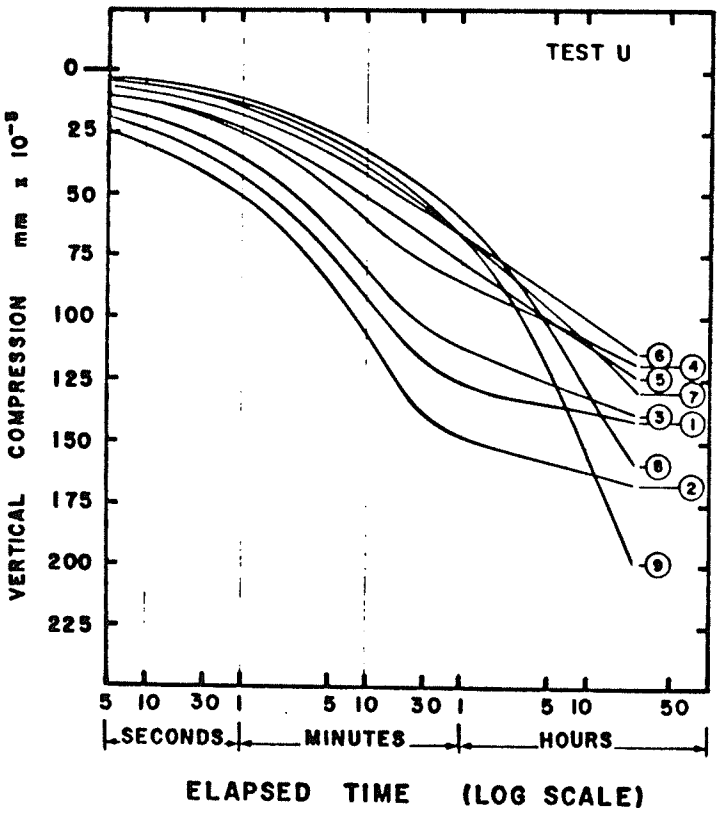

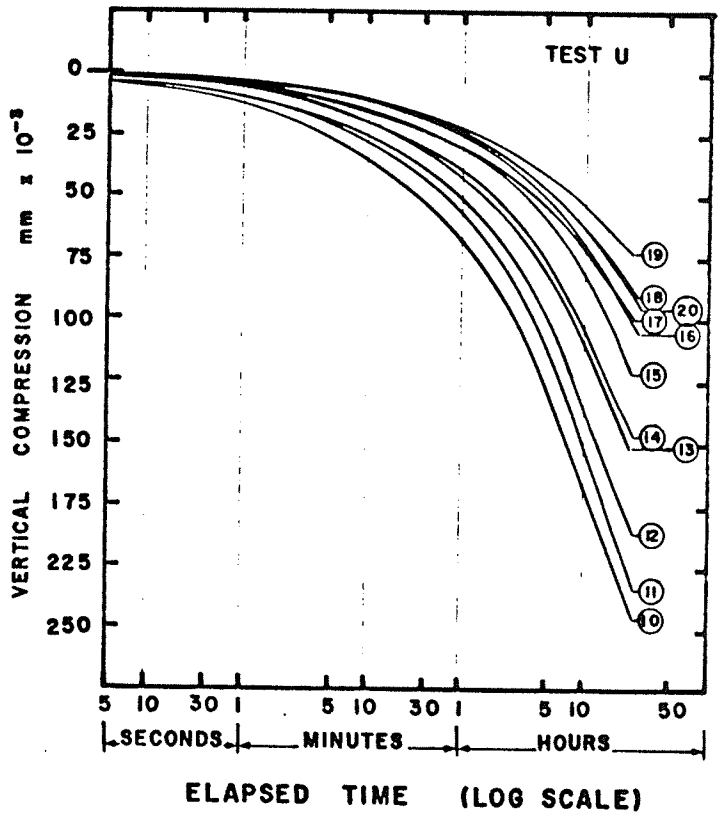

Notes: Constant Increment Test, $\Delta\sigma$ = 48.5 kPa. Increment (1) 18.5 to 67 kPa

Figure 4.9 Oedometer Test U, 9.0 m Depth. Consolidation versus Log. Time Curves in order of Loading.

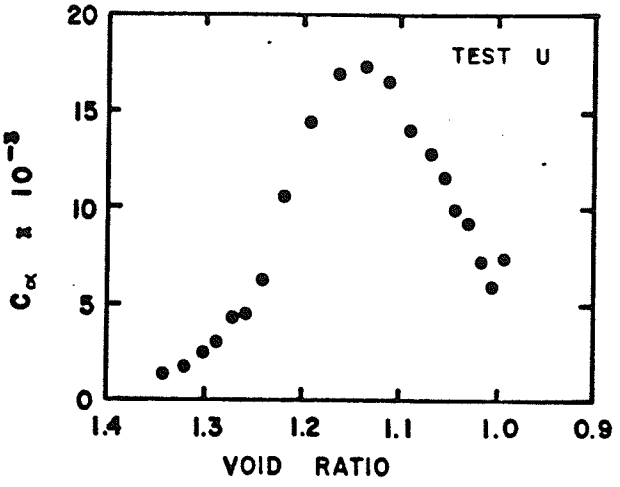

Figure 4.10 Oedometer Test U, 9.0 m Depth.
C_α versus e

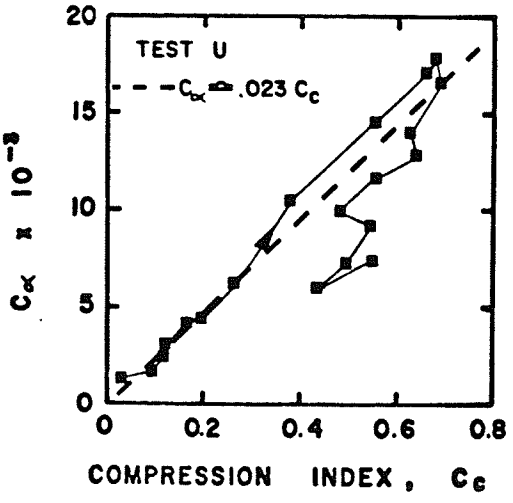

Figure 4.11 Oedometer Test U,
9.0 m Depth.
C_α versus C_c

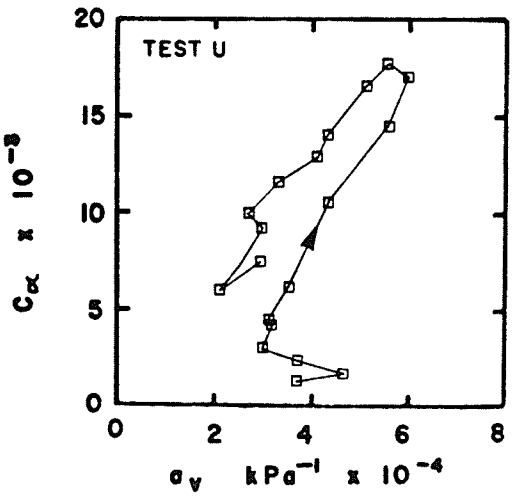

Figure 4.12 Oedometer Test U,
9.0 m Depth.
C_α versus a_v

characteristic for small load increment ratios, (Chapter 3), and in test U the ratio is decreased at each loading. The L.I.R for curve 4 equals 1.30, and that for curve 5 equals 1.23; that for curve 20 equals 1.05. Withoug direct pore-pressure measurement it is not possible to obtain an experimental value of C_v from type III curves, but the curves become approximately linear after sufficient times, and C_α is measured from the logarithmic slope at the end of ΔT, in this case 24 hours. The variation of C_α with void ratio (Figure 4.10), and the dependence of C_α upon C_c (Figure 4.11) can be compared with results from test C, (Figures 4.5 and 4.6). Figure 4.12 shows that C_α/a_v is also approximately constant.

4.2.4 Test I, 11.5 m, Blue Clay

Constant Increment Test, $\Delta\sigma$ = 43.0 kPa, ΔT = 8 hours

Samples of blue clay from 11.5 m had a higher initial moisture content and void ratio than samples of blue clay from 9.0 m discussed above. The behaviour was found to be similar to that at 9.0 m but there was typically an increase in compressibility, a marked decrease in preconsolidation pressure, and a much more striking yield.

The e versus σ'_c curve (Figure 4.13), shows that P'_c is only 215 kPa as compared to 410 kPa at 9.0 m and the compressibility, a_{vo}, is 6.7 x 10^{-4} kPa^{-1}, approximately twice that at 9.0 m. There is also a much more dramatic yield, characterised by very high peak values of a_v, C_α, and also C_c (Figure 4.14). Figure 4.15(a) shows that the ratio C_α/C_c is also high.

At a stress well beyond the preconsolidation pressure, (increment 17, 754 to 797 kPa), a constant stress was sustained for 10 days and then three more loads were applied using a L.I.R. of 1.6 and ΔT =

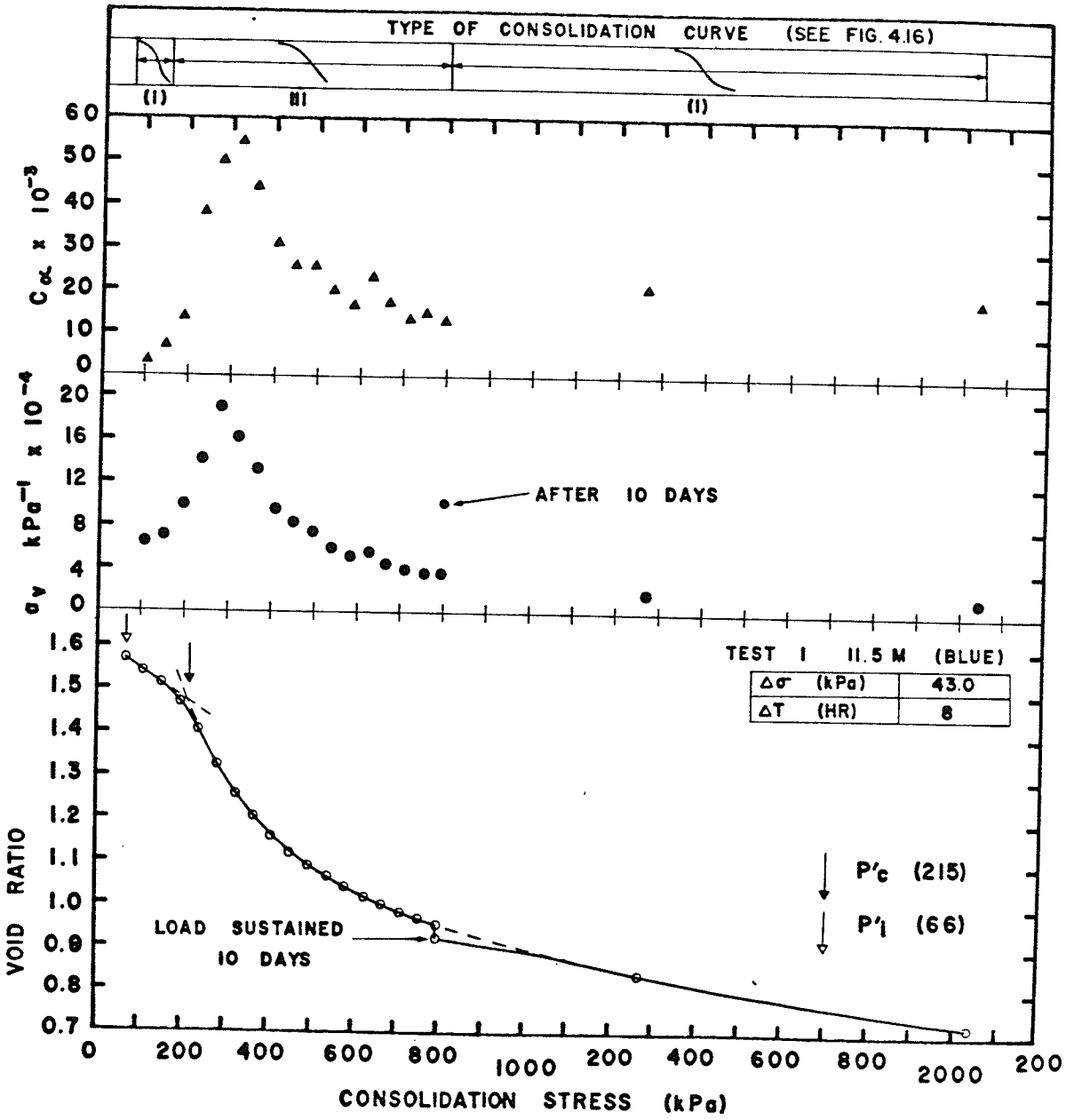

Figure 4.13 Oedometer Test I, 11.5 m Depth.
Void Ratio versus Consolidation Stress, and
Coefficients a_v and C_α for Each Increment.

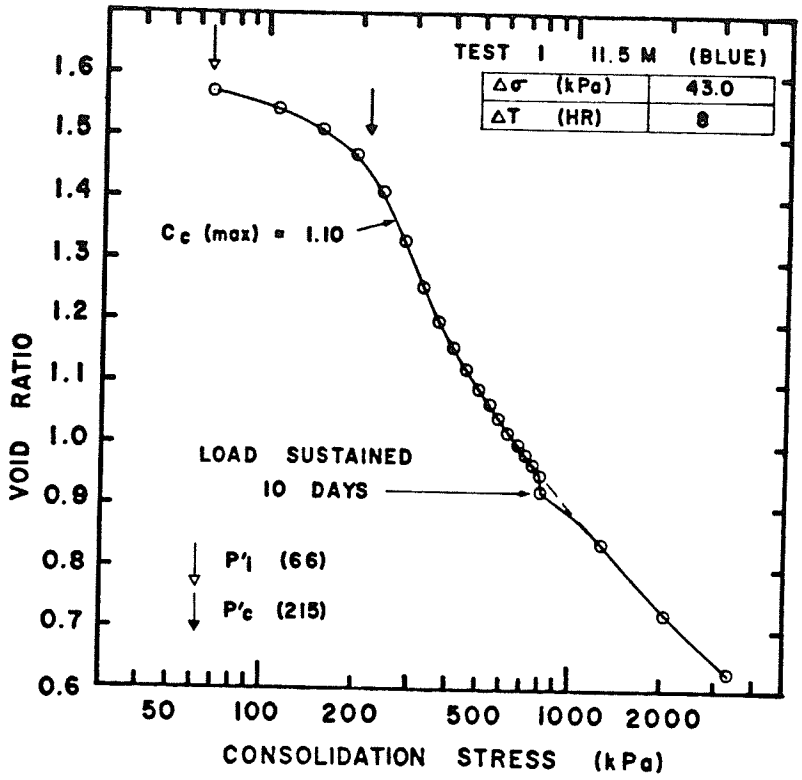

Figure 4.14 Oedometer Test I, 11.5 m Depth.
Void Ratio versus Log. Consolidation Stress.

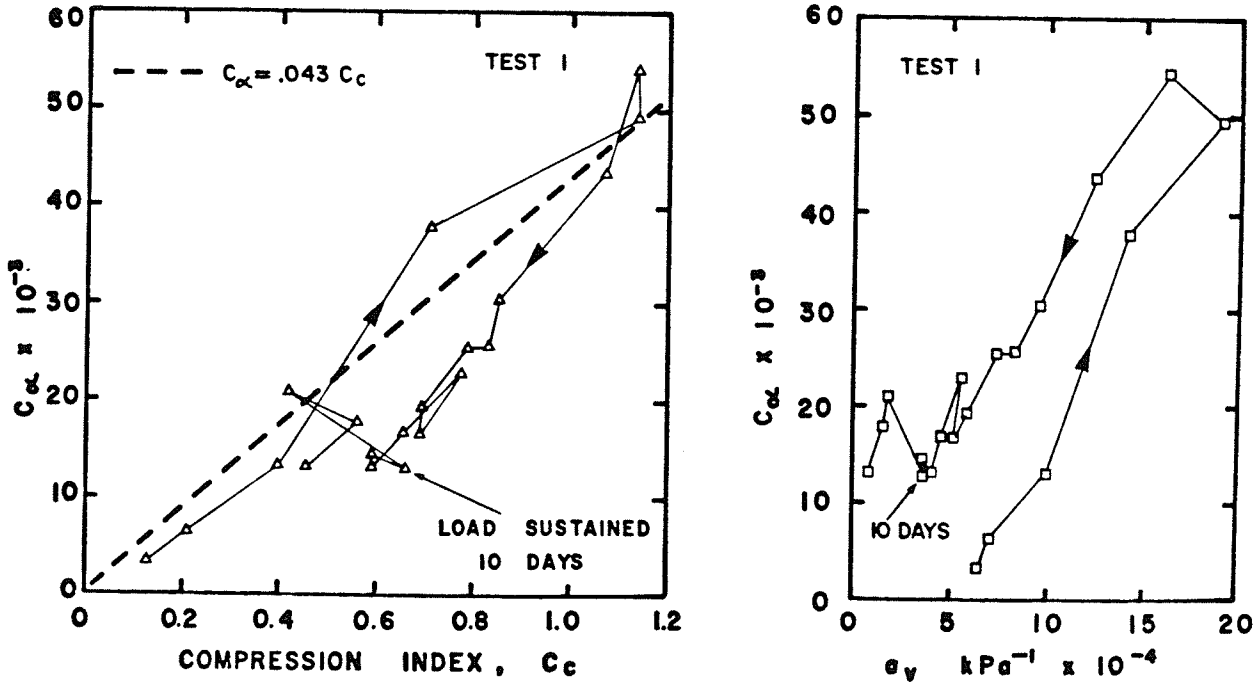

(a) (b)

Figure 4.15 Oedometer Test I, 11.5 m Depth.
(a) C_α versus C_c
(b) C_α versus a_v

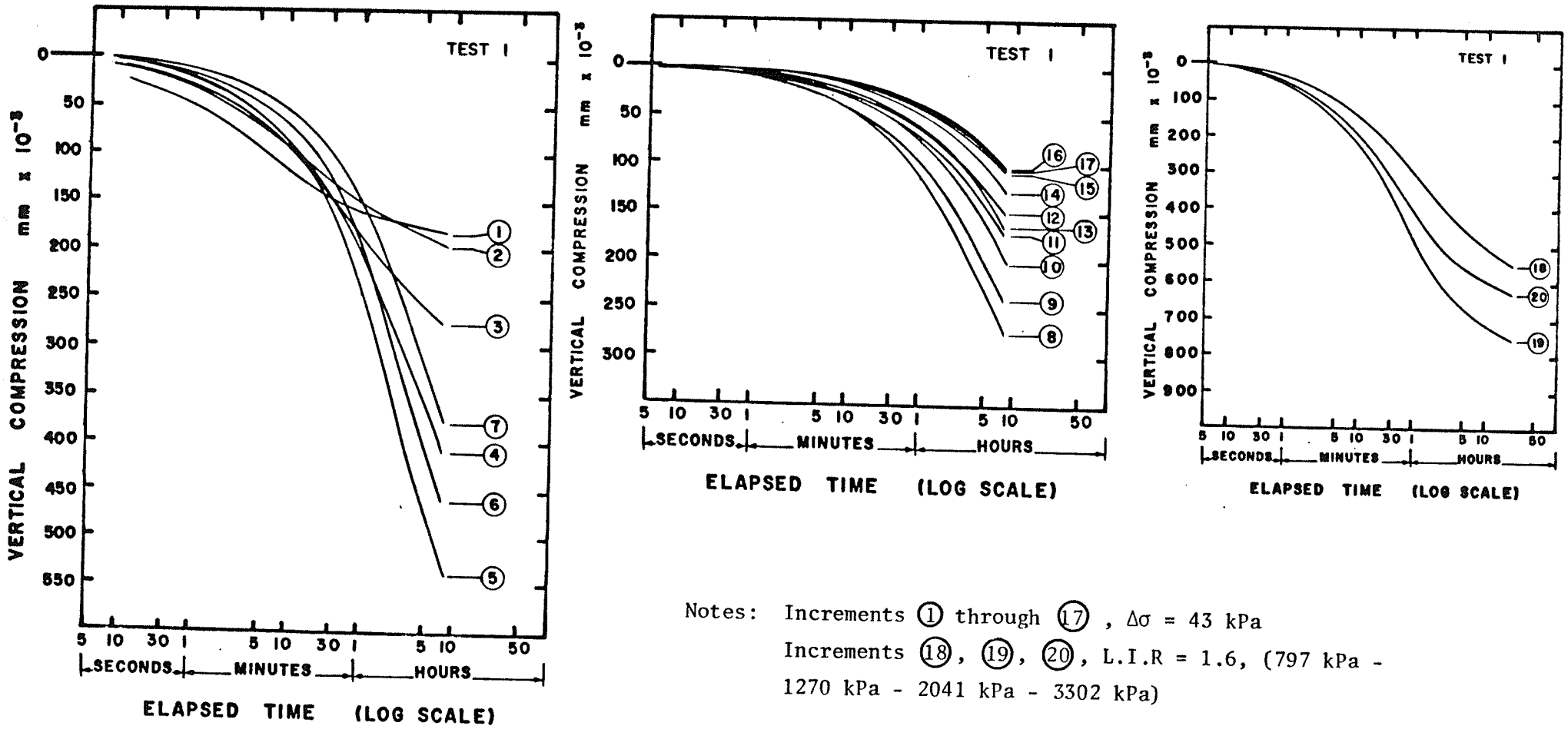

Notes: Increments ① through ⑰ , $\Delta\sigma$ = 43 kPa
Increments ⑱, ⑲, ⑳, L.I.R = 1.6, (797 kPa - 1270 kPa - 2041 kPa - 3302 kPa)

Figure 4.16 Oedometer Test I, 11.5 m Depth.
Consolidation versus Log. Time Curves in order of Loading.

24 hours, (Figures 4.13 and 4.14). A quasi-preconsolidation pressure then developed (Leonards and Altschaeffl, 1964; Bjerrum, 1967).

Consolidation versus logarithmic time curves for each increment are shown in Figure 4.16. Curves 1 through 16 are for an increment of 43 kPa and period ΔT of 8 hours. The transition to a type III curve occurs for the 4th increment, 195 to 238 kPa, L.I.R = 1.22, a span which includes the preconsolidation pressure. The sample was most compressible, however, under increment number 5. Increment 17 was sustained for 10 days, before increments 18, 19, 20 were applied using a L.I.R = 1.6, (see above). The return to a high load increment ratio resulted in development of type I curves.

4.2.5 Test T, 5.5 m Brown Clay

Constant Increment, $\Delta\sigma$ = 162 kPa, ΔT = 24 hours

The average initial void ratio of the brown clay from the 5.5 m depth lies in-between that of the blue clay strata at 9.0 m and 11.5 m. However the behaviour of the brown clay was quite different. The e versus σ'_c curve, (Figure 4.17), can for practical purposes be described as linear for stresses less than 1,000 kPa, (a_{vo} = 4.5 x 10^{-4} kPa^{-1}), with strain stiffening at higher stresses. There are some signs of a preconsolidation effect; a weak yield appears to occur at about 500 kPa, and the value of C_α rises to a maximum of 28 x 10^{-3} at about 1,000 kPa. There are also slight peaks in a_v at about 150 kPa and 800 kPa, the former being probably due to swelling (Section 4.2.3) and the latter being a preconsolidation effect. From the above evidence the apparent preconsolidation pressure is estimated to have been from 500-800 kPa, but as a practical parameter, P'_c has no significance.

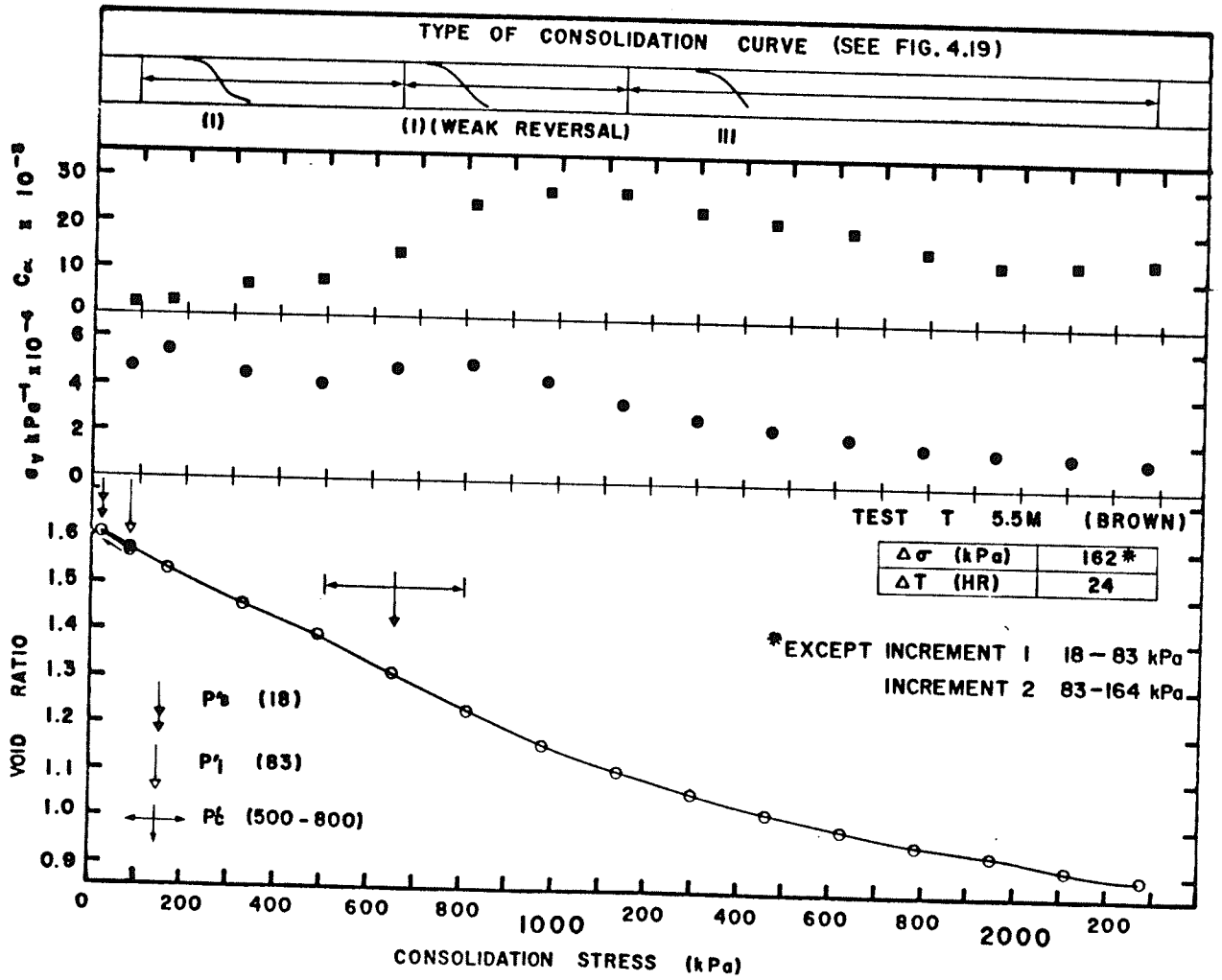

Figure 4.17 Oedometer Test T, 5.5 m Depth.
Void Ratio versus Consolidation Stress

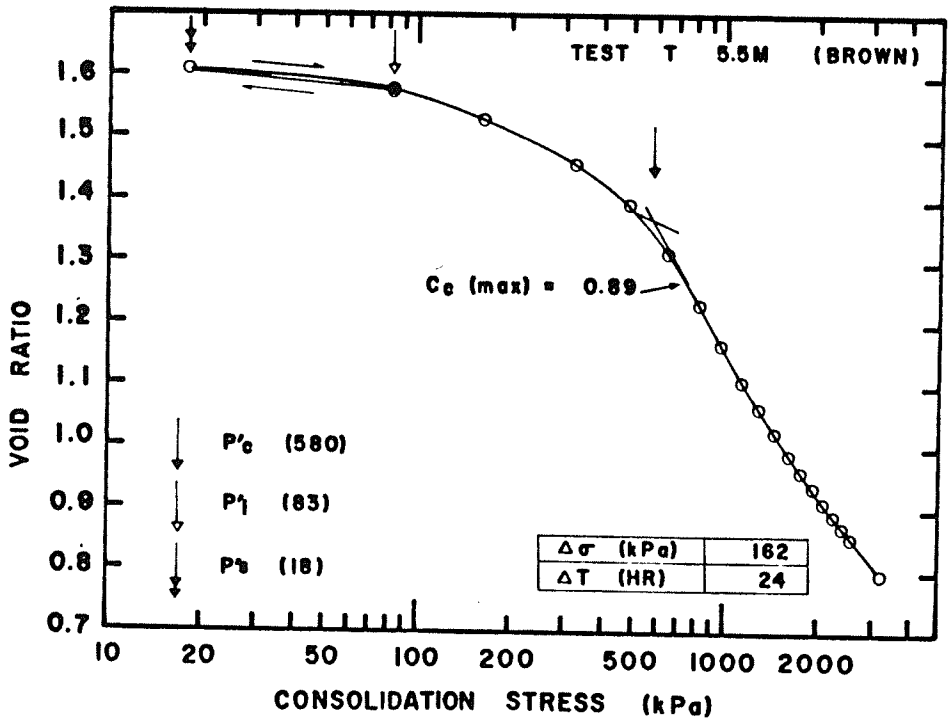

Figure 4.18 Oedometer Test T, 5.5 m Depth.
Void Ratio versus Log. Consolidation Stress

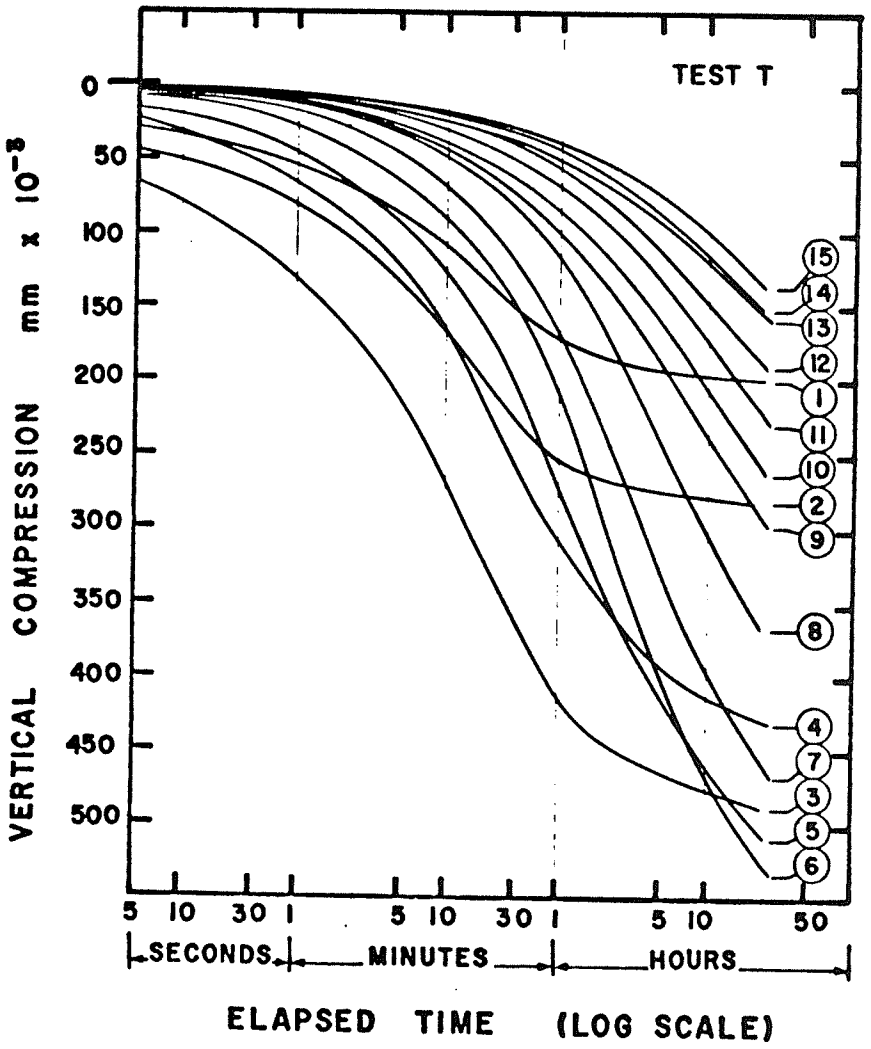

Figure 4.19 Oedometer Test T, 5.5 m Depth.
Consolidation versus Log. Time Curves
in order of Loading.

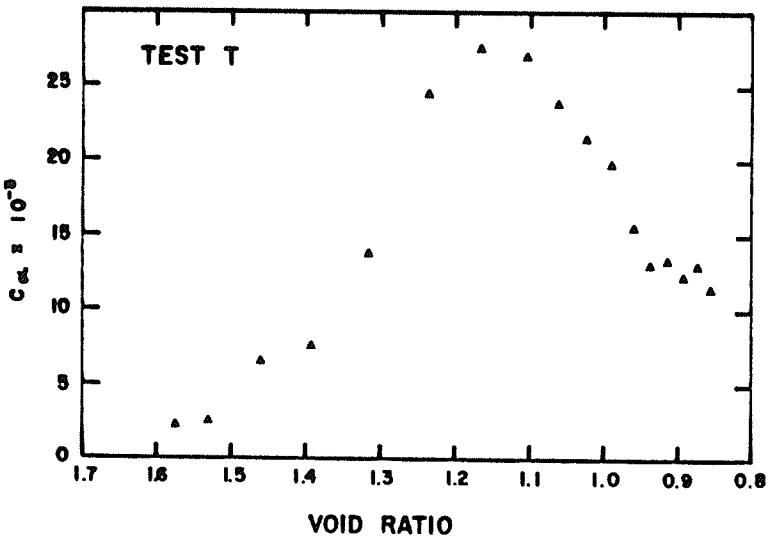

Figure 4.20 Oedometer Test T, 5.5 m Depth.
C_α versus C_c

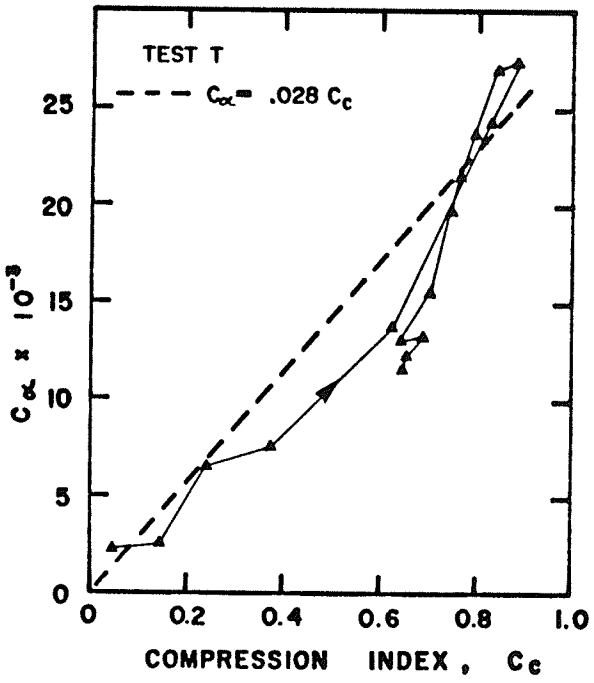

Figure 4.21 Oedometer Test T, 5.5 m Depth.
C_α versus Void Ratio

It can be seen that the traditional e versus log. σ'_c plot (Figure 4.18) is very misleading when used for Winnipeg brown clay. A value of P'_c can easily be defined by the Casagrande construction, and it is not apparent that P'_c is of no practical significance. Furthermore, the point of maximum curvature used as a starting point in the Casagrande Construction is dependent upon the relative vertical to horizontal scales used, and thus the value of P'_c is not unique. For further information the reader is directed to the technical note, "On curve fitting and laboratory data", (Graham, J., Pinkney, R.B., Lew, K.V., and Trainor, P.G.S., 1982) which is reproduced in Appendix A.

The consolidation versus log. time curves for Test T are shown in Figure 4.19. After initial consolidation to P'_i = 83 kPa, the oedometer sample was unloaded to P'_s = 18 kPa. The first two positive load increments were unequal, no. 1 ≡ 18 kPa back to 83 kPa, no. 2 ≡ 83 kPa to 164 kPa, but the remaining increments no. 3 to no. 15 were all 162 kPa. Curves 1 to 5 are distinctly type I, whereas curves 9 to 15 are distinctly type III. Curves 6, 7 and 8, (L.I.R = 1.20, 1.17 and 1.14), appear to be type I, but the reversal in curvature is very slight. Figures 4.20 and 4.21 show a $C_\alpha - C_c$ interelationship and a C_α versus void ratio curve similar to those found for the blue clay.

4.2.6 Summary of Oedometer Tests, Brown Clay 5.5 m

The results of constant increment oedometer test T were reviewed in the previous section. The e versus σ'_c curves for the remaining 5 tests on clay from 5.5 m are similar, (Figures 4.22 through 4.26), in that there is only the barest hint of a yield, which is of no practical significance. Table 4.2 allows numerical comparison of the curves. To

compensate for different initial void ratios, the values of e at 100 kPa, e(100), were used as an origin to calculate Δe at higher stresses. Example, $\Delta e(300) = e(100) - e(300)$.

As described in Section 4.1 and shown in Table 4.1, tests were grouped in control pairs, M and N; O and P; and S and T. The control pair M and N were trimmed from piston samples (BH4 July, 1980), and were tested using L.I.R = 1.6, ΔT = 24 hours. Sample M contained some stiff, crumbly, patches and had a low initial void ratio, e_o = 1.38. Despite this the compression Δe for each test was similar up to 1,000 kPa after which sample M was less compressible (Table 4.2). It is interesting to note that C_α did not reach a maximum value in either test, even at σ'_c = 1,600 kPa.

The remaining samples, O, P, S, T were trimmed from block samples (BH5, January, 1981). Control pair O and P were each loaded with the same increments, $\Delta\sigma$ = 48.5 kPa, but the loading periods, ΔT, were 8 and 24 hours respectively. The e versus σ'_c curves (Figures 4.24 and 4.25), are so similar that it is not possible to identify any trend caused by the change in the rate of loading. Some scatter in the C_α and a_v values is probably due to fluctuations in the amount of side friction. Control pair S and T (Figures 4.26 and 4.17), were loaded with larger increments, $\Delta\sigma$ = 162 kPa, and ΔT = 24 hours. Although Test T was unloaded from P'_i = 83 kPa to P'_s = 18 kPa and allowed to swell, the e versus σ'_c curves for the two tests were very similar.

The shape of all curves at 5.5 m was very similar, and the coordinates of an average e versus σ'_c curve were calculated from the average values of e(100 kPa), and Δe(300 kPa), Δe(500 kPa) etc. (Table 4.2).

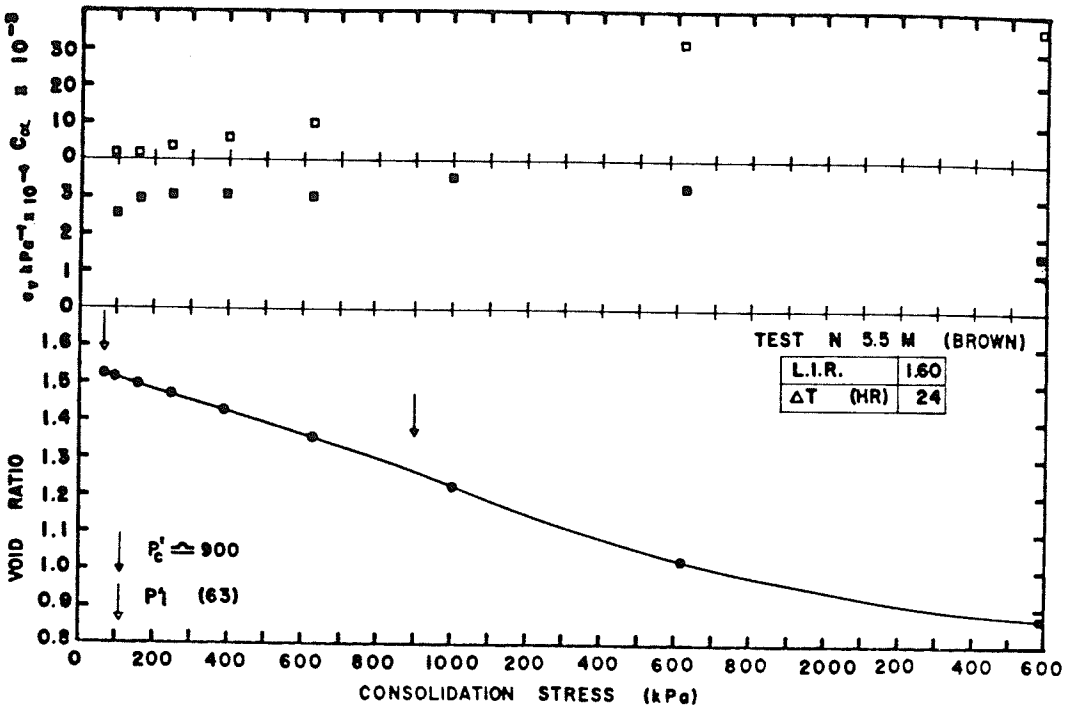

Figure 4.22 Oedometer Test M, 5.5 m Depth
Void Ratio versus Consolidation Stress

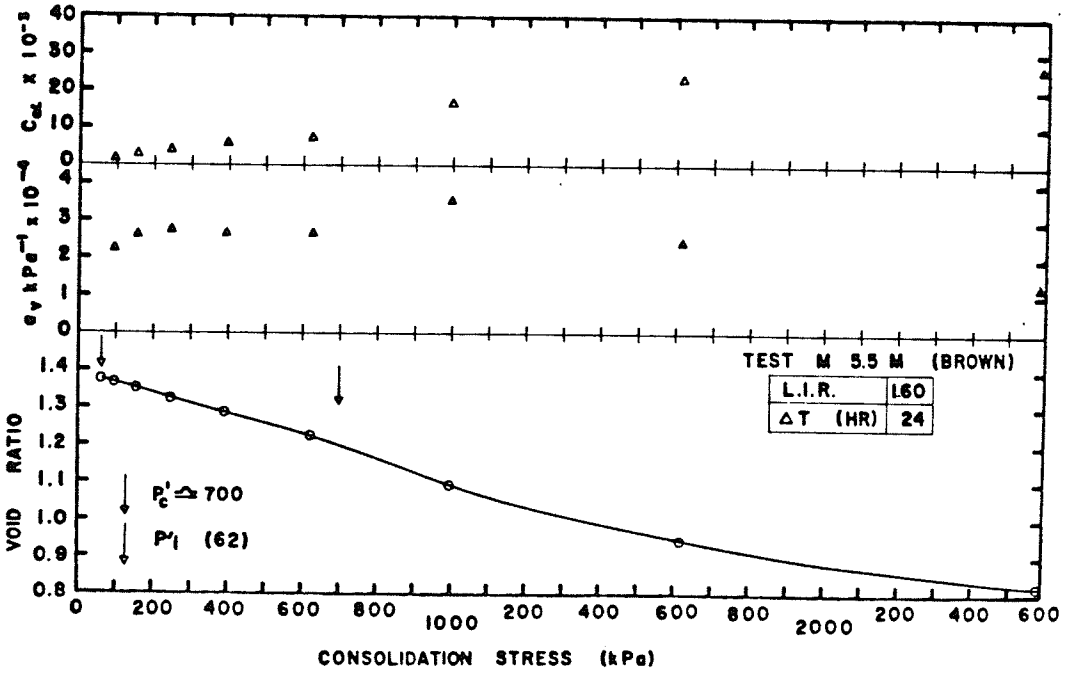

Figure 4.23 Oedometer Test N, 5.5 m Depth
Void Ratio versus Consolidation Stress

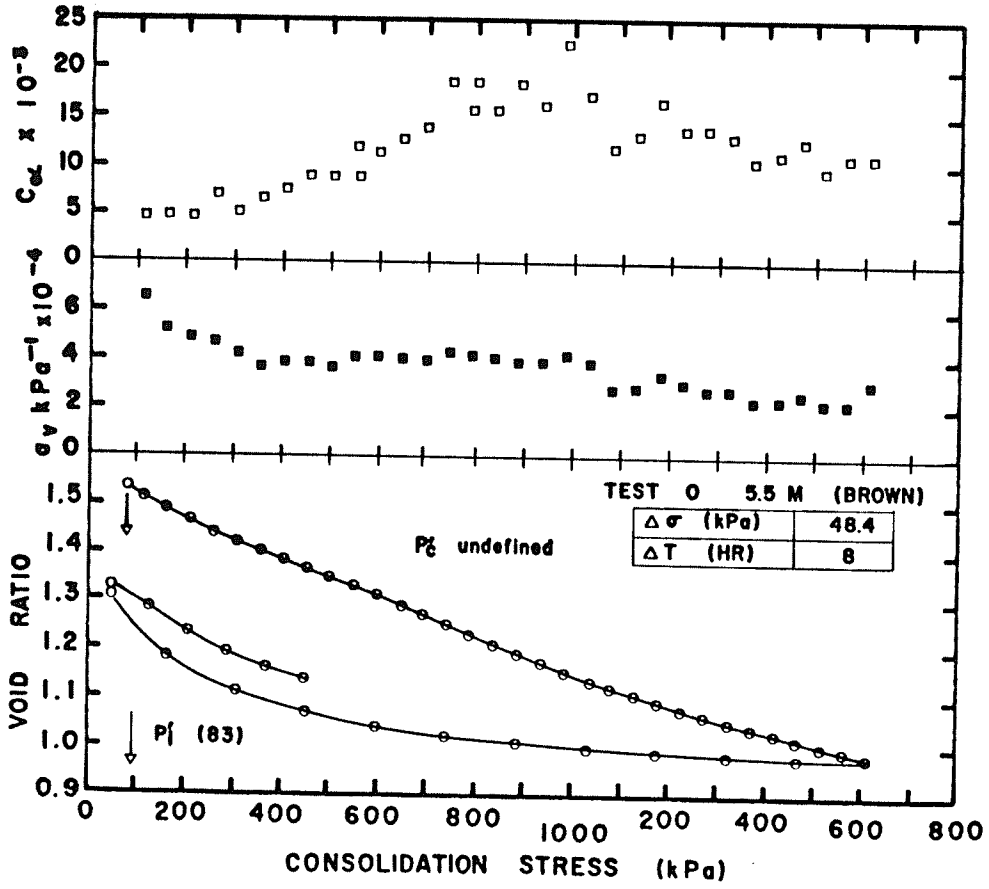

Figure 4.24 Oedometer Test O, 5.5 m Depth
Void Ratio versus Consolidation Stress

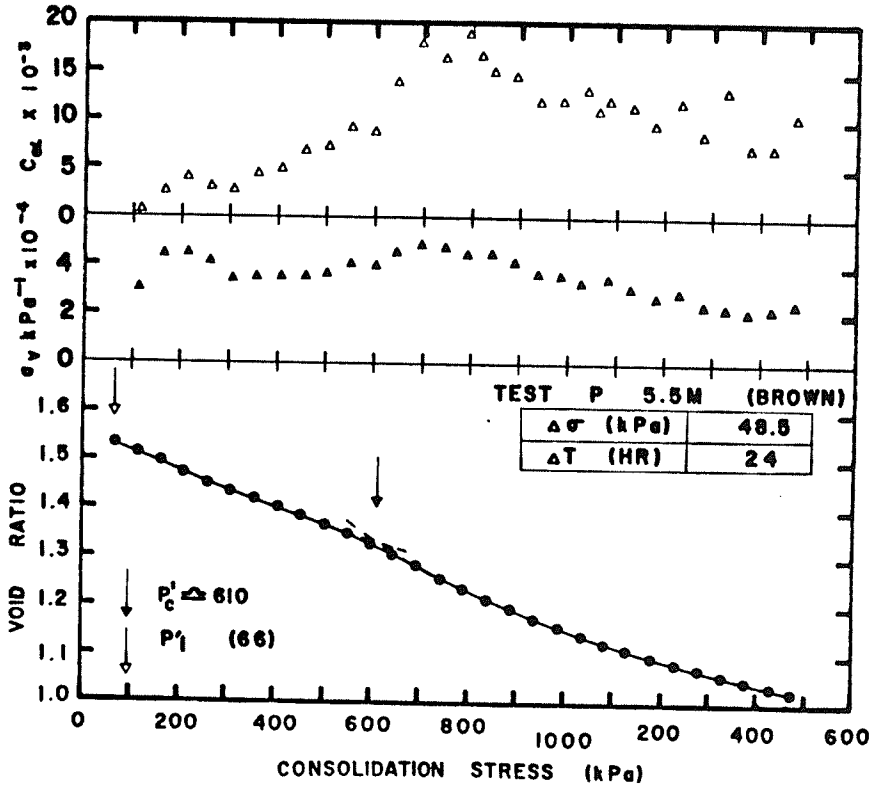

Figure 4.25 Oedometer Test P, 5.5 m Depth
Void Ratio versus Consolidation Stress

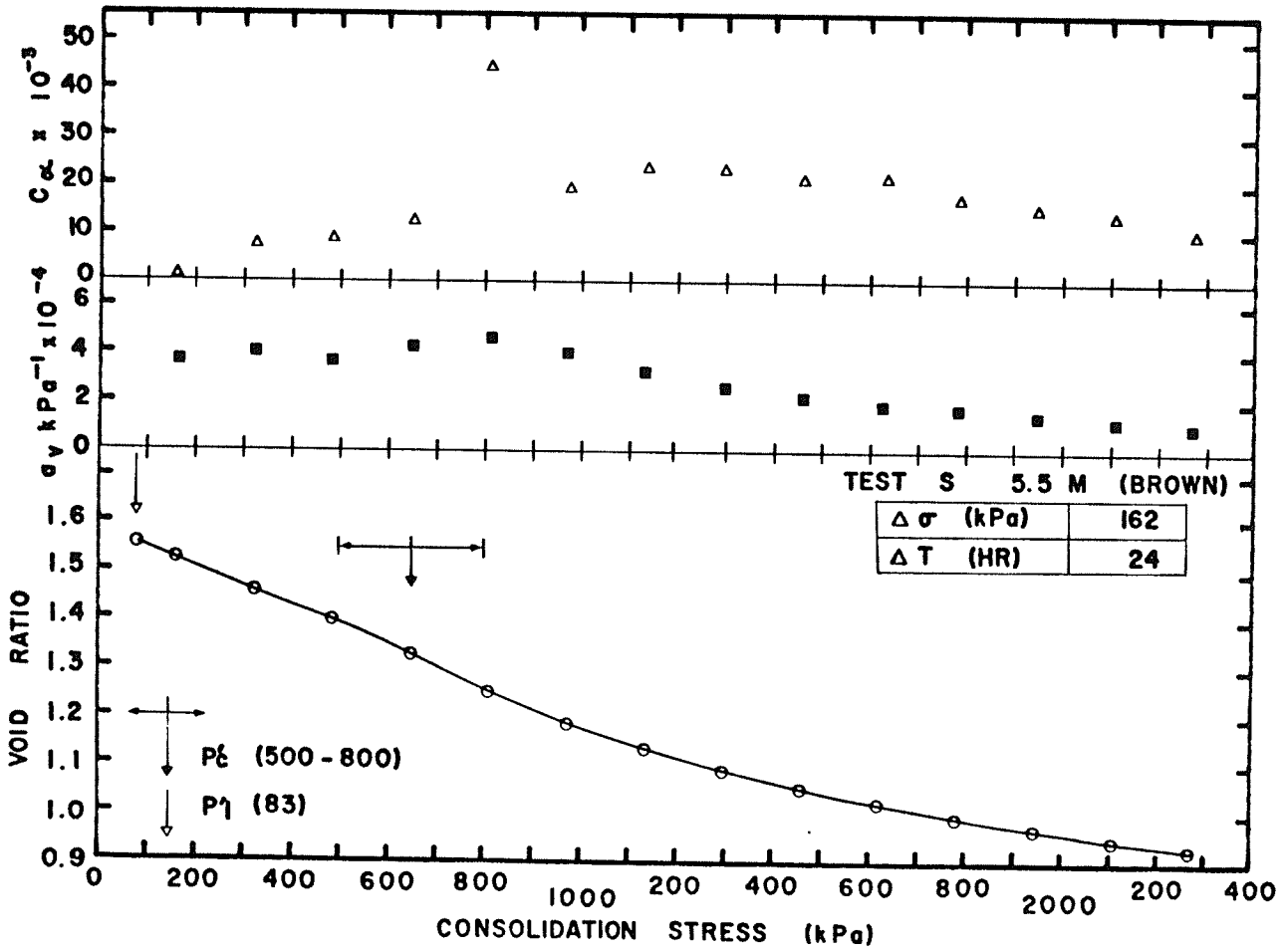

Figure 4.26 Oedometer Test S, 5.5 m Depth
Void Ratio versus Consolidation Stress

VOID RATIO	TEST M	TEST N	TEST O	TEST P	TEST S	TEST T	AVERAGE $\bar{X}$	SED. DEV. S
e at 100 kPa	1.368	1.516	1.523	1.520	1.546	1.567	1.507	0.071
Δe(300 kPa)	0.055	0.061	0.098	0.081	0.080	0.095	0.078	0.017
Δe(600 kPa)	0.136	0.151	0.213	0.193	0.198	0.226	0.186	0.035
Δe(900 kPa)	0.240	0.253	0.334	0.329	0.332	0.368	0.309	0.051
Δe(1200 kPa)	0.323	0.353	0.436	0.428	0.431	0.475	0.408	0.057
Δe(1500 kPa)	0.396	0.451	0.514	*	0.501	0.550	0.486	0.054
Δe(1800 kPa)	0.447	0.518	*	*	0.555	0.607	0.540	0.053
Δe(2100 kPa)	0.484	0.565	*	*	0.598	0.651	0.582	0.056

*For purposes of Averaging assume similar to Test S

Note: The average value of a_{vo} from 100 kPa to 600 kPa = 3.7×10^{-4} kPa^{-1}

Table 4.2 Numerical Characteristics of e versus σ'_c Curves from Oedometer Tests on Winnipeg Brown Clay.

4.2.7 Summary of Oedometer Tests, Blue Clay, 9.0 m

Oedometer tests C and U were reviewed in Sections 4.2.1 and 4.2.2. The e versus σ'_c curves for all ten tests, including the above are presented in sets according to the initial void ratio (Figure 4.27). Control groups consisted of samples C and D; E, F and G; and J, K and L. Samples Q and U were tested individually. Samples for the first control group, C and D, were trimmed from a block sample and tested in an identical fashion, L.I.R = 1.6, ΔT = 24 hours, and the results were almost identical (Figure 4.27(b)). Group E, F and G, also cut from a block sample were tested as above, but with a variation in ΔT; E and F - 12 hours, G - 48 hours. The latter sample was slightly more compressible after the preconsolidation pressure, (Figure 4.27(c)). Control group J, K and L were trimmed from piston samples and the P'_c values for each test were marginally lower. There is little difference between Test J (L.I.R = 1.6, ΔT = 24 hours) and Test L ($\Delta\sigma$ = 43 kPa, ΔT = 8 hours) (Figure 4.27(a)). Test K is shown in Figure 4.27(b) since the sample had a slightly lower initial void ratio, e_o, but in terms of the shape, (Δe versus σ'_c), K is similar to L and J. Tests Q and U used clay from bore hole 5 (January, 1981), whereas all other samples at 9.0 m came from bore hole 4 (July, 1980). The decreased compressibility of Tests Q and U after yield (Figure 4.27(a)) is probably due to soil variation rather than test procedure.

Overall the shapes of the e versus σ'_c curves were remarkably similar except for a slight variation in P'_c. Because of this variation a simple averaging of coordinates would smooth out the yield, and so the coordinates of the average curve were calculated as shown in Figure 4.28 In effect the average coordinates of points 1 to 4 were calculated by

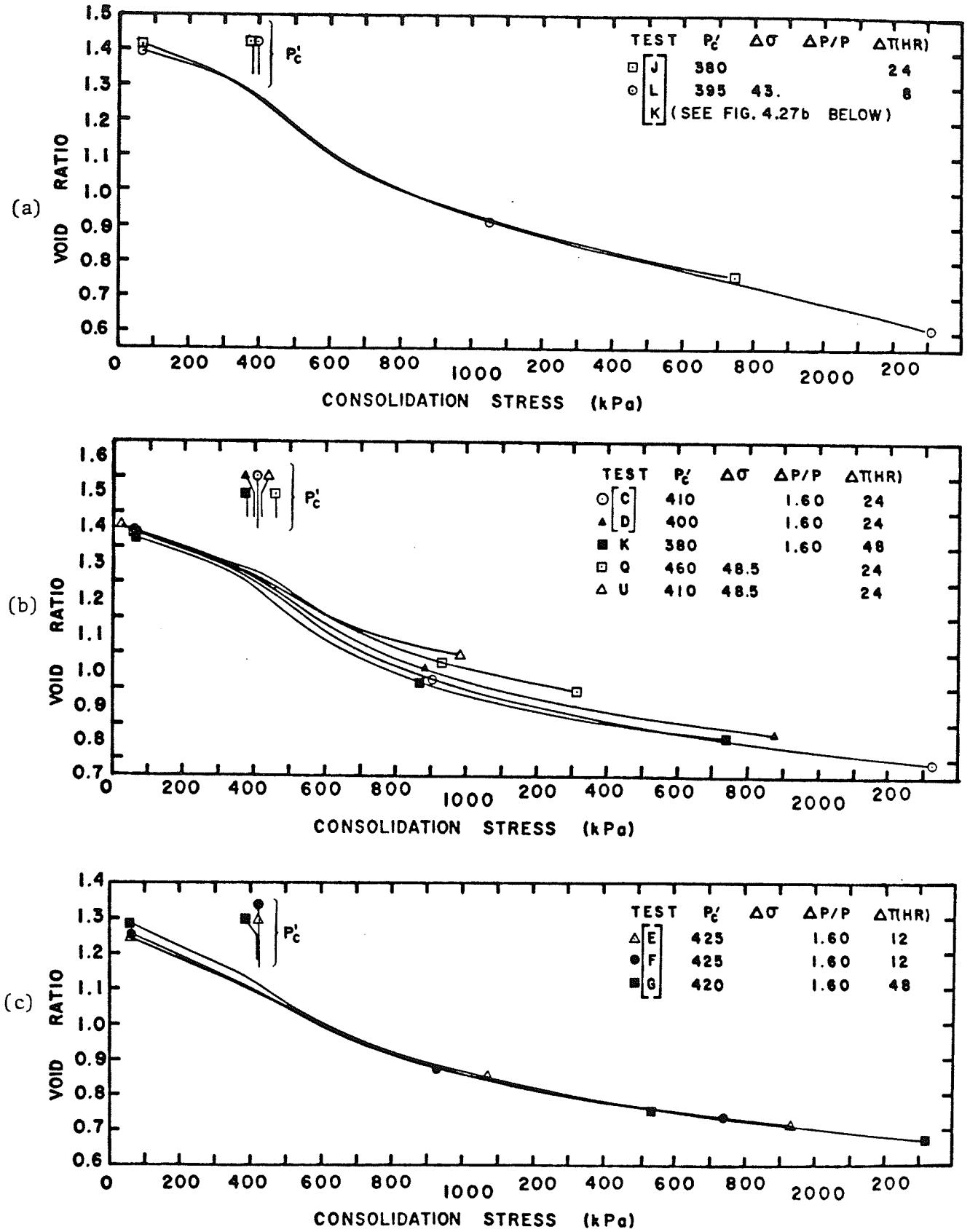

Figure 4.27 Winnipeg Blue Clay, 9.0 m Depth. Comparison of e versus σ'_c Curves for Ten Oedometer Tests.

(a) $e_o \simeq 1.4$ (b) $e_o \simeq 1.35$ (c) $e_o \simeq 1.3$

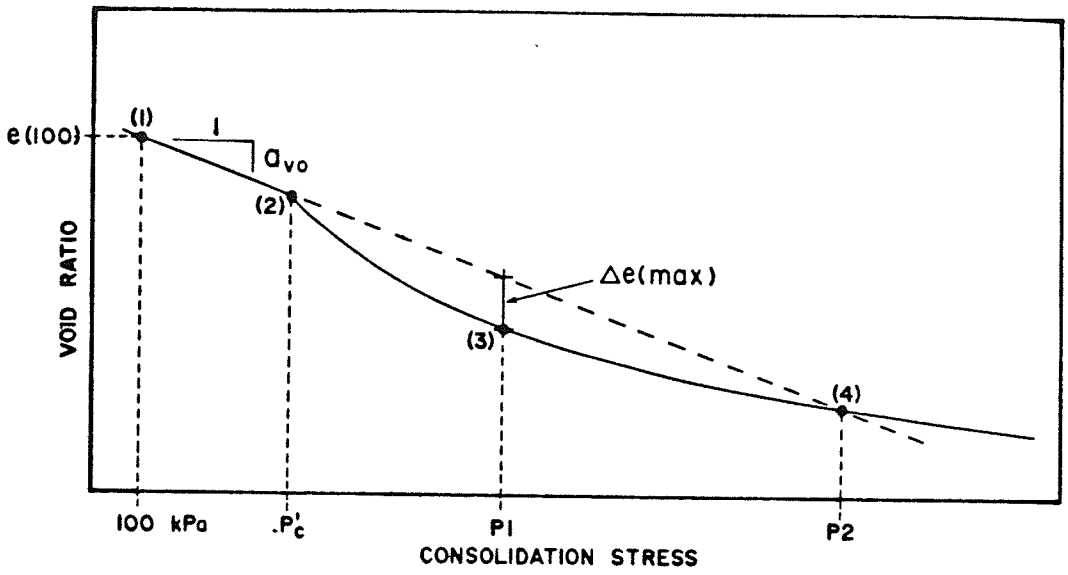

Figure 4.28 Method of Averaging e versus σ'_c Curves from Oedometer Tests on the Blue Clay at 9.0 m and 11.5 m.

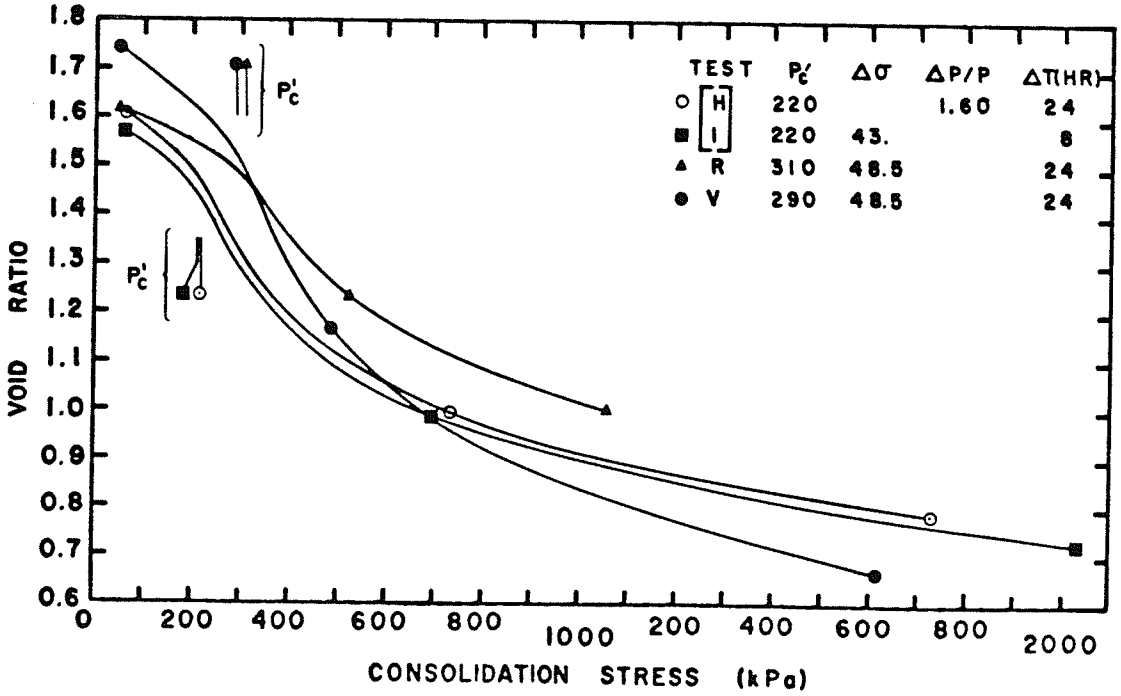

Figure 4.29 Winnipeg Blue Clay, 11.5 m Depth. Comparison of e versus σ'_c Curves from Four Oedometer Tests.

general averaging of:

(a) The void ratio at 100 kPa, e(100).

(b) The recompression slope, a_{vo}.

(c) The preconsolidation pressure, P'_c.

(d) The maximum amount of yield, Δe max, and the corresponding pressure, P1.

(e) The pressure P2, at which the virgin curve intersects the extended linear section (Dashed line).

The values of the above parameters and averages are shown in Table 4.3.

4.2.8 Summary of Oedometer Tests, Blue Clay, 11.5 m

The results of oedometer test I were presented in detail in Section 4.2.3. The e versus σ'_c curves for all four tests on clay from 11.5 m are shown in Figure 4.29, and the numerical characteristics of each are recorded in Table 4.3. As compared with the blue clay at 9.0 m depth, all samples showed increased initial compressibility, a_{vo}, a marked decrease in P'_c, and a more dramatic yield. There was however a definite difference in the preconsolidation pressures of samples from borehole 4 and bore hole 5. Samples H and I, a control pair from borehole 4, showed preconsolidation pressures of 220 and 215 kPa, and there is very little difference in the two e versus σ'_c curves, despite the difference in loading procedures. Tests R and V from bore hole 5 showed preconsolidation pressures of 310 and 290 kPa. The value of a_{vo} for Test R is only slightly higher than that of the blue clay samples from the 9.0 m depth. Test V was taken from a very moist layer in the bottom 200 mm of a block sample, and which had a very high initial void ratio. It was

Table 4.3(a) 9.0 m Depth

Test No	e @ 100 kPa	a_{vo} kPa x 10^{-4}	P'_c kPa	Δe^* (max)	P_1^* kPa	P_2^* kPa
C	1.335	3.72	410	0.115	850	1600
D	1.330	3.40	400	0.110	950	1700
E	1.235	4.26	425	0.033	650	950
F	1.227	4.15	425	0.025	650	950
G	1.262	4.35	420	0.048	730	1080
J	1.400	3.52	380	0.165	1000	2100
K	1.313	3.20	380	0.150	950	1900
L	1.382	3.22	395	0.170	1000	2400
Q	1.325	3.03	460	0.105	900	1700
U	1.325	3.50	410	0.060	750	1200
AVERAGE, $\bar{X}$	1.313	3.64	411	0.098	843	1558
STD. DEV., S	0.057	0.47	24	0.054	138	500

Table 4.3(b) 11.5 m Depth

H	1.582	7.53	220	0.165	450	980
I	1.546	6.70	215	0.190	500	1100
R	1.593	4.65	310	0.185	700	1600
V	1.703	8.05	290	0.240	600	1300
AVERAGE $\bar{X}$	1.606	6.73	259	0.195	562	1245
STD. DEV., S	0.068	1.50	48	0.032	111	271

*See Figure 4.28 for Definition.

Table 4.3 Numerical Characteristics of e versus σ'_c Curves from Oedometer Tests on Winnipeg Blue Clay.

anticipated that p'_c for this sample would be very low, however, although the initial compressibility was very high ($a_{vo} = 8 \times 10^{-4}$ kPa^{-1}), the value of p'_c was 290 kPa.

4.2.9 Values of the Coefficient of Secondary Compression, C_α versus Void Ratio Curves

The C_α versus e curves for the 5.5 m, 9.0 m and 11.5 m depths are shown in Figures 4.30, 4.31, 4.32, respectively. The most noticable feature is the large amount of scatter in peak values, and in post-peak behaviour. Peak Values of C were 20-30 x 10^{-3} for the 5.5 m depth 20-30 x 10^{-3} for the 9.0 m depth and 40-60 x 10^{-3} for the 11.5 m depth. As discussed earlier, for an individual test, C_α can be expressed as a linear function of C_c (Mesri, 1977). In this study, however, C_α/C_c varied from 0.023 to 0.045 between tests so that C_α cannot be accurately predicted from an e versus $\log\sigma'_c$ curve.

It is very difficult to determine whether the large variation in values of C_α is due to material variation, the direct affect of loading procedure on the compression process, or an indirect effect such as side friction. The experimental evidence presented here however does not support the contention that C_α is dependent on void ratio and independent of $\Delta\sigma$ or L.I.R. (Wahls, 1962). The latter contention leads to the expectation that for a group of samples exhibiting a narrow range of p'_c values at each depth, the peak C_α values should be close at each depth. Further, the post-peak behaviour should be defined by an unique "Virgin - Secondary compression - Void ratio curve", and this is clearly not shown.

The values of C_α in the vicinity of p'_c are fairly high,

suggesting that in cases where final stresses might exceed the preconsolidation pressure, the use of Terzaghi theory may lead to a significant underestimate of "final" settlement. There is, however, a wide scatter in experimental values of C_α, and an appropriate theory to explain the direct significance of high laboratory values of C_α on the consolidation of a thick layer is lacking. Suggested upper and lower bound settlement estimates for known values of C_α are given in Chapter 3.

Given the high values of C_α and the low value of p'_c at the 11.5 m depth, it is possible that the clay at this depth has never been subjected to a higher stress than p'_o. The difference between p'_c and p'_o would then be a quasi-preconsolidation effect (see Figure 4.13). This would mean that at a constant stress of p'_o, the void ratio has been reduced from $e_{n/c}$ to the present value, e_o, by secondary compression.

$$\therefore \quad C_\alpha \cdot \Delta \log t = e_{n/c} - e_o \text{ (at } p'_o)$$

$$\text{and} \quad e_{n/c} - e_o = C_c \log(p'_c/p'_o) - a_{vo}(p'_c - p'_o)$$

so that the number of log. cycles of secondary compression required to reach p'_c is given by:

$$\Delta \log t = \frac{C_c \log(p'_c/p'_o) - a_{vo}(p'_c - p'_o)}{C_\alpha}$$

Assuming for the 11.5 m depth;

$C_c = 1.1$

$p'_c = 220$ kPa

$p'_o = 115$ kPa

$a_{vo} = 6 \times 10^{-4}$ kPa^{-1}

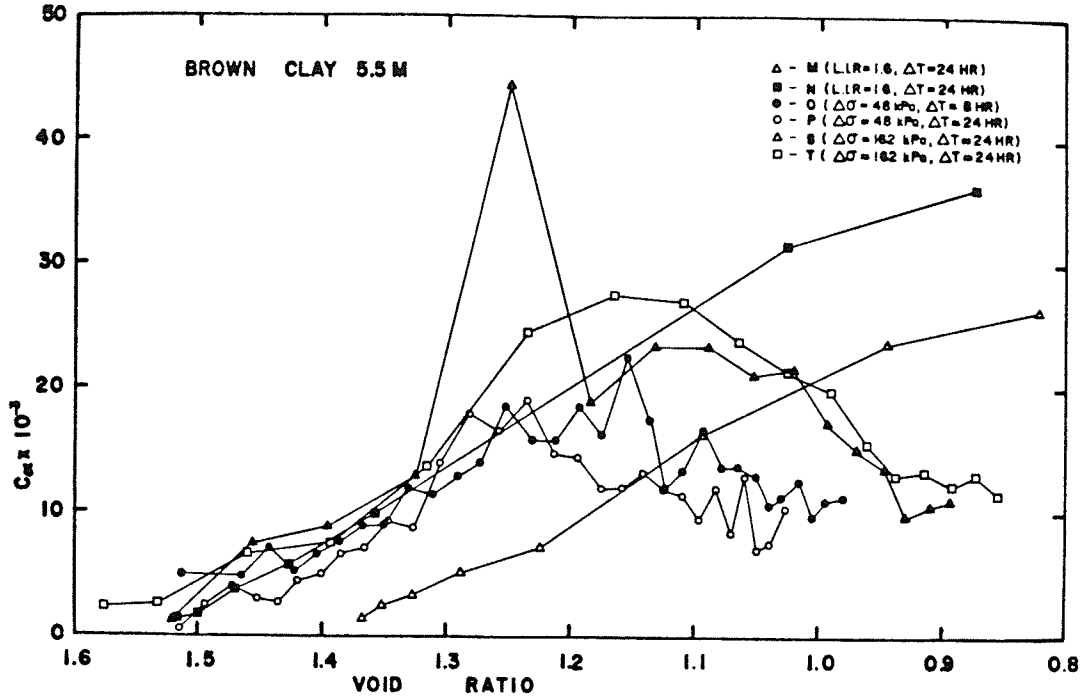

Figure 4.30 Summary of C_{α} versus Void Ratio Curves from Oedometer Tests at 5.5 m.

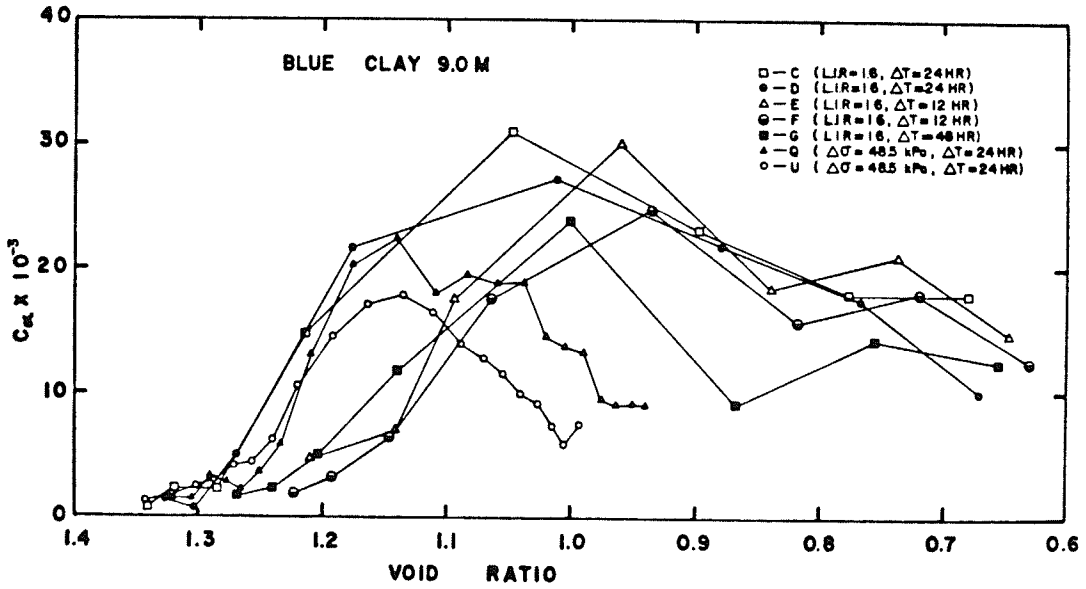

Figure 4.31 Summary of C_{α} versus Void Ratio Curves from Oedometer Tests at 9.0 m.

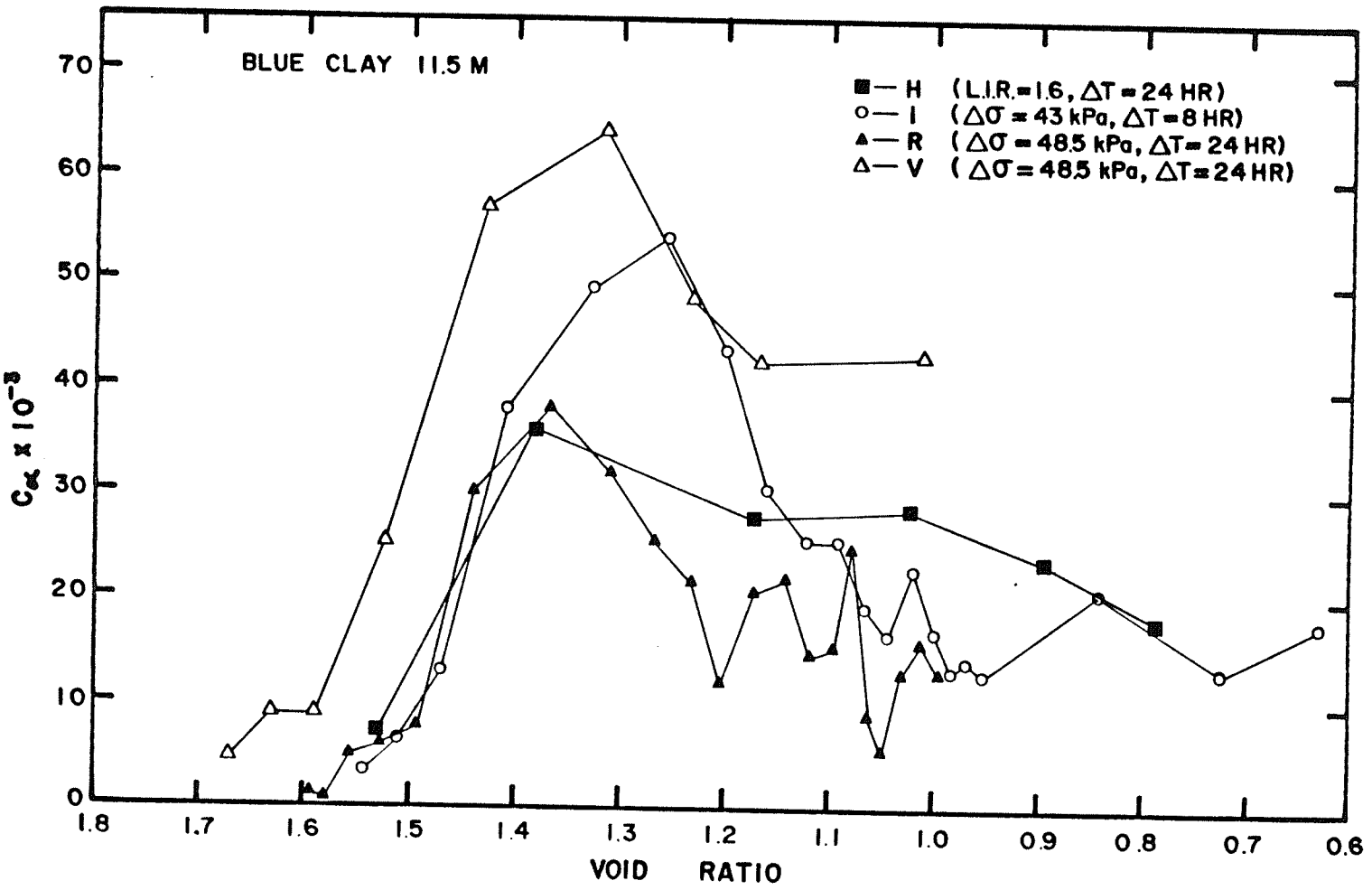

Figure 4.32 Summary of C_α versus Voids Ratio Curves from Oedometer Tests at 11.5 m

$$C_\alpha = 50 \times 10^{-3}$$

then $\Delta \log t = 4.9$ cycles

Thus for a thin laboratory sample loaded to 115 kPa in virgin compression, with secondary compression occuring after say 10 hours, then p'_c would advance to 220 kPa after 91 years. It is difficult to estimate the equivalent time for a thick layer in which substantial excess pore-pressures were probably never developed. The above calculation does show, however, that at 11.5 m depth the overconsolidation may be mostly due to quasi-preconsolidation effects.

4.2.10 General Discussion and Summary

The main reason for the use of the small constant increment loading method, was to provide equally spaced data points on the e versus σ'_c curves and thus give better definition of the recompression, yield, and virgin compression behaviour. As the time period, ΔT, was also varied this allowed a limited study of the effects of loading rate on compressibility and preconsolidation pressure. However, by means of testing control groups of oedometer samples taken from adjacent soil, it was possible to show that the slight variations in p'_c and compressibility were mainly due to variations within the strata. From this limited study it would appear that Winnipeg clay is not particularly strain-rate sensitive. Further research, however, is needed on this topic, and the author suggests that a series of strain-controlled oedometer tests with pore-pressure measurement would give definitive results.

Prior to the present research there had been some uncertainty regarding the rounded recompression curve on e versus log σ'_c curves

from oedometer tests on Winnipeg clay. The results presented in this chapter, however, show that the recompression behaviour as measured in oedometer tests represents undisturbed behaviour and can thus be applied to field settlement calculations. It was shown that in an e versus σ'_c plot, recompression behaviour is essentially linear, and the scatter in p'_c values and a_{vo} values from different tests was very low (Table 4.3). The well rounded recompression curve on an e versus log σ'_c plot is merely a result of the fact that a_{vo} for Winnipeg clays is very high. Had sample disturbance been a problem, there would have been a wide fluctuation in a_{vo} values and the yield would have been reduced or become non-existent. Also C_α values for the initial increments would have been high.

Figure 4.33 shows a comparison between the e versus σ'_c and e versus log σ'_c curves for:

(a) A sensitive, cemented, Leda clay from eastern Canada, (results taken from Crawford, 1965, Figure 1).

(b) Winnipeg blue clay, 9.0 m depth, (Test C).

Both clays show linear recompression behaviour (Figure 4.33(b)), but the value of a_{vo} for Winnipeg clay is approximately 8 times greater. Because a_{vo} for Leda clay is very small the recompression behaviour in a logarithmic plot (Figure 4.33(a)) is also approximately linear. Although the overall compressibilities, (values of Δe), from 100 to 800 kPa are approximately equal, the yield in the Leda clay is much sharper. Both clays exhibit high rates of secondary compression beyond p'_c, but whereas the Leda clay is very strain rate sensitive for increments in the vicinity of the preconsolidation pressure, it appears that the Winnipeg clay is not.

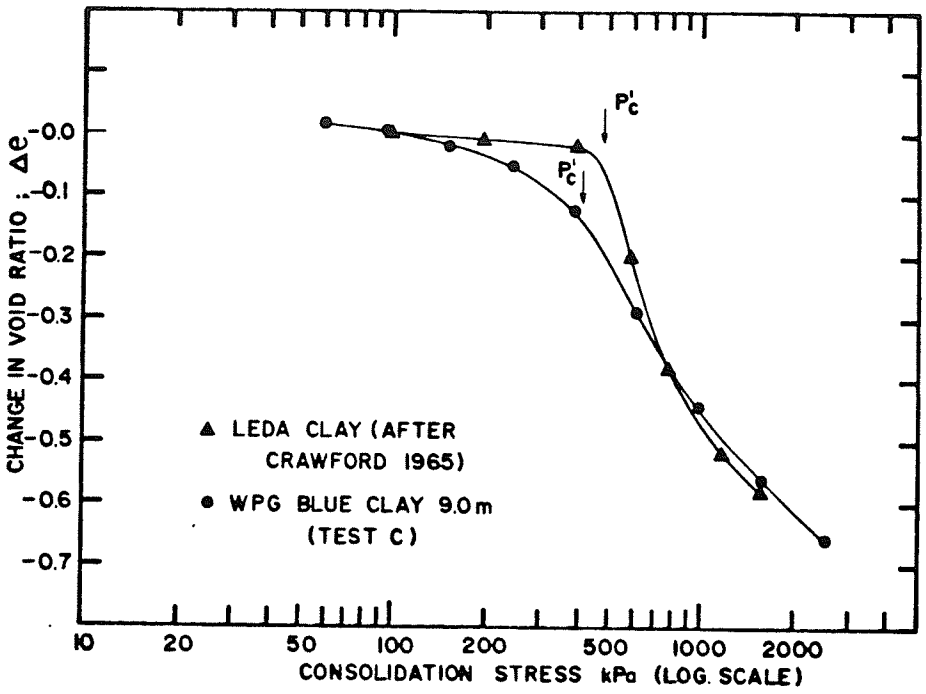

(a)

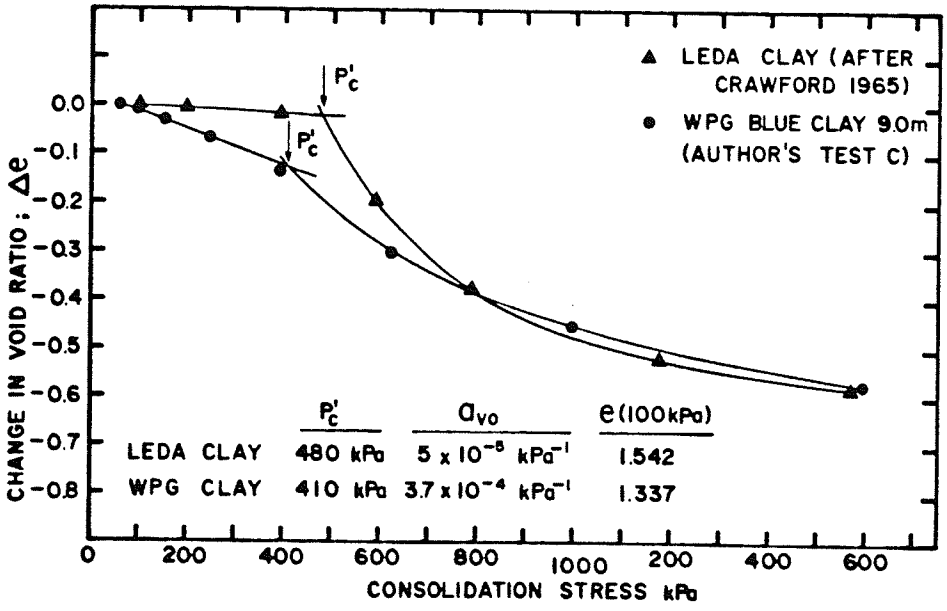

(b)

Figure 4.33 Comparison of Compressibility in Oedometer Tests between Leda Clay (After Crawford (1965), Figure 1) and Winnipeg Blue Clay from 9.0 m (Test C).

(a) e versus log σ'_c (b) e versus σ'_c

A good comparison of the differences in compression behaviour for the three depths of Winnipeg clay under study, 5.5 m, 9.0 and 11.5 m, is shown by the average e versus σ'_c curves (Figure 4.34). The methods of averaging were discussed in Section 4.26 and 4.27. The virgin compression curves for the blue clay, (at 9.0 m and 11.5 m), are almost identical, except for different preconsolidation pressures. Both average curves show the characteristic yielding. The brown clay at 5.5 m, however, shows almost no yield, and the preconsolidation pressure is of virtually no practical significance. The curve for the brown clay can be normalized, however, by a vertical shift, Δe, to the position by the dashed line. It can then be seen that the lack of a significant yield is probably a result of a higher preconsolidation pressure. Because of the relative slopes of the recompression curve and the virgin compression branch for Winnipeg clay it is apparent that the yield would be expected to become almost unnoticeable for stresses above about 600 kPa. The reason for the shift, Δe, between the virgin compression curves of the brown and blue clay can easily be explained by an increase in plasticity at the 5.5 m depth, (Chapter 2).

For the Winnipeg site tested, there is continuous decrease in p'_c with depth in the Lake Agassiz I deposits. A possible explanation is that this has been caused by the combination of a desiccation front, acting from the surface, and upward seepage from the underlying till and limestone aquifer.

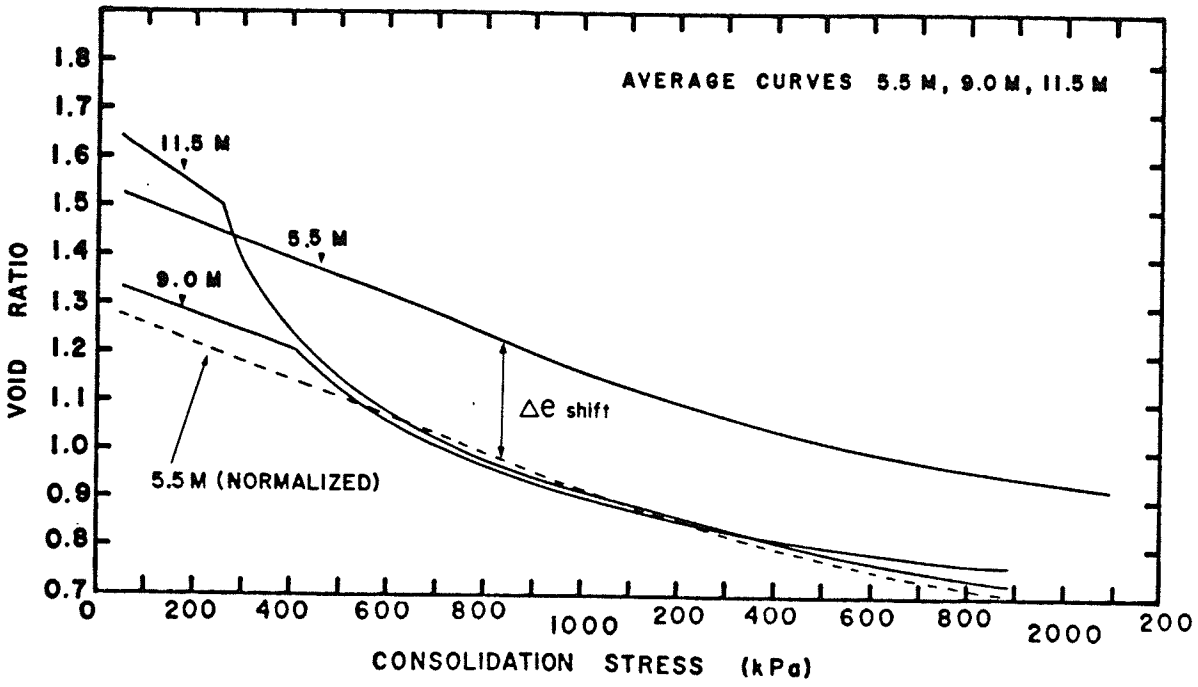

Figure 4.34 Variation in the Compressibility of Winnipeg Clay with Depth. Average e versus σ'_c Curves at Depths of 5.5 m, 9.0 m and 11.5 m.

CHAPTER 5

CONSOLIDATED-UNDRAINED (CIŪ) TRIAXIAL TESTING PROGRAM

5.1 INTRODUCTION

Triaxial tests on small diameter samples (35 mm) were used to investigate the peak effective stress strength envelope of Winnipeg clay from depths of 5.5 m, 9.0 m, and 11.5 m.

Previous testing by Pietrzak (1979), using Winnipeg blue clay from depths of 6.3 m and 9.6 m, had indicated two almost identical tri-linear failure envelopes. It was subsequently suggested, (Baracos et. al., 1980), that a single tri-linear envelope is operative for the entire depth of blue clay at the University of Manitoba campus as follows:

(a) A steep low stress branch, $\phi' \simeq 32^{o}$, $c' \simeq 6$ kPa

(b) A flat overconsolidated branch, $\phi' \simeq 13^{o}$, $c' \simeq 33$ kPa

(c) A normally consolidated branch, $\phi' \simeq 22.5^{o}$, $c' \simeq 3$ kPa

The aims of the present study were to substantiate Pietrzak's results by tests on the blue clay from the 9.0 m and 11.5 m depths, and extend the study to the brown clay at 5.5 m depth. The influence of normal stress on the mode of failure was also of interest in view of the three apparent stages of the strength envelope.

5.2 OUTLINE OF TESTING PROGRAM, AND TRIMMING PROCEDURES

A total of 63 undisturbed samples were carefully prepared, consolidated in a triaxial cell, and then sheared in undrained axial compression at a constant rate of strain. Table 5.1(a) and 5.1(b) show

a breakdown of tests by depth, and show the wide range of consolidation pressures used. A pilot study of 9 tests, (series AA), was conducted using a block of blue clay sampled in october 1977 from a depth of 8.0 m (Block #4, Bore Hole #3*). Subsequent testing used freshly sampled clay from B.H. 4 (July, 1980), and B.H. 5 (January, 1981). Fifteen tests were performed using blue clay from 9.0 m (series A), 18 tests using blue clay from 11.5 m (series B), and 21 tests using brown clay from 5.5 m (series C). All samples were trimmed with zero angle of inclination between the major axis, and the original vertical direction in the field. Sections of the clay blocks were cut to the required diameter using a wire saw and a manually-rotated lathe. Two types of lathe were available:

- Type A, in which the sample was rotated relative to a fixed cutting guide.
- Type B, in which the sample was held fixed and the cutting guide rotated.

A commercially-made type A lathe was used with success on many of the blue clay samples, which contained no noticable fissures. However, the slight, but unavoidable torsional stresses induced by rotating the sample, tended to open up fissures or cause cracks in the brown clay. This problem was overcome by use of a type B lathe designed by Dr. J. Graham, and constructed in the civil engineering workshop.

All but two of the triaxial samples were trimmed to a diameter of 35.5 mm, and a height/diameter ratio, h/d, of 2:1. At high consoli-

---

*Part of the same block was used by Noonan (1980), to investigate yield envelopes in the Winnipeg clay.

Series AA

Blue Clay, 8.2 m (BH3)

Test	σ'_c kPa	e_o
AA1	33.3	1.43
AA2	51.4	1.32
AA3	149	1.60
AA4	188	1.49
AA5	311	1.50
AA6	486	1.52
AA7	571	N. Avail.
AA8	587	1.48
AA9	695	1.45

Series AA

Blue Clay, 9.0 m (BH4)

Test	σ'_c kPa	e_o
A1	6.6	1.34
A2	12.2	1.21
A3	21.7	1.47
A4	38.2	N. Avail.
A5	80.1	1.33
A6	114	1.37
A7	151	1.39
A8	144	1.43
A9	201	1.35
A10	213	1.38
A11	268	1.37
A12	296	1.33
A13	328	1.34
A14	383	N. Avail.
A15*	246, 172	1.42

*σ'_1 = 246 kPa, σ'_3 = 172 kPa

Table 5.1(a) Program of Triaxial Tests on Winnipeg Clay at Depths of 8.2 m and 9.0 m

Series B

Blue Clay, 11.5 m (BH5)

Test	σ'_c kPa	e_o
B1	5.1	1.66
B2	14.2	N. Avail.
B3*	27.0	N. Avail.
B4	35.0	1.57
B5	46.6	1.52
B6*	65.6	1.62
B7*	86.4	N. Avail.
B8	109	1.52
B9	130	1.76
B10*	139	N. Avail.
B11	151	1.74
B12	165	1.63
B13	166	1.72
B14	179	1.71
B15	204	1.65
B16	210	1.74
B17	252	1.77
B18	301	1.71

*From BH4

Series C

Blue Clay, 5.5 m (BH5)

Test	σ'_c kPa	e_o
C1	4.1	1.44
C2	11.6	1.60
C3	27.4	1.37
C4	41.2	1.28
C5	62.6	1.36
C6	83.9	1.45
C7	113	1.35
C8	132	1.28
C9	151	1.44
C10	164	1.52
C11	173	1.32
C12	221	1.34
C13	248	1.33
C14	258	1.49
C15	271	1.32
C16	324	1.41
C17	366	1.50
C18	375	1.43
C19	457	1.49
C20	526	1.33
C21	666	1.41

Table 5.1(b) Program of Triaxial Tests on Winnipeg Clay at Depths of 11.5 m and 5.5 m

dation stresses, however, samples of the blue clay with these dimensions consistently failed by deformation into an S-shaped "buckling" mode. To investigate the effect of height and diameter on strength, and mode of failure, the height of one sample (A14) was reduced to 61.75 mm, (h/d = 1.7), and the diameter of another sample (A12) was increased to 51 mm, (h/d = 1.8).

5.3 TRIAXIAL CONSOLIDATION - TEST PROCEDURES

The experimental set-up used during triaxial consolidation is shown in Figure 5.1. All samples were consolidated for 24 hr. ± 1 hr. The sample is isolated from the cell water by means of two close-fitting rubber membranes, which are sealed by O-rings at the loading cap and pedestal. Radial drainage is achieved by means of individual side filter paper strips extending to a bottom porous stone; the filter strips must not be too long, otherwise they may become trapped by the O-ring seals and inhibit swelling at low confining pressures. To dissolve any air that could not be mechanically removed during installation, de-aired, distilled water was used exclusively in the drainage lines, and samples were consolidated under a back pressure of 140 kPa. A mercury-water manometer wheel (Bishop and Henkel, 1962) was used to measure volume changes under pressure. Both the cell pressure and back pressure were provided by self compensating mercury pot manometer systems (Bishop and Henkel, 1962), which can supply a constant pressure and have a capacity for volume change of about 200 mL. At the top of the cell a layer of thick oil was used to provide a seal between loading piston and cell bushing, and also to provide lubrication.

To permit axial displacement during isotropic consolidation

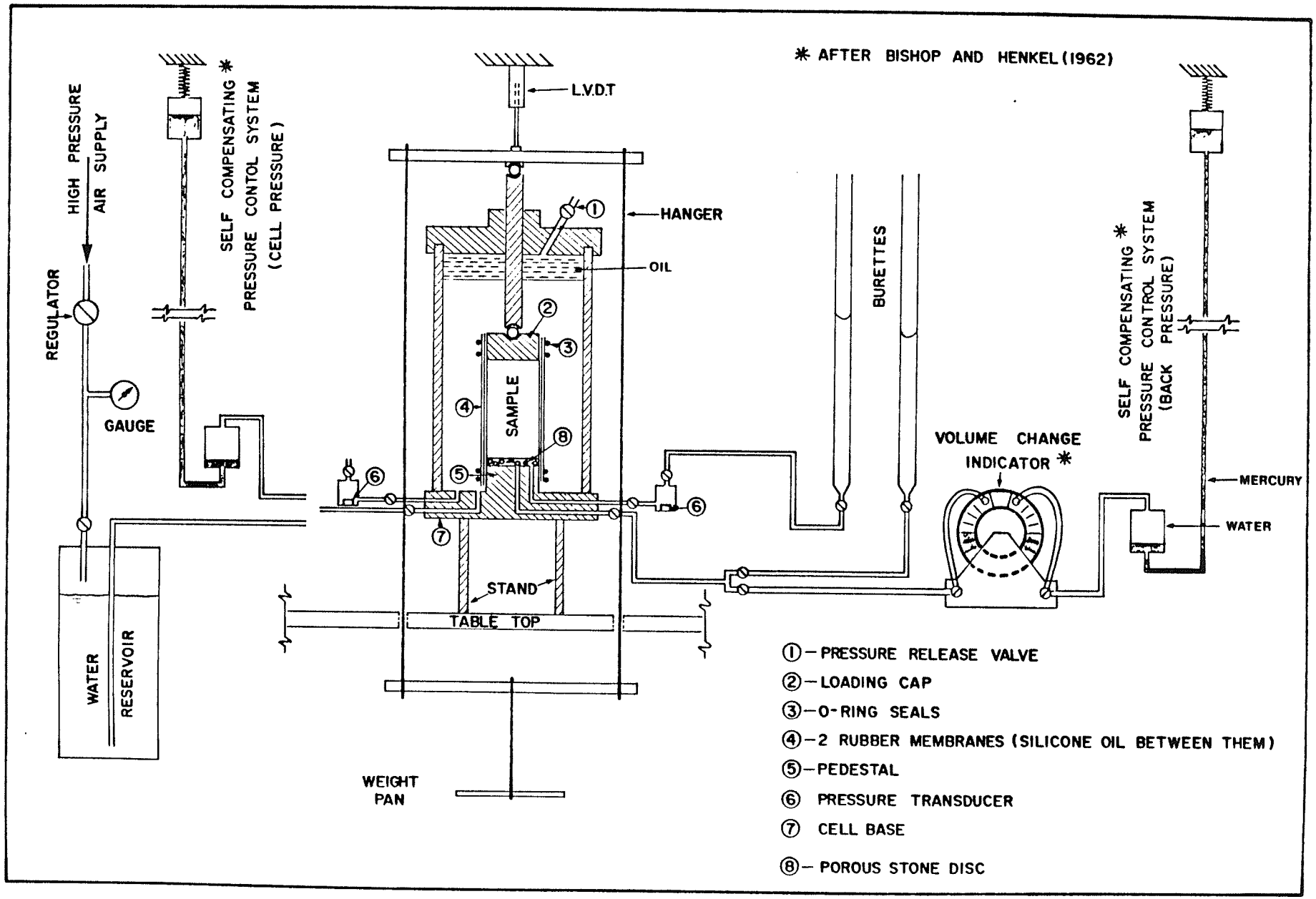

Figure 5.1 Triaxial Test Apparatus (Schematic Representation)

(compression or swell) to be measured, the reaction on the piston caused by the cell pressure was counterbalanced by weights. A slight excess load of 0.5 to 1.0 N ensures that a slight increase in cell pressure will not blow out the piston. Axial displacement, pore-pressure, and cell pressure, were all measured by electronic transducers and automatically recorded by a data logger.

Different consolidation procedures to those outlined above were used in a few special cases. Sample A15, was consolidated anisotropically to stresses $\sigma_1' = 246$ kPa, $\sigma_3' = 172$ kPa, ie. $\sigma_1'/\sigma_3' = 1.43$. This stress state was achieved by using additional weight on the hanger, above that required for balance. Samples B4 and C4 were not actually "consolidated", but allowed to reach equilibrium with a small volume of water under undrained conditions; the details of this procedure are described in Section 5.6. After 24 hours sample B4 had reached equilibrium at a swelling pressure of 35 kPa, and sample C4 at a swelling pressure of 41 kPa.

5.4 UNDRAINED SHEAR - TEST PROCEDURES

During undrained loading, the measured pore-pressure response must accurately reflect pore-pressure changes within the sample, so that the effective stress state can be properly evaluated. For the measurements to be reasonable there are two basic requirements:

(a) The sample should be completely saturated and there should be no air bubbles in the surrounding filter drains and pore-pressure measuring system.

(b) The rate of strain must be slow enough, so that non-uniformity in excess pore-pressures due to end restraint

does not become significant.

The first requirement can be satisfied by proper installation procedures. As a check on the undrained response after 24 hours of consolidation, the cell pressure, σ_3, is temporarily increased by 50 to 100 kPa. Skempton's pore-pressure parameter, B, can then be computed from the response, Δu.

$$\Delta u = B \, \Delta\sigma_3 \tag{5.1}$$

Values of B in the range 0.95 to 0.995 were obtained in response times of 30 seconds to 4 minutes. These values indicate satisfactory saturation. The second requirement, (b), above, was satisfied by using a slow rate of strain, 0.7% per hour, the same rate as used by Pietrzak (1979). The time to failure varied from about 3 hours at low stresses to as long as 12 hours for tests at high stresses. These times are long enough to allow 95% equalization of non-uniform pore-pressures according to the following equation, (Blight, 1963):

$$t_f = 0.07 \frac{H^2}{C_v} \tag{5.2}$$

where t_f = time to failure

H = half sample height

C_v = coefficient of consolidation

Axial load was measured at the external end of the loading piston by means of a load transducer attached to the frame of the compression machine. To avoid errors due to friction in the cell bushing, the piston was slowly rotated by a small electric "clock" motor (1 rev./min).

5.5 CORRECTION FOR THE STRENGTH OF MEMBRANES AND FILTER DRAINS

To minimize the error in deviator stress caused by the strength of the membranes and the filter drains, very thin membranes and very thin individual filter paper strips were used. An estimate of the required correction at peak strength was then made, using the methods described by Bishop and Henkel (1962), and the correction was found to be negligible (Appendix C). After the formation of a failure plane, the correction becomes more severe (Symons, 1967), however, the present study was not designed to measure post-peak strengths.

5.6 SAMPLE INSTALLATION

Winnipeg clays contain a significant proportion of highly-swelling clay minerals, and so it is important that samples be installed in the triaxial cell in as short a time as possible. The operation should be well organised but unhurried. All equipment should be checked prior to the start of installation, and all tools and materials arranged within easy reach. A checklist of operations and materials, plus some useful tips, are given in Appendix B. With practice the inner membrane can be secured by one bottom O-ring, and the air expelled from between the membrane, the sample, and the filter drains, within 3-5 minutes. From this time on, further swelling can be prevented. The excess water is removed from between membrane and sample by lowering a drainage burette a metre or two below the sample for 30 seconds. This imposes a suction pressure of 5 to 10 kPa below atmospheric, which can easily be maintained if the fit of the membrane around the greased loading cap is good. As a bonus the sample is then confined during the subsequent operations, and is held tightly against the pedestal. The

negative pore-pressure gradually rises showing the swelling tendency of the clay. As mentioned in Section 5.3, samples B4 and C4 were not actually consolidated, but allowed to reach equilibrium after a cell pressure of 200 kPa had been applied. After 24 hours the pore-pressures had stabilized at values of 35 kPa and 41 kPa below the cell pressure.

5.7 SPECIAL PRECAUTIONS IN LOW STRESS TESTS

As there is very little difference between the back pressure and cell pressure, it is especially important that the pressure transducers be matched. After filling an empty cell to mid-height with water, the zero reading of both transducers is adjusted. Next, air pressure is supplied through the top valve so that both transducers read a value equal to the desired cell pressure. One of the transducers is adjusted slightly so that both read exactly the same value.

Samples consolidated for 24 hours at very low confining pressures have very low strength, and preparation for undrained shear must be done with extra care.

5.8 THE END OF THE TEST AND SAMPLE REMOVAL

Samples were not compressed much beyond failure so that the initial mode of failure could be determined. The removal and examination of the sample was considered an important part of each test. To avoid swelling, drainage lines were left closed until the moment the sample and membranes were removed from the pedestal. After weighing each sample, a vertical section was taken to reveal the failure mode which was accurately sketched and then the remainder of the sample was chopped up to make sure that there were no large stones.

In the pilot series of tests, (series AA), it was discovered that for normally consolidated samples the time to failure was about 12 hours. If the samples were left to shear overnight, it was not possible to determine whether initial failure was due to buckling or the formation of a rupture zone. In the subsequent testing programs (A, B and C), undrained shear on normally consolidated samples was commenced before 9 am, so that failure would occur before midnight of the same day. To ensure 24 hours consolidation, installation was commenced very early on the previous day.

5.9 RESULTS OF TRIAXIAL CONSOLIDATION

The most accurate determination of total volume change during isotropic consolidation was obtained from the sample's change in weight. The total volumetric strains from such data are plotted versus consolidation stress in Figure 5.2. There is some scatter of results, mainly due to the non-homogeneity of the deposit, and these curves can be compared to the e versus σ'_c curves from oedometer tests on individual samples, (Chapter 4). For the samples of brown clay, the relationship appears to be approximately linear at stresses above 50 kPa. For the blue clay there appears to a slight yield, but the value of the isotropic pre-consolidation pressure, $P'_{c(iso)}$ appears to be about 200 kPa for both the 9.0 m and 11.5 m strata. At stresses below 50 kPa it appears that there were considerable swelling strains, and a departure from linearity at all three depths. The linear portion of each curve can be described by a drained modulus, $a_{v(iso)}$ defined by:

$$a_{v(iso)} = \frac{\Delta e}{\Delta \sigma'_c} = \frac{\Delta V/V(1+e_o)}{\Delta \sigma'_3} \qquad (5.3)$$

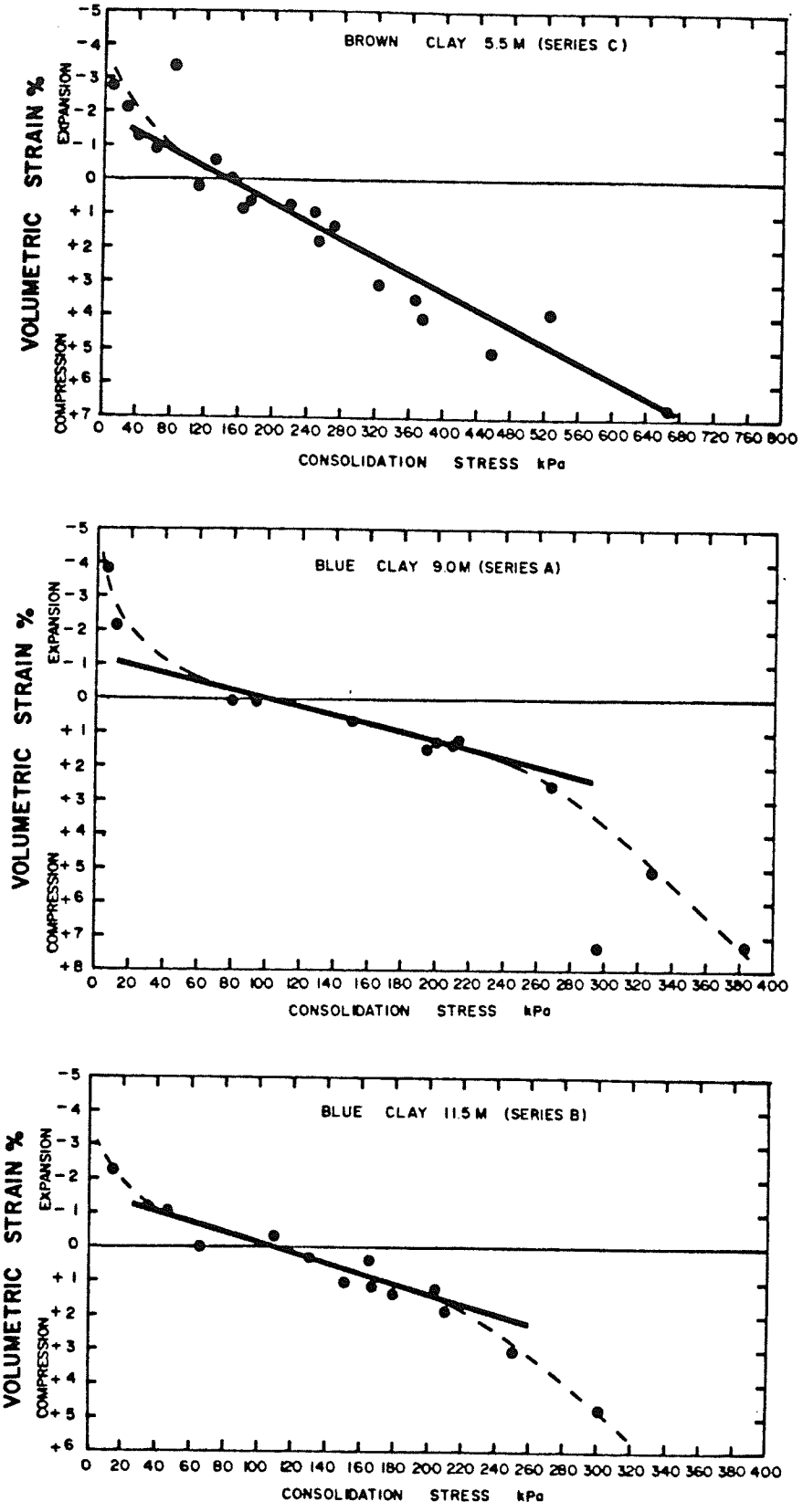

Figure 5.2 Volumetric Strain versus Isotropic Consolidation Stress, from Triaxial Tests on Winnipeg Clay

where e_o = average value of initial void ratio for each depth

The values of $a_{v(iso)}$ are approximately 3 x 10^{-4} kPa^{-1} at the 5.5 m and 9.0 m depths, and 4 x 10^{-4} kPa^{-1} at 11.5 m depth. Thus the values of $a_{v(iso)}$ are slightly lower than the values of a_{vo} calculated from oedometer tests, (Chapter 4). a_{vo} and $a_{v(iso)}$ are of course different parameters in that $a_{v(iso)}$ describes the volumetric response to a spherical pressure increase $\Delta\sigma'_c$, (where $\Delta\sigma'_1 = \Delta\sigma'_2 = \Delta\sigma'_3$), whereas a_{vo} describes the response to a vertical pressure increase $\Delta\sigma'_c$ (where $\Delta\sigma'_1 = \Delta\sigma'_c$, $\Delta\sigma'_2 = \Delta\sigma'_3 = K_o\ \Delta\sigma'_c$).

5.10 RESULTS OF UNDRAINED SHEAR, BLUE CLAY AT 9.0 m

5.10.1 Stress Paths and Failure Envelopes

The stress paths, $q = \frac{(\sigma_1 - \sigma_3)}{2}$ versus $p' = \frac{(\sigma'_1 + \sigma'_3)}{2}$ shown in Figure 5.3 include the results of the pilot series of 9 tests from a depth of 8.0 m (series AA), as well as the 15 tests at 9.0 m (series A). As will be shown later in this chapter, samples A1 to A7 and AA1 to AA4 were overconsolidated and failed in a brittle fashion, whereas A8 to A14 and AA5 to AA9 were normally consolidated, and failed in a ductile fashion. In Figure 5.3, the normally consolidated samples have stress paths which curve gradually to the left. As failure is reached, the effective stress, p', continues to decrease because of increasing pore-pressures, but the decrease in shear strength is only gradual. The overconsolidated samples have stress paths which curve to the right, and shear strength decreases rapidly after failure. At very low confining stresses, the stress paths fall close to the line $\alpha = 45^o$ which in Figure 5.3 separates tension and compression states. It is of course not practically possible for a

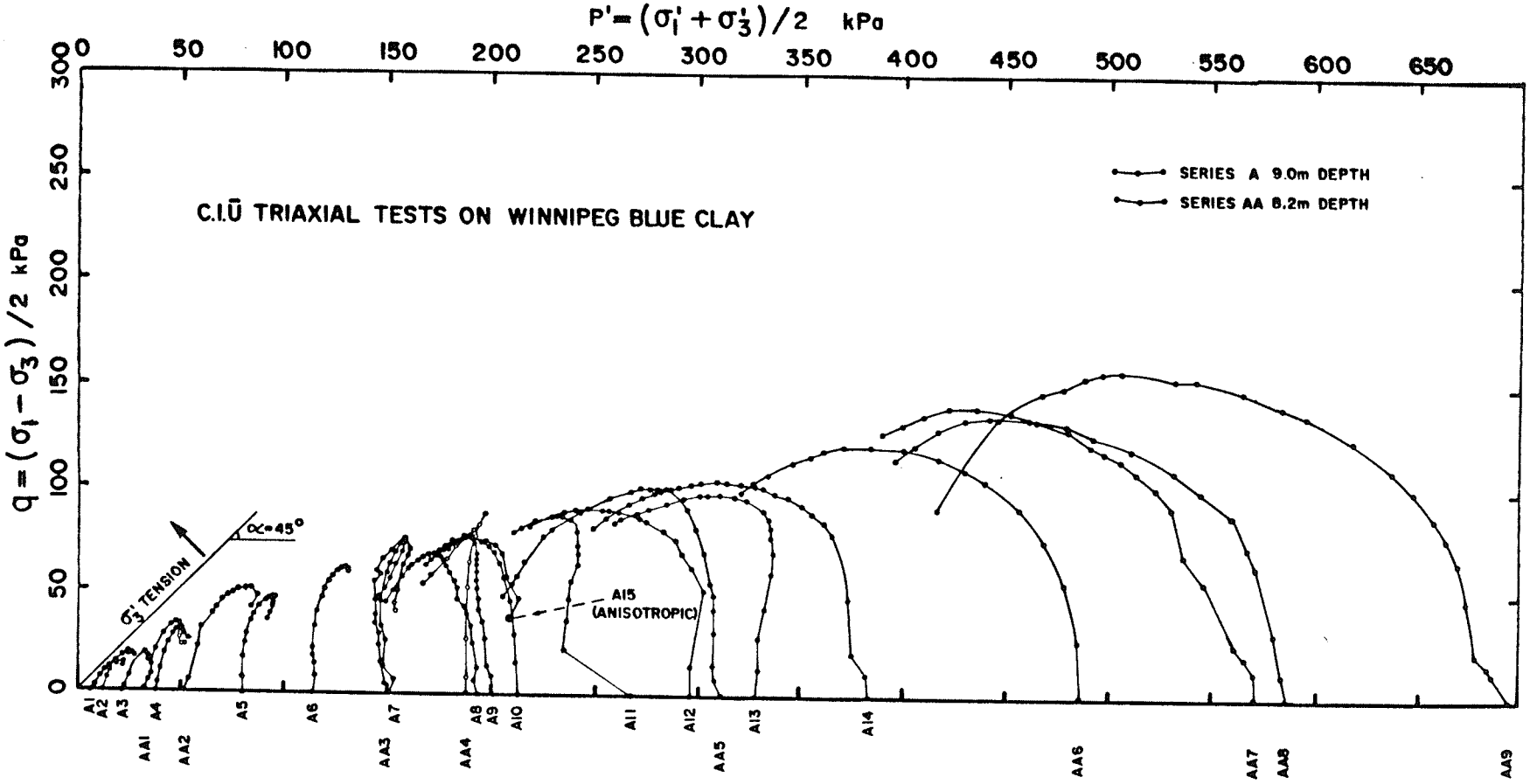

Figure 5.3 Effective Stress Paths, 9.0 m and 8.2 m Depths

sample to reach a state of tension in a triaxial test. Sample A15 was consolidated anisotropically to a stress of $\sigma_1' = 246$ kPa, $\sigma_3' = 172$ kPa. This stress state lies well inside the yield envelopes for the blue clay defined by Baracos et. al. (1980) for the 6-12 m depth, and by Noonan (1980) for the 8.2 m and 10.0 m depths (see Appendix D). The stress path to failure however of sample A15 was almost identical to that of the isotropically consolidated sample A10, and both samples failed in a normally consolidated, ductile fashion.

In constructing the failure envelope, there are two criteria which can be used to establish the critical points on each stress path:

Point (a) - The point at which the shear stress, q, is a maximum.

Point (b) - The point at which the effective stress ratio, σ_1'/σ_3', is maximum, ie. the largest equivalent frictional resistance, σ', is mobilized. The maximum ratio occurs at the point on the stress path which subtends the largest angle with the horizontal axis at the origin.

In Figure 5.4, for tests in which the critical points (a), and (b), did not coincide, both points are shown, together with the interconnecting stress path. At high stresses there is a significant difference between the points defined by the two criteria, and there is also some difference at very low stresses. The construction of the collective failure envelope however, is unaffected by this difference, as in between points, (a), and, (b), the stress paths of individual samples follow the collective envelope. The envelope is curved at low stresses, and then becomes approximately linear over a very wide range of stresses,

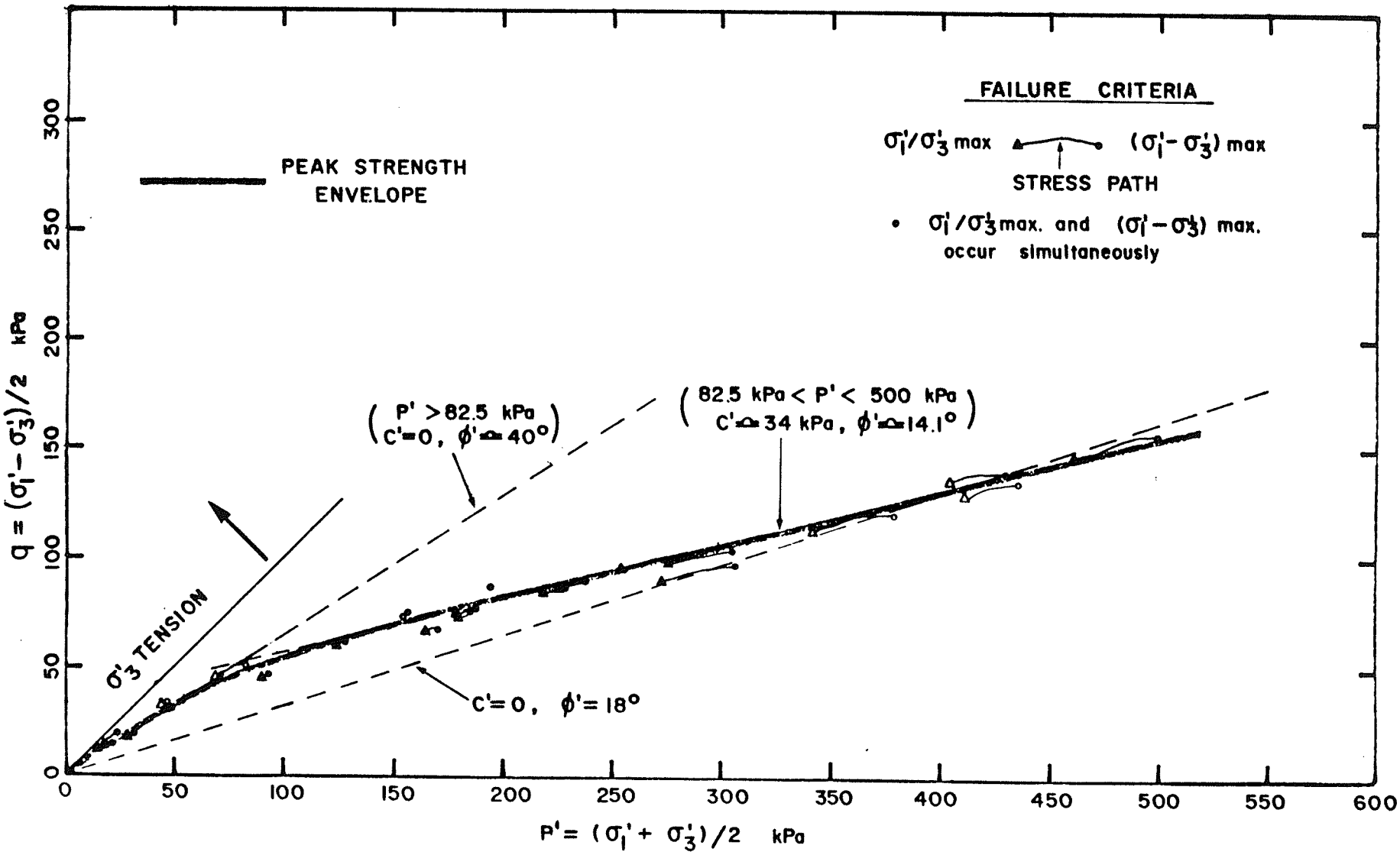

Figure 5.4 Failure Envelope for the Blue Clay from 9.0 m Depth

100 kPa < p' < 500 kPa. What is really susprising, is that although there is a definite difference between the behaviour of normally consolidated and overconsolidated samples, and the transition occurs at a stress level, p', of approximately 175 kPa (Figure 5.3), there is no discontinuity, or change in shape, in the failure envelope.

Strength envelopes are usually approximated by linear sections as follows:

$$q_f = a' + p'_f \tan \alpha' \tag{5.4}$$

where a' is the intercept, and α' the gradient of each section of the envelope in q' - versus p' space.

These parameters are then converted to the parameters c' and ϕ' which define the Mohr-Coulomb failure envelope.

$$T_{ff} = c' + \sigma'_{ff} \tan \phi' \tag{5.5}$$

$$\text{and } \phi' = \sin^{-1}(\tan \alpha') \tag{5.6}$$

$$c' = a'/\cos \phi' \tag{5.7}$$

The curved envelope shown in Figure 5.4 can be represented by a bilinear approximation as follows:

At normal stress	$\phi' \simeq 14.5^o$, $(\alpha' \simeq 14^o)$
levels, p', above 90 kPa	$c' \simeq 34$ kPa, $(a' \simeq 33$ kPa$)$
At normal stress	$\phi' \simeq 40^o$, $(\alpha \simeq 32^o)$
levels, p', below 90 kPa	$c' \simeq 0$

The fit is good except in the transition range, 80 kPa < p' < 110 kPa.

5.10.2 Comparison with Previous Failure Envelopes

Previous CIŪ triaxial tests on undisturbed Winnipeg blue clay have lead to the postulation of a variety of peak strength envelopes, usually without the specification of the applicable range of normal stresses. For example:

(a) Mishtak (1964), 9.3 m Red River Floodway

Normally consolidated	$c' = 0$, $\phi' = 16^o$
Overconsolidated	$c' = 45$ kPa, $\phi' = 12^o$

(b) Crawford (1964), 9.3 m Red River Floodway

	(As above)
One envelope	$c' = 59$ kPa, $\phi' = 9^o$

(c) Freeman and Sutherland (1974), 7.8 m, blocks 1 and 2

Overconsolidated	$c' = 11$ kPa, $\phi' = 17.6^o$

(d) Pietrzak (1979), University of Manitoba Site.

Tri-linear envelopes:

(1) 6.4 m depth

Low stress	$c' = 6$ kPa, $\phi' = 32^o$
Intermediate stress	$c' = 33$ kPa, $\phi' = 14.5^o$
High stress	$c' = 1$ kPa, $\phi' = 23^o$

(2) 9.6 m depth

Low stress	$c' = 8$ kPa, $\phi' = 30.5^o$
Intermediate stress	$c' = 36$ kPa, $\phi' = 10.5^o$
High stress	$c' = 0$, $\phi' = 24^o$

As there is a large discrepancy in the above values of c' and ϕ', it would at first appear that there must have been a large scatter in the test results produced by the above researchers. However the author has examined the original publications, to determine the normal stress range over which each researcher conducted tests. In Figure 5.5, each of the above envelopes are shown only over the stress range in which

tests were performed. Most of the envelopes are in good agreement with that defined by the author's tests. Exceptions are Pietrzak's normally consolidated envelope for the 6.4 m depth, and Freeman and Sutherland's envelope. In the latter case, strength envelopes were selected to fit the lower boundary of test results, and many of the actual test data points fall close to the author's curved envelope.

Two of Pietrzak's samples from the 6.9 m depth, (at the University of Manitoba campus), did have higher strengths in the normally consolidated range, and the reason for this deviation is not certain. These samples were consolidated to very high stresses, p' = 520 kPa and 640 kPa, and the results were used to justify the normally consolidated envelope $\phi'_{n/c} = 23^{o}$, c' = 0.

The otherwise good correlation between the different envelopes shown in Figure 5.5, despite the wide variation in c' and ϕ' parameters, illustrates two important points. Firstly, values of c' and ϕ' used to approximate test results should not be extrapolated to estimate strength outside the range of testing. Secondly, the parameters c' and ϕ', which give the best linear approximation to a failure envelope, are not soil parameters but merely mathematical coefficients. The contribution of a real cohesion, c'(real), to failure strength is very difficult to determine, and may be insignificant unless strong cementation bonds exist. A large portion of the reserve strength of an overconsolidated clay originates from the fact that, for a given stress p', it exists at a lower void ratio than a similar normally consolidated deposit, and therefore has greater interlocking of particles, and a tendency to dilation.

In the normally consolidated stress range, the structure of

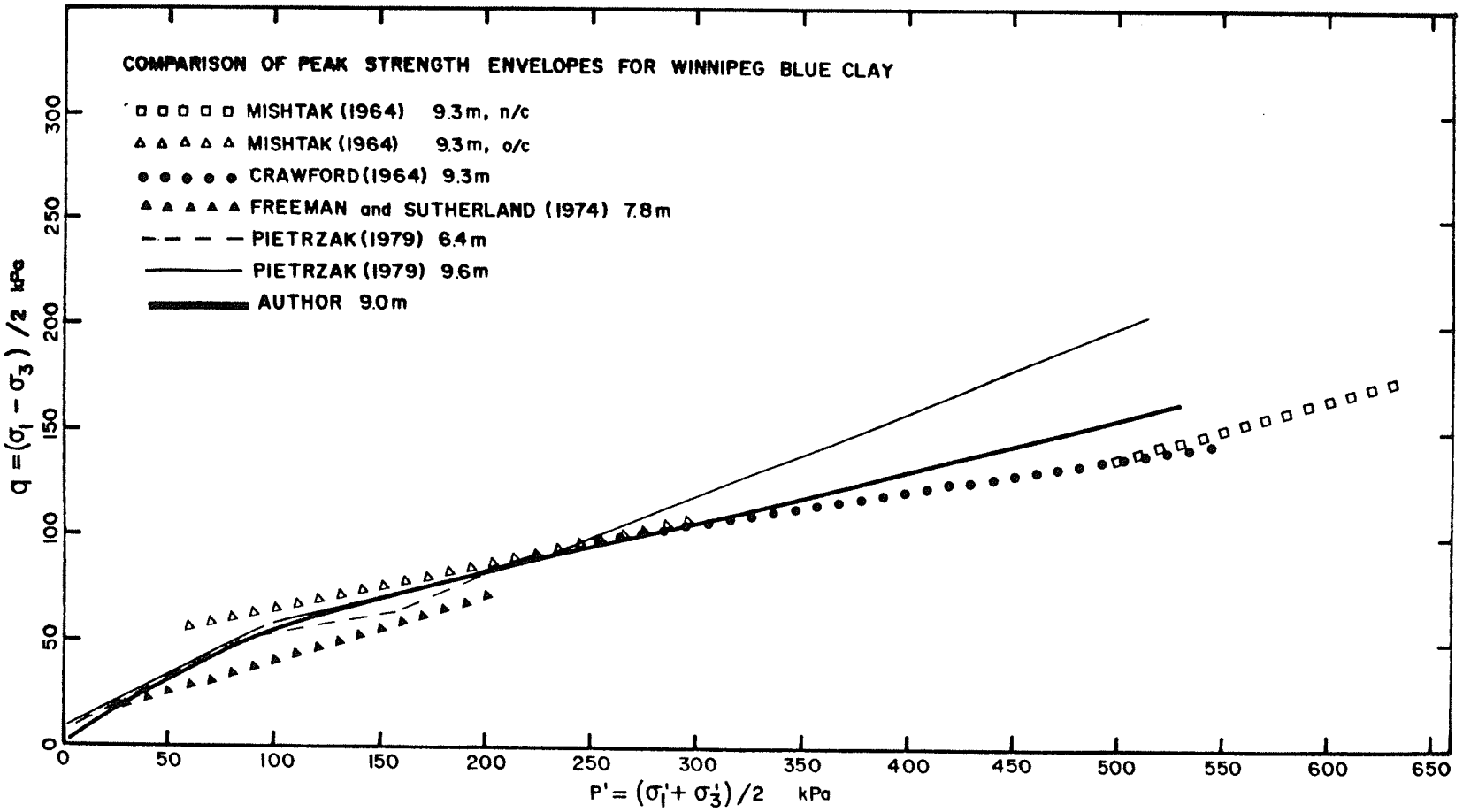

Figure 5.5 Comparison of Failure Envelopes for Winnipeg Blue Clay

the soil has been disturbed, so that any effects of aging have been removed. It is generally accepted that the real cohesion, c'(real), is negligible, and experimentally the best linear fit to normally consolidated test results is usually $\phi_{n/c}$ = constant, c' = 0. The parameter $\phi'_{n/c}$ is in this special case considered to be a real soil friction parameter, independent of the normal stress. A study of the strength envelope shown in Figure 5.4, however, shows that if c'(real) is zero, then in the normally consolidated range, ϕ' varies from about 24^{o} at p' = 200 kPa to 18^{o} at p' = 500 kPa. This variation in $\phi'_{n/c}$ is an unusual result, which must signify a difference in behaviour of the Winnipeg clays as compared to most other clays.

Winnipeg clay contains about 75 to 85% of clay size material (<2μ)(Figure 2.1), and most of the larger size material is contained in clasts. The clay minerals are mainly illites and smectites* in roughly equal amounts, with lesser amounts of kaolinites present, (Wicks, 1965; Baracos, 1977). The dominant exchange cation has been found to be calcium, (Wicks, 1965). A literature survey revealed an interesting study on the peak strength of calcium montmorillonite and this is discussed in the next section.

5.10.3 Comparison of Failure Envelope with the Peak Strength of Calcium Montmorillonite

Peak strength envelopes for calcium montmorillonite are shown in Figure 5.6 (after Mesri and Olson, 1970). They were derived from drained and undrained triaxial tests on artificially sedimented calcium

---

*Generic name, includes montmorillonites and bentonites.

montmorillonite prepared from a Wyoming Bentonite deposit. Both the normally consolidated and overconsolidated envelopes are highly curved. The normally consolidated peak values of $\phi'_{n/c}$ vary from about 27^o at $p' = 60$ kPa to 14^o at $p' = 650$ kPa, so that the envelope is highly curved at low stresses and approximately linear (but with a c' intercept) at high stresses. The overconsolidated envelope, produced by precompression to 800 kPa, shows increased strength but also curves markedly at low stresses. This behaviour contrasts with that of calcium illite, for which $\phi'_{n/c}$ is constant at about 24^o (Olson, 1962).

The above results suggest that the cause of the cohesion intercept, c', for the normally consolidated envelope of Figure 5.4, might be similar behaviour of the Winnipeg clay to that of calcium montmorillonite. It might also be expected then, that the normally consolidated envelope at low stresses should be curved, although it is difficult to test this hypothesis.

5.10.4 Failure Modes

Figure 5.7 shows sketches of vertical sections through each sample after failure. There was a distinct difference between the failure modes of the normally consolidated samples, A8 to A14; and the overconsolidated samples, A1 to A7. The normally consolidated samples failed, ie. exceeded maximum q, = $(\sigma_1-\sigma_3)/2$, and maximum σ'_1/σ'_3, by a ductile distortion into an S-shape or buckling mode. Tests were concluded as soon as failure had definitely been established. When compression was continued, a failure plane eventually formed, (eg. A12, A8), but this appears to be a secondary occurrence. During the pilot series of tests, (AA), it was thought that perhaps the buckling mode was a

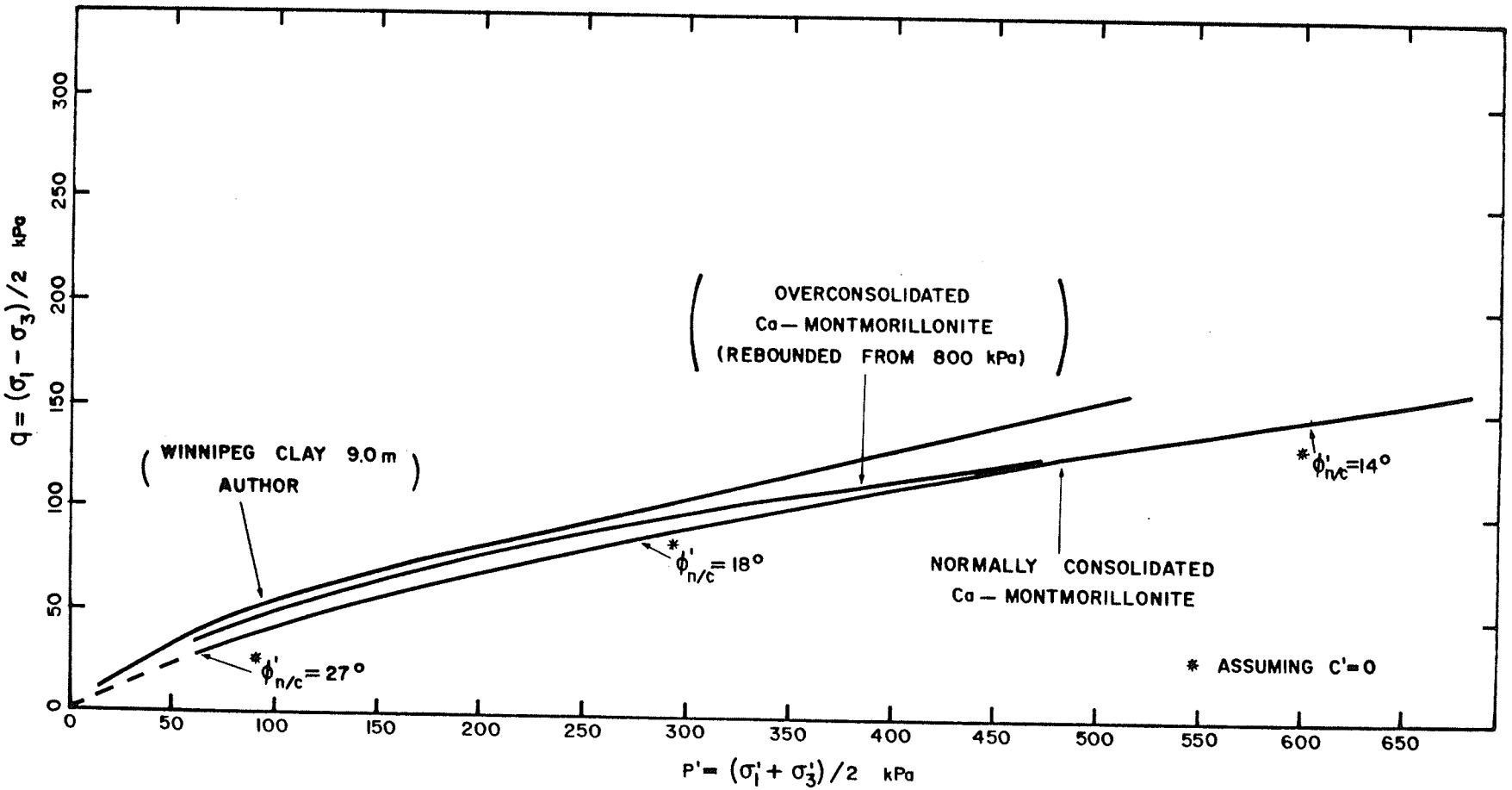

Figure 5.6 Failure Envelope for the 9.0 m Depth Compared to n/c and o/c Envelopes for Calcium Montmorillonite (After Mesri and Olson, 1970, (Figures 3 and 4))

premature failure due to one of the following causes:

(a) The height/diameter ratio of 2:1 was too great.

(b) The ends of the sample were perhaps not cut quite square.

(c) There was slight initial eccentricity of the loading piston, due to lateral movement during consolidation. The latter occurred because of non-homogeneity.

The eccentricity problem was eliminated by use of the system of weights and hangers to keep the piston in contact with the loading cap during consolidation. To improve end-trimming, a cutting jig was made, using a specially machined, closely fitting piece of pipe. However the samples still consistently failed by buckling. Test A14 was then conducted using a shortened sample, height/diameter = 1.7, and Test A12 using a 50 mm diameter sample, with height/diameter = 1.8. These samples also failed by buckling, and had similar stress paths to failure and similar strengths. It was concluded that the deformation into the buckled shape was not really a buckling phenomenon, but was due to spreading of the sample accompanied by rotation of the top cap, once shear stresses reached critical values. The spreading and top cap rotation may not be as noticable in larger diameter samples, but it does not appear to affect failure strength.

Further evidence that the normally consolidated failure envelope based on buckled samples is not an underestimate of strength, is provided by the work of Noonan (1980) and Lew (1981). The latter authors tested 76 mm diameter triaxial samples of blue clay from a depth of 8.2 to 11.5 m at the University of Manitoba campus site. Their research was primarily directed to the mapping of yield envelopes, but some samples were tested to failure in the normally consolidated range.

These samples did not buckle, but had strengths slightly below the author's envelope, c' = 34 kPa, ϕ ' = 14.10 (Figure 5.4).

All overconsolidated samples, A1 to A7, formed clearly defined failure planes, (Figure 5.7). Particular attention was paid to the development of failure in the low normal stress range. Failure planes first formed in samples A1 to A4 as soon as maximum σ_1'/σ_3 was reached, but the deviator stress, $\sigma_1-\sigma_3$, continued to increase for a significant time after this, (Figure 5.3 and 5.4). The failure planes were straight, and easily visible internally as a zone of soft material, (1-2 mm thick), which had apparently dilated significantly. There was no evidence of fissuring or cracking, or of a nuggety structure. It appeared that the failures had occurred because the strength of the microstructure had been exceeded in a region of previously intact material. This is contrary to the proposition that macrostructure fissuring is responsible for the low cohesion intercept, c', and high friction angle, ϕ ', at low stresses (Baracos et. al., 1980). Further evidence that even at low stresses, failure in the blue clay occurs through intact material, rather than through fissures, has been gathered from a recent series of tests on 76 mm diameter samples (Au, 1982, Personal Communication - M.Sc. Thesis in preparation).

The suggested conclusion is that at low normal stresses, general softening of the entire material occurs, consistent with the high swelling strains noted in Section 5.9. The behaviour is again probably similar to that of calcium montmorillonite, for which the overconsolidated envelope is highly curved at low normal stresses (Figure 5.6).

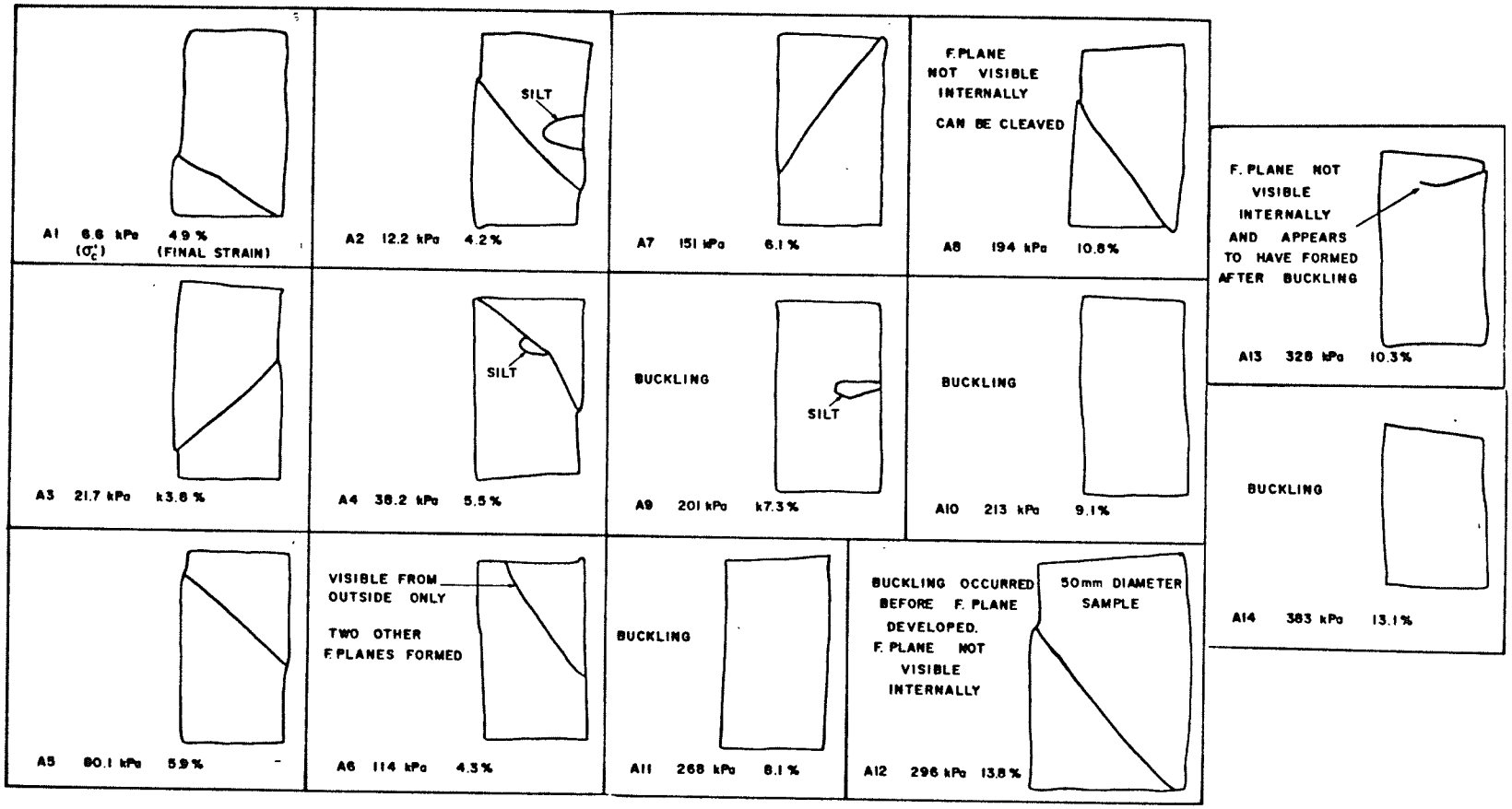

Figure 5.7 Failure Modes for Triaxial Samples of Winnipeg Blue Clay from 9.0 m Depth (Series A)

5.10.5 Stress-Strain and Pore-Pressure Generation Curves

The shapes of the stress-strain, and pore-pressure generation curves, give an indication of the soil particle structure, and can be correlated with the mode of failure. In Figures 5.8 and 5.9, the pore-pressure, Δu, and the deviator stress $(\sigma_1-\sigma_3)$, have been normalized by the isotropic consolidation stress σ'_c. Figure 5.10 shows the effective stress ratio, σ'_1/σ'_3 versus strain. The overconsolidated samples (A1 to A7) showed brittle behaviour, with failure strains of 1% to 4%, and in general, the higher the overconsolidation ratio, the sharper the peak in deviator stress or stress ratio, and the lower the failure strain. The pore-pressure curves have corresponding sharp peaks which occurred at slightly lower strains than the peaks in shearing resistance, thus indicating a tendency to dilation.

The behaviour of the normally consolidated samples, (A8 to A14), was in comparison ductile. Shearing resistances decreased only gradually from maximum values occurring at strains of 4% to 8%, and pore-pressure values continued to increase or stabilized, even when the deviator stress had peaked and was decreasing.

5.11 RESULTS OF UNDRAINED SHEAR, BLUE CLAY AT 11.5 m

In Chapter 4 it was shown that in oedometer tests, the behaviour of the blue clay at 11.5 m was very similar to that of the blue clay at 9.0 m. The former, however, was less overconsolidated, and had a higher initial void ratio. The overall average values of P'_c were 260 kPa at 11.5,m and 410 kPa at 9.0 m depth. The clay from borehole 4 at 11.5 m,however,appeared to have a P'_c of 220 kPa (2 tests) as compared to a P'_c of 300 kPa (2 tests) for the clay from borehole 5. Of

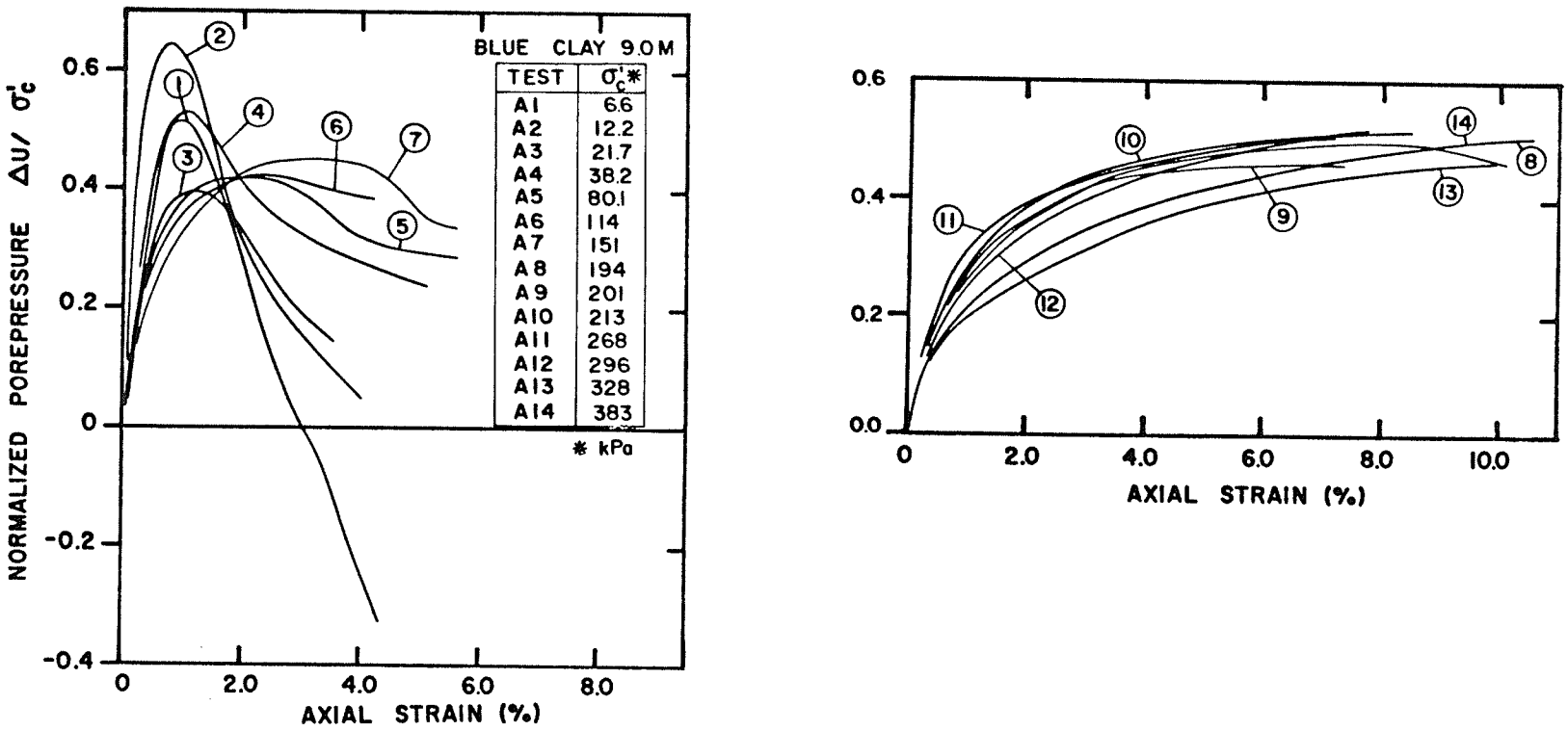

Figure 5.8 Porepressure Response $\Delta U/\sigma_c'$ versus Axial Strain at 9.0 m Depth. (Series A)

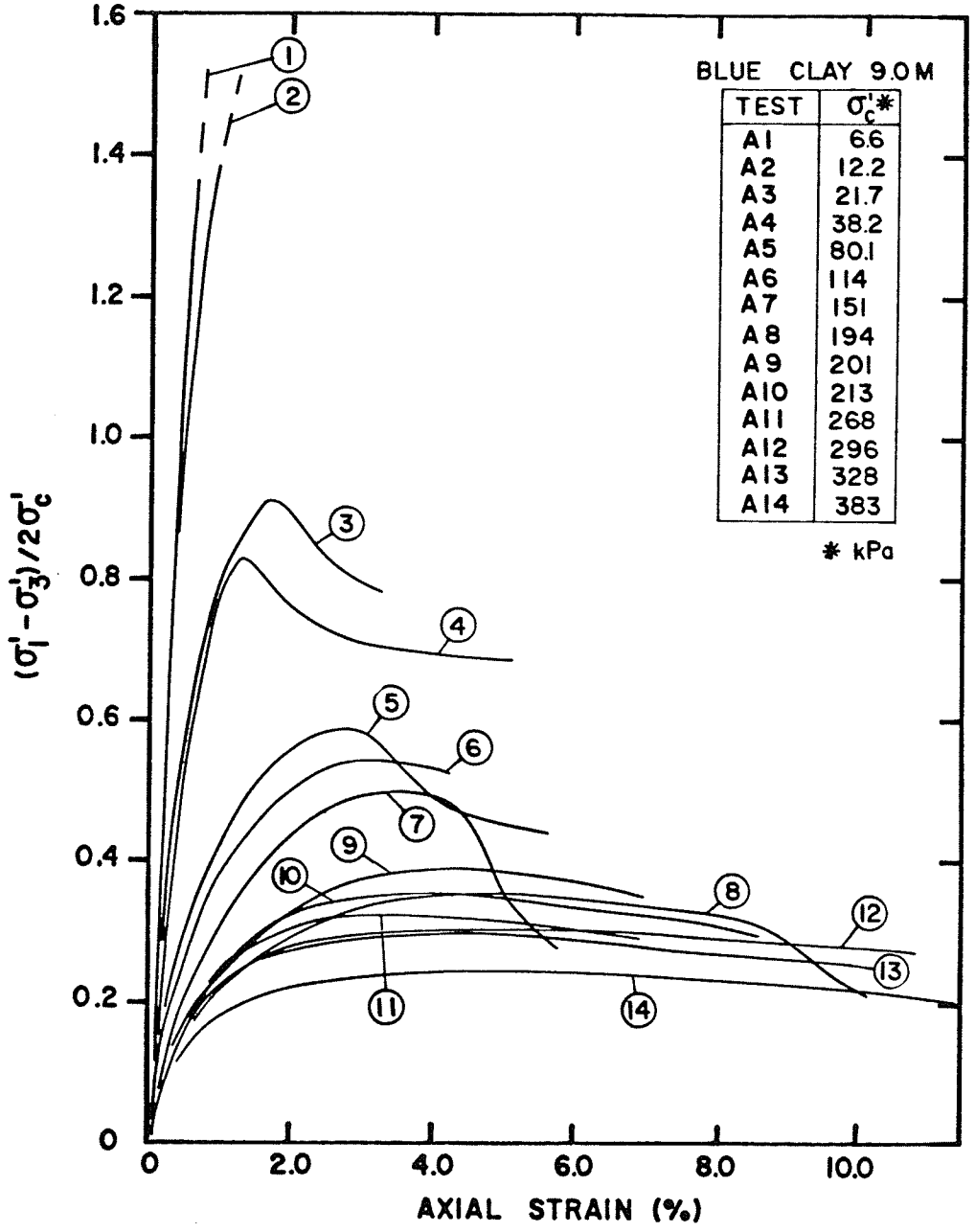

Figure 5.9 Normalized Deviator Stress versus Axial Strain at 9.0 m Depth. (Series A)

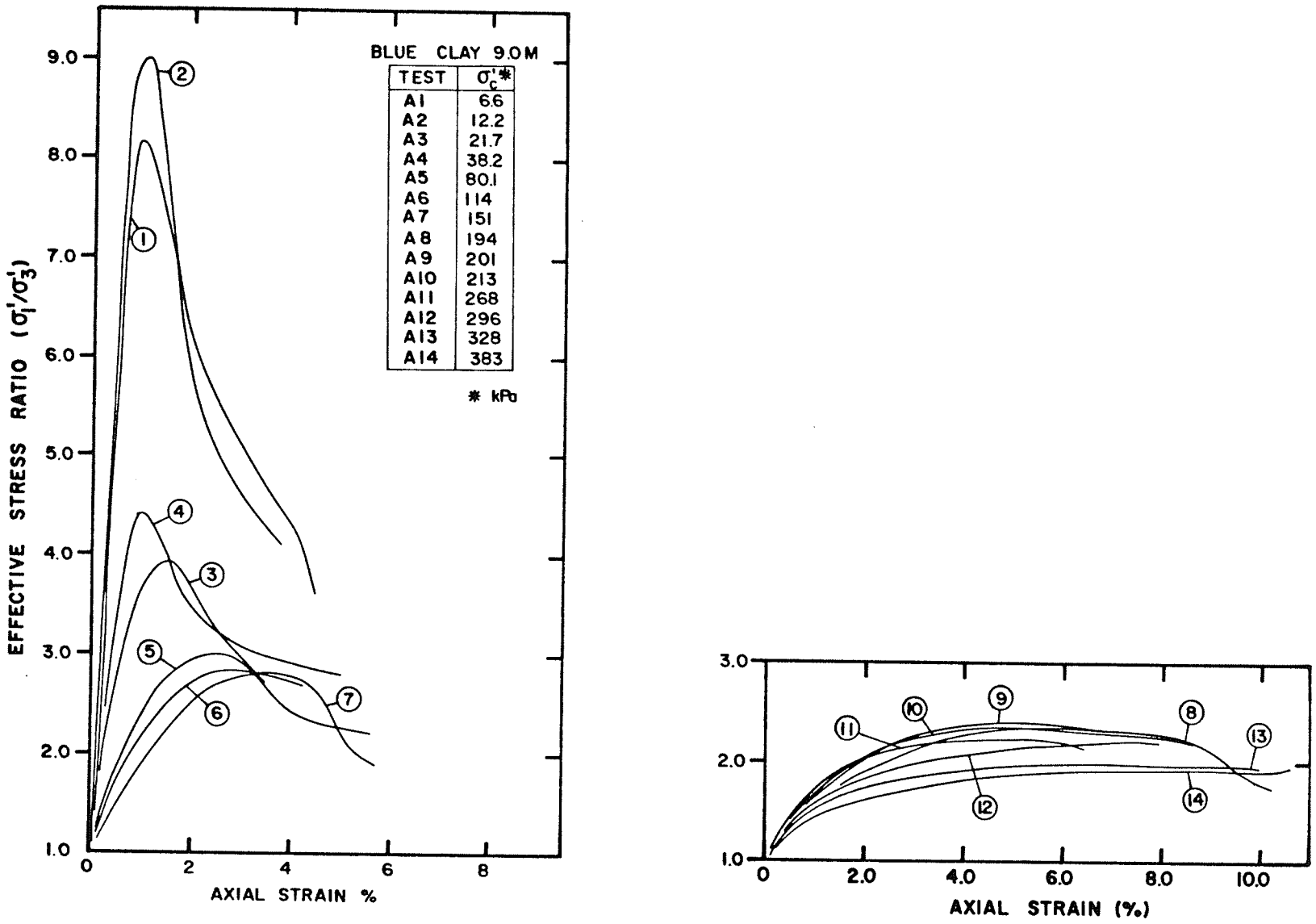

Figure 5.10 Effective Stress Ratio versus Axial Strain at 9.0 m Depth (Series A)

the 18 triaxial samples from a depth of 11.5 m, only samples B3, B6, B7, and B10, were from borehole 4, which had the lower preconsolidation pressure.

Figure 5.12 shows that the peak strength envelopes for the 9.0 m and 11.5 m depths are very similar. However an inspection of the stress paths, failure modes, and stress-strain curves (Figures 5.10 to 5.16), shows that the clay at 11.5 m depth did behave as a less overconsolidated deposit. In Figure 5.10, samples B1 to B9, (σ'_c = 5.1 to 130 kPa) were overconsolidated, whereas B15 to B18, (σ'_c = 204 to 301 kPa), were normally consolidated and failed by buckling. Sample B10 (σ'_c = 139 kPa) was also clearly normally consolidated, and failed by buckling, but this sample was from borehole 4 (lower preconsolidation pressure). For clay from borehole 5, samples B11 (σ'_c = 151 kPa) and B12 (σ'_c = 165 kPa) were close to the transition between overconsolidated and normally consolidated behaviour. Sample B11 failed by buckling, and B12 formed a failure plane, although the stress paths for the two samples are very similar. Stress paths for samples B13 and B14 (σ'_c = 166 kPa and 179 kPa) were not available due to a malfunction of the measuring equipment.

5.12 RESULTS OF UNDRAINED SHEAR, BROWN CLAY 5.5 m DEPTH

In comparison with the blue clay deposits, the brown clay at 5.5 m depth was much more heterogeneous. The clay blocks contained fissures, and there were swirls and patches of dark coloured and light coloured material of different plasticity (Chapter 2).

As can be seen in Figure 5.17, it is more difficult to distinguish between overconsolidated and normally consolidated behaviour from the stress paths. Only sample C21, which was consolidated to a

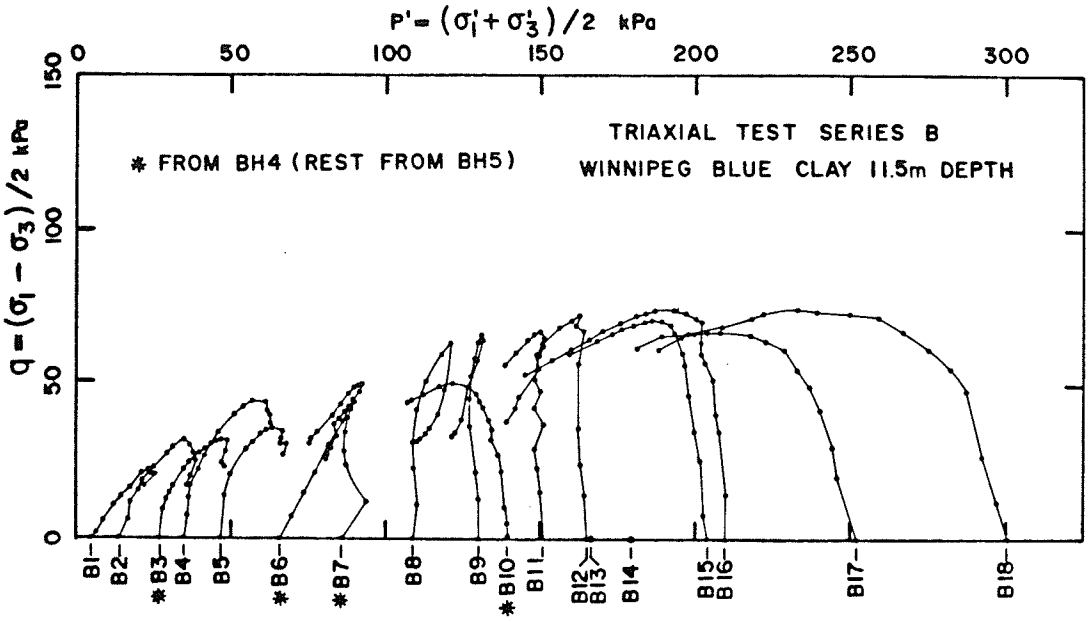

Figure 5.11(a)

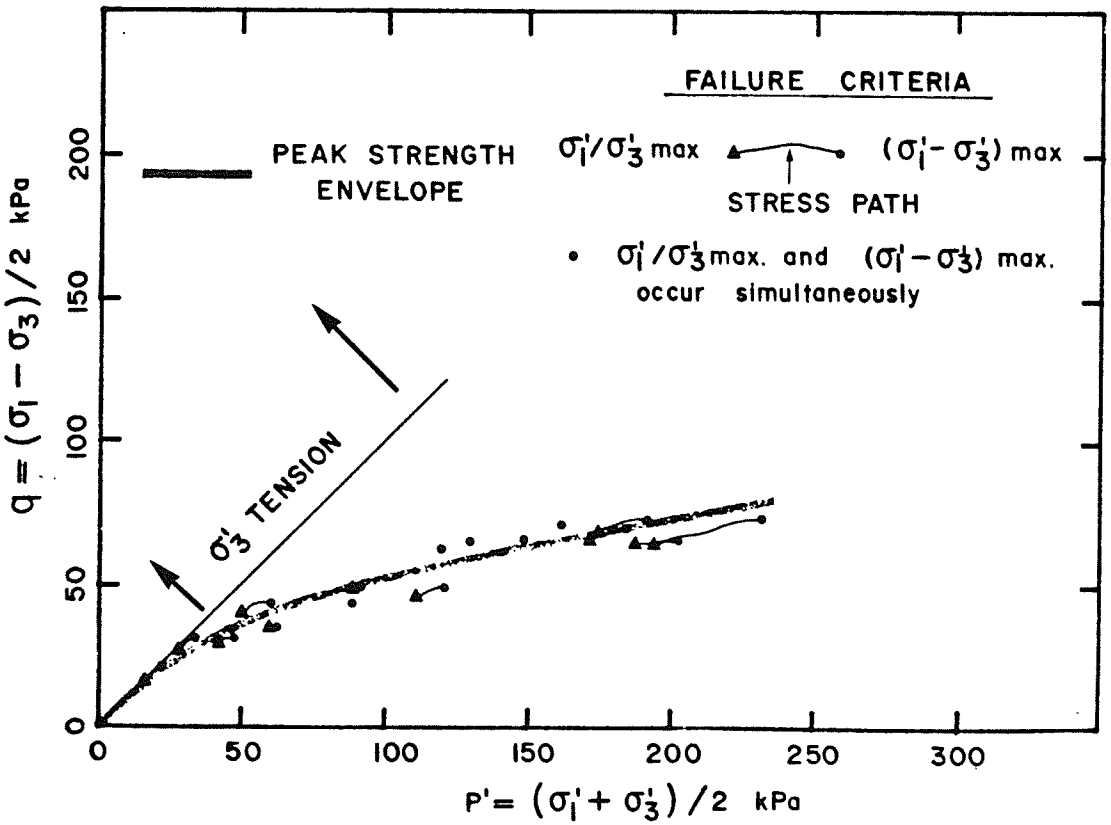

Figure 5.11(b)

Figure 5.11 Stress Paths and Failure Envelope for Winnipeg Blue Clay from 11.5 m Depth (Series B)

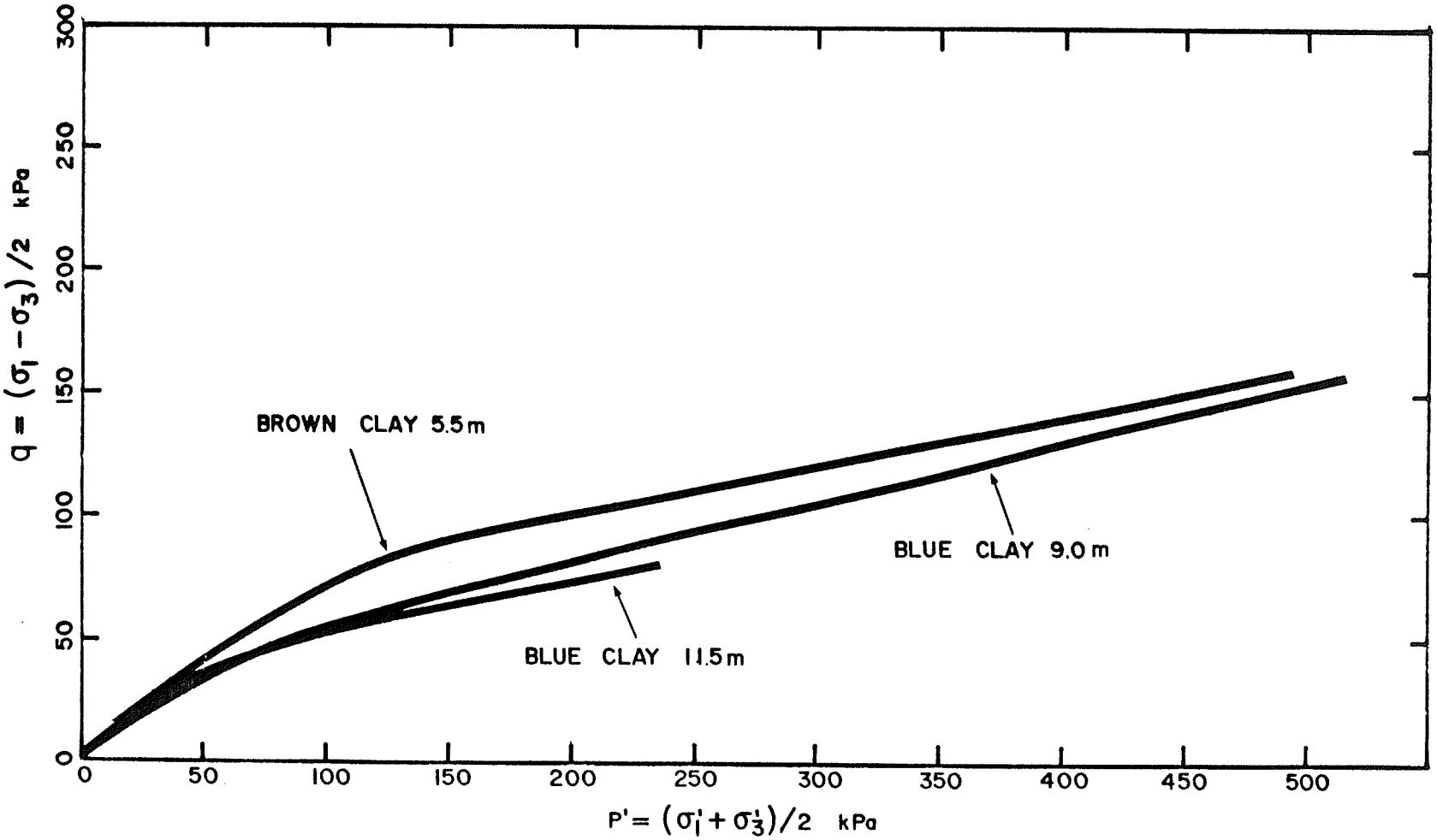

Figure 5.12 Comparison of Failure Envelopes for Depths of 5.5 m, 9.0 m and 11.5 m

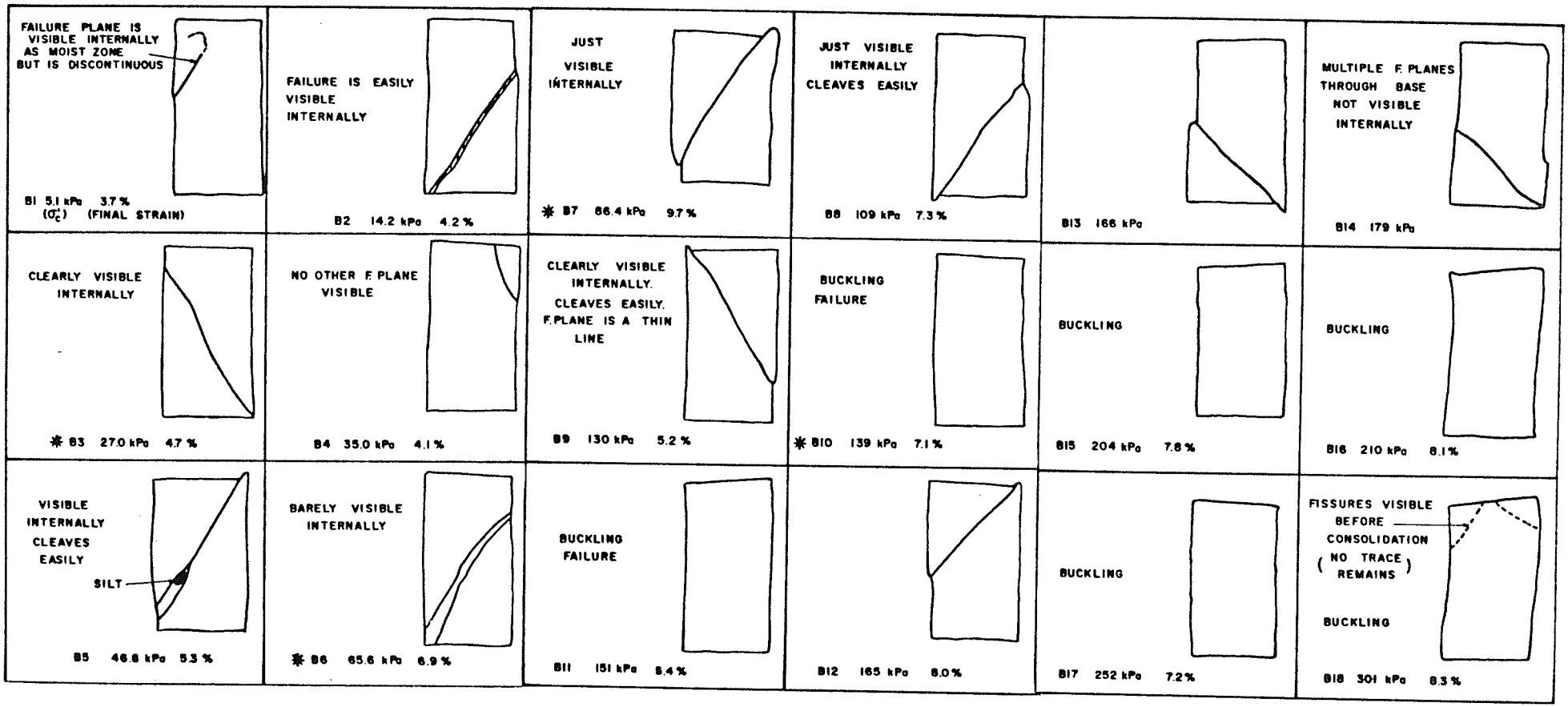

Figure 5.13 Failure Modes for Triaxial Samples of Winnipeg Blue Clay from 11.5 m Depth (Series B)

*From BH4, rest from BH5

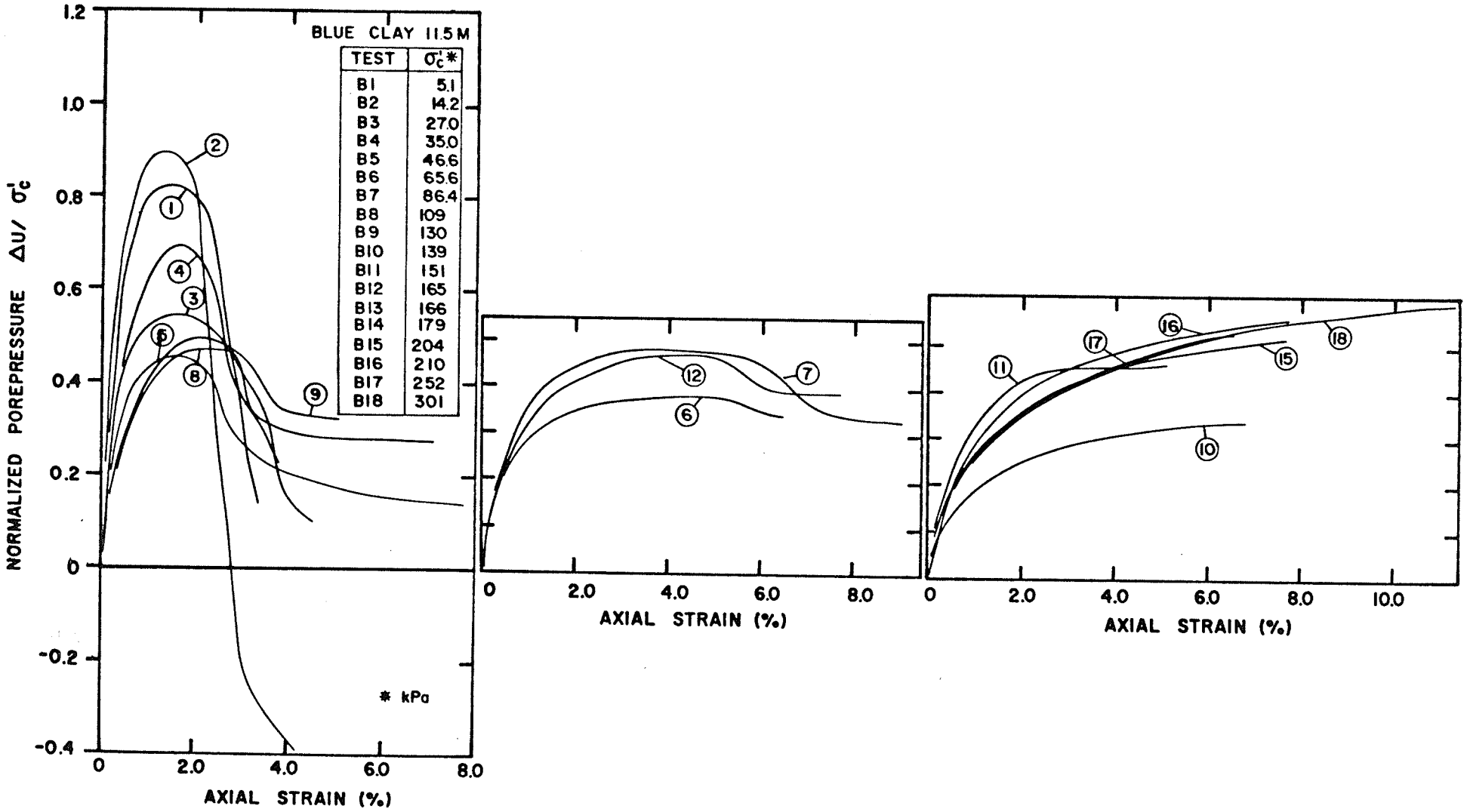

Figure 5.14 Porepressure Response $\Delta U/\sigma'_c$ versus Axial Strain at 11.5 m Depth (Series B)

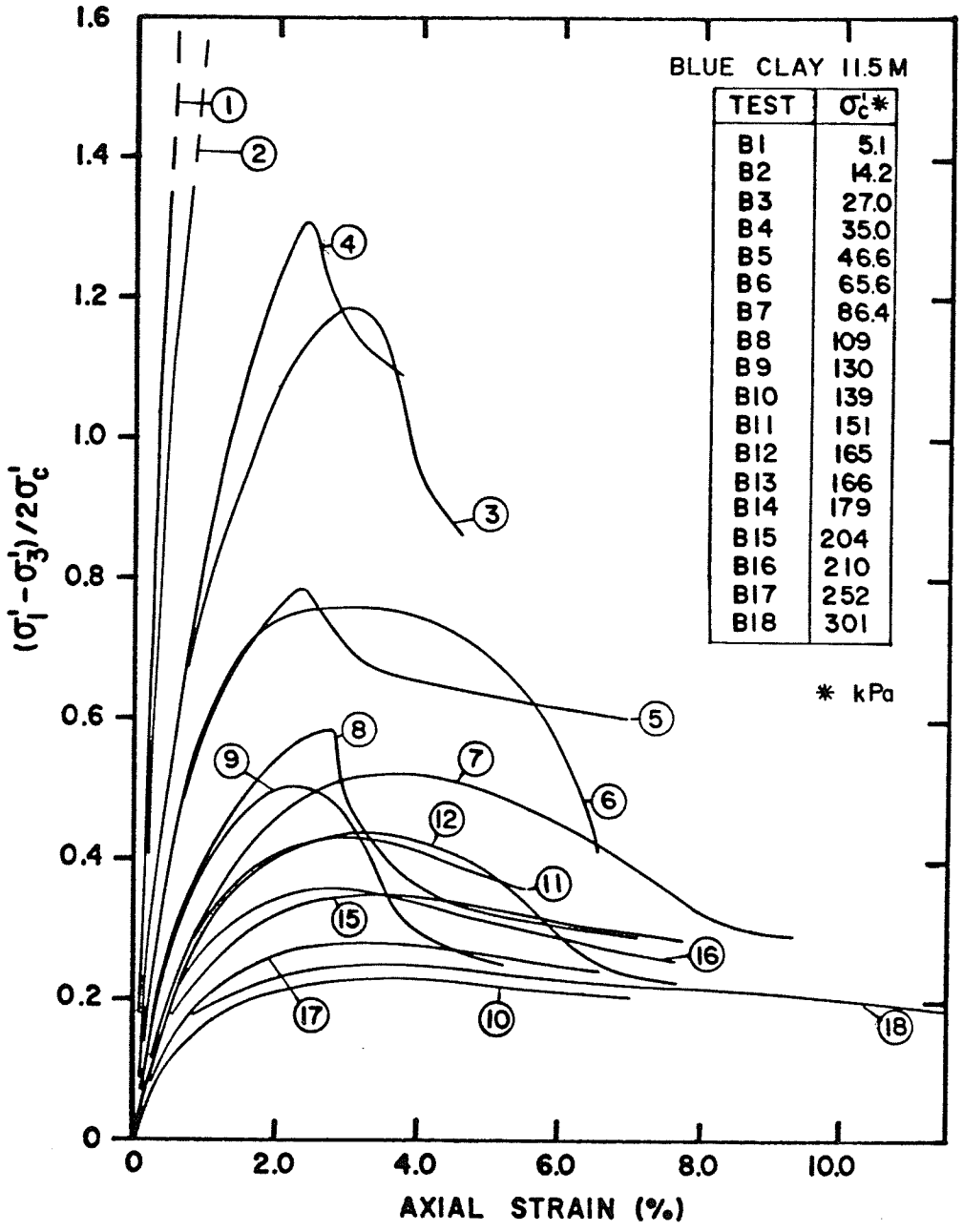

Figure 5.15 Normalized Deviator Stress versus Axial Strain at 11.5 m Depth (Series B)

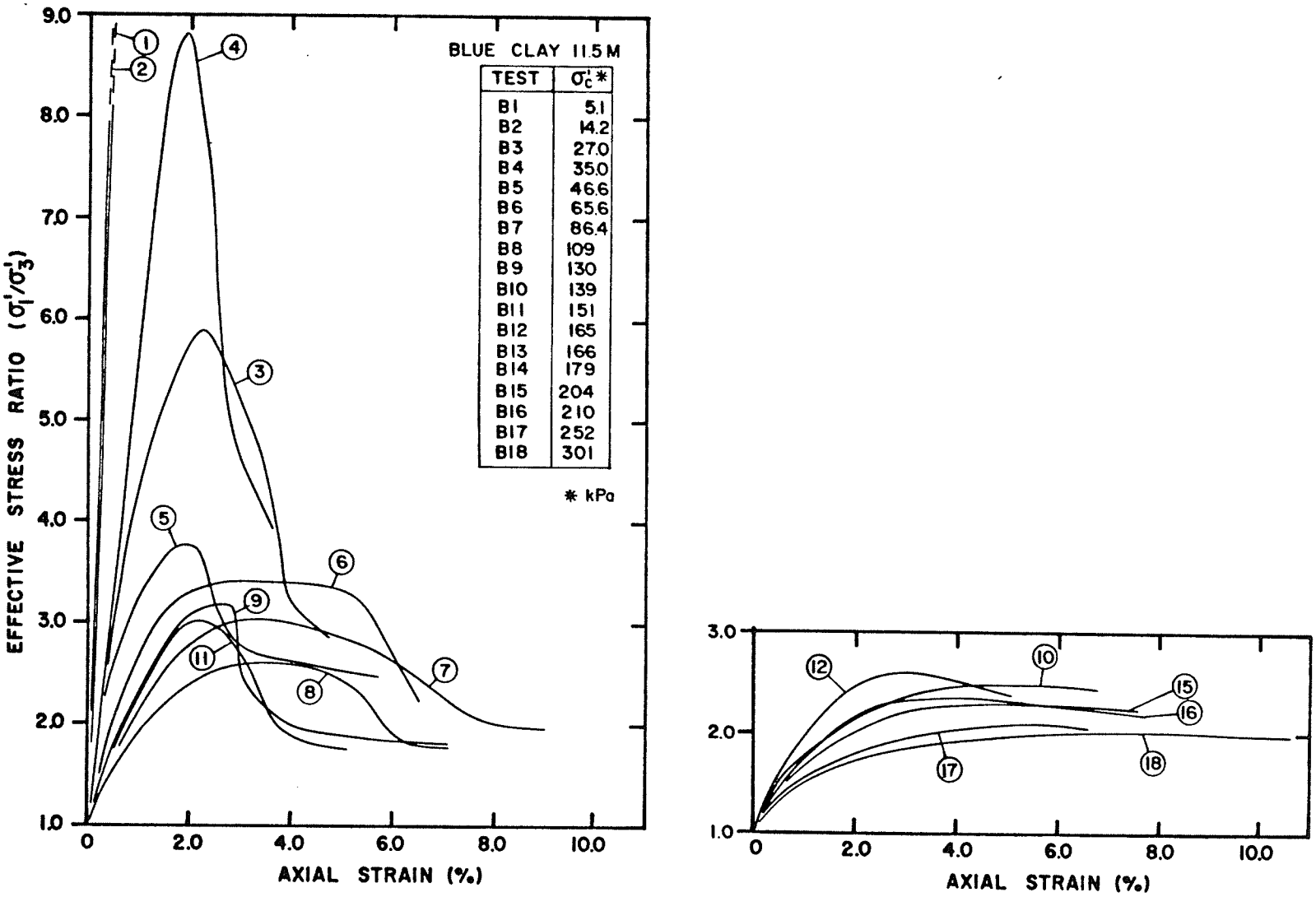

Figure 5.16 Effective Stress Ratio versus Axial Strain at 11.5 m Depth (Series B)

very high stress (666 kPa) showed signs of the buckling failure noted in the blue clay, (Figure 5.19). It is likely that the non-homogeneity mentioned above causes more brittle behaviour as compared to the blue clay, and that failure planes develop much sooner, even in the normally consolidated range. Nevertheless, at higher consolidation stresses the peaks in shearing resistance and generated pore-pressure become less sharp, and the failure planes become less visible internally, (Figures 5.20, 5.21 and 5.22). If a distinction is to be made between normally and overconsolidated behaviour, it appears that the transition occurs at about 200 kPa to 300 kPa, and that samples C16 to C21 were normally consolidated.

In Figure 5.18, an upper bound strength envelope has been fitted to the failure strength data. At high stresses the envelope was constructed using as a model the envelope for the blue clay, which had no discontinuity in slope between overconsolidated and normally consolidated branches. It should be noted, however, that although this envelope fits the data points well, the model $\phi'_{n/c}$ = constant, c' = 0 could also have been used to fit the test results at stresses, p', greater than 300 kPa. Using a bilinear approximation to the envelope of Figure 5.18, the parameters c' = 60 kPa, ϕ' = 11.5^{o} can be used for normal stresses, p', greater than 120 kPa, and the parameters c' = 0, ϕ' = 50^{o} can be used for stresses, p', less than 120 kPa.

In the mid-range of stresses, 80 kPa to 200 kPa, there is a large amount of scatter. Samples C7, C10, C12, C13 and C17 all failed at rather low strengths (Figure 5.17). Whether these low strengths were due to the prescence of pre-existing fissures, or due to fissures which formed during testing as a result of stress concentration, is not

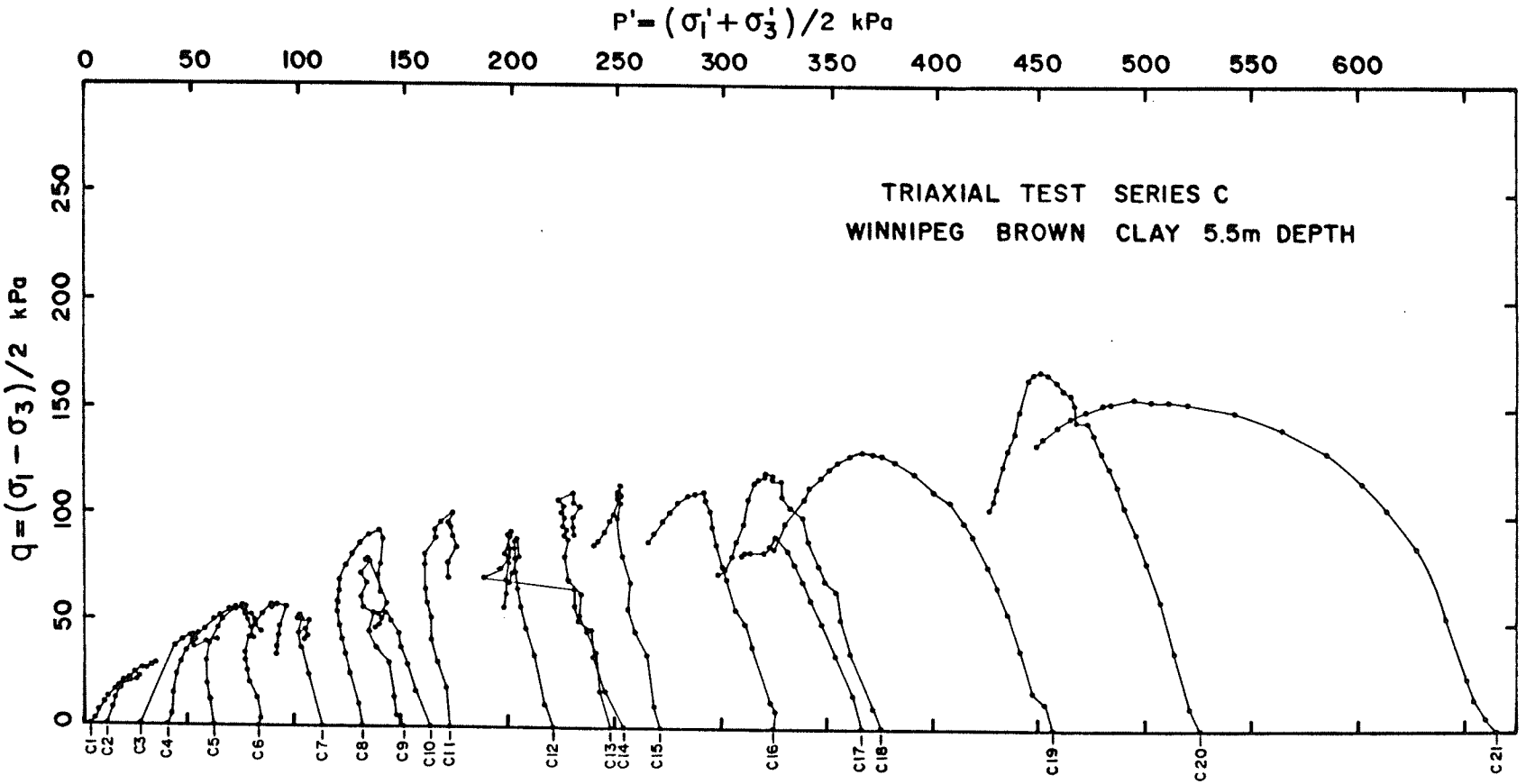

Figure 5.17 Effective Stress Paths, 5.5 m Depth

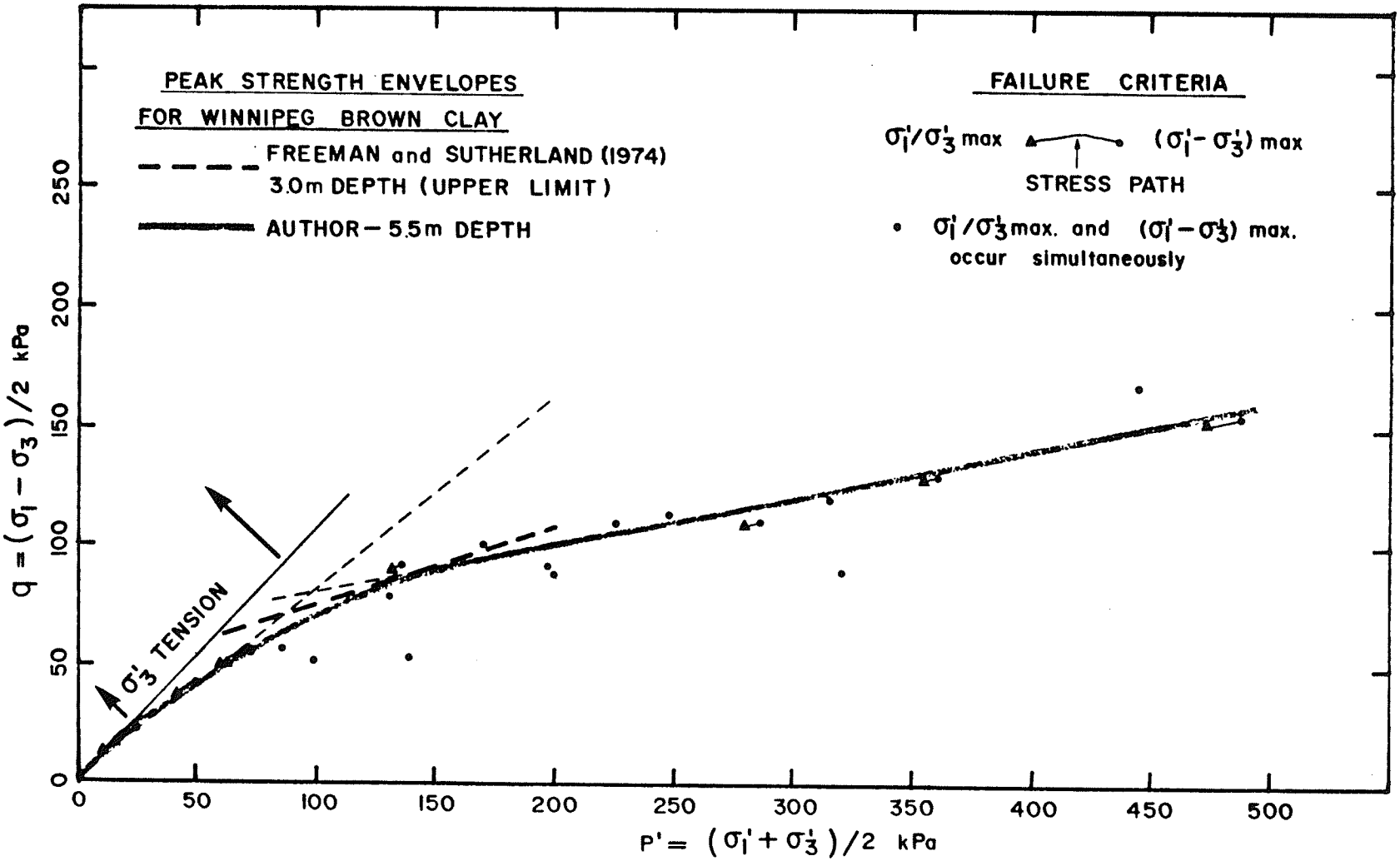

Figure 5.18 Failure Envelope for the Brown Clay from 5.5 m Depth

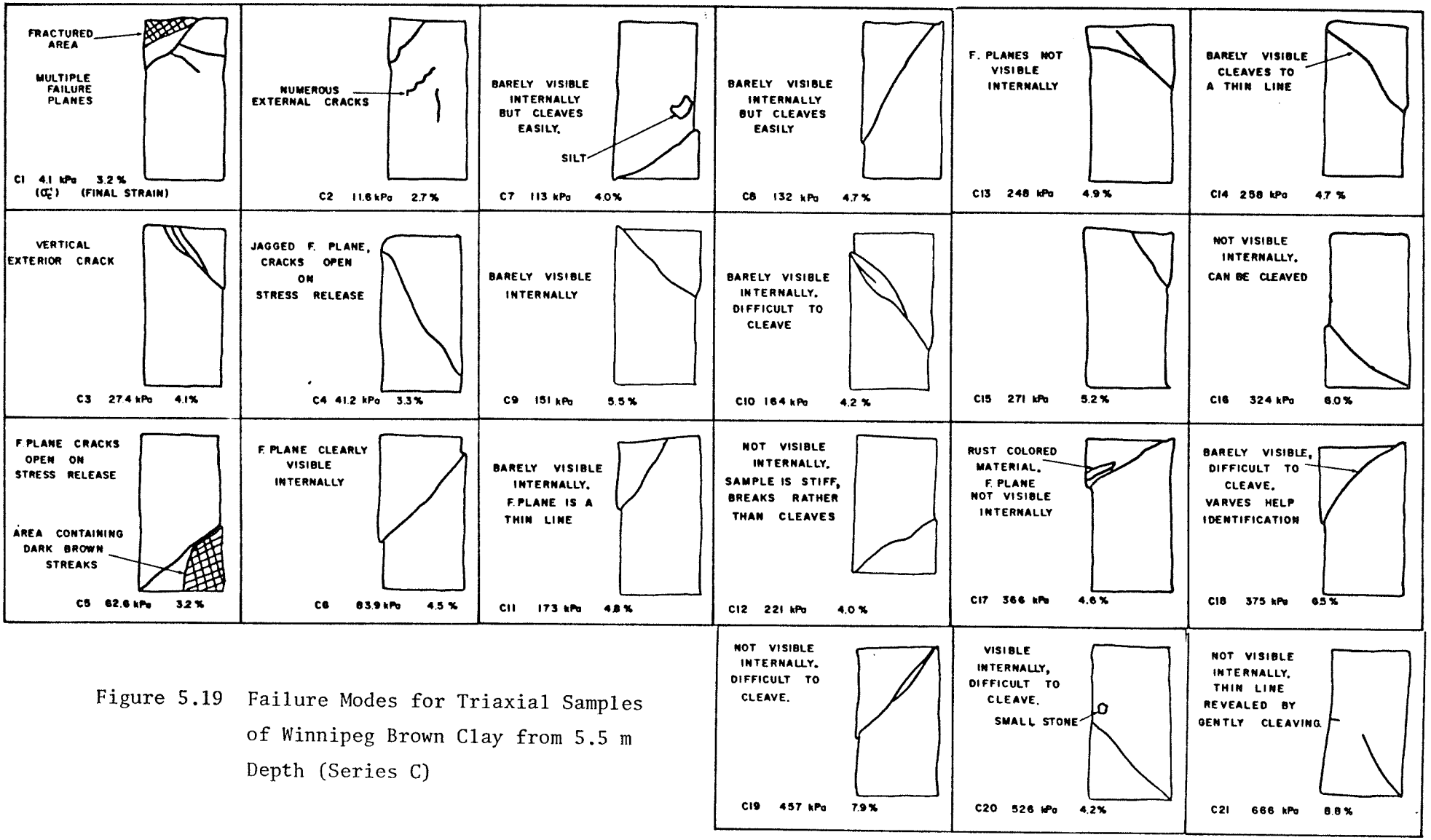

Figure 5.19 Failure Modes for Triaxial Samples of Winnipeg Brown Clay from 5.5 m Depth (Series C)

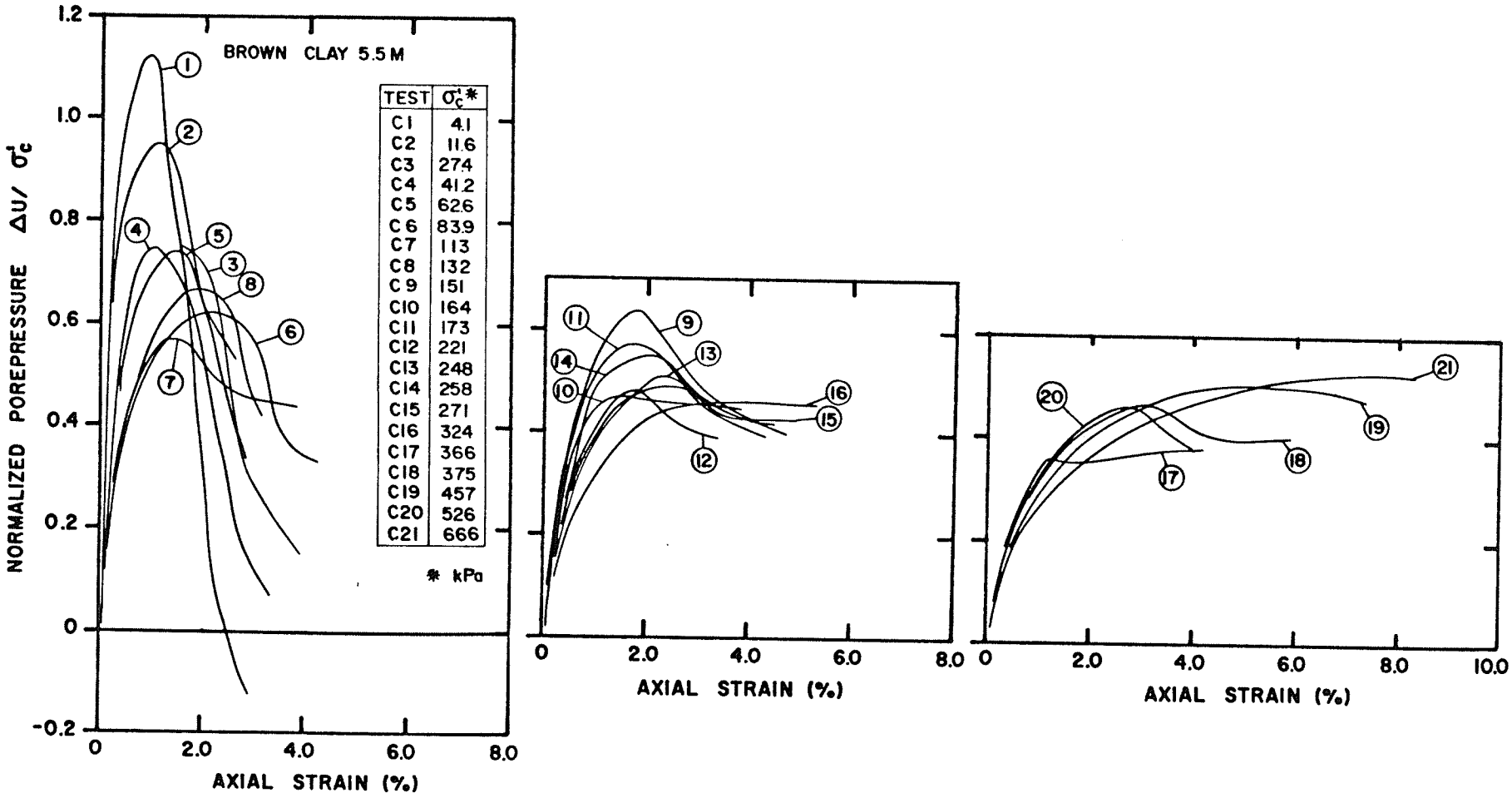

Figure 5.20 Porepressure Response $\Delta U/\sigma'_c$ versus Axial Strain at 5.5 m Depth (Series C)

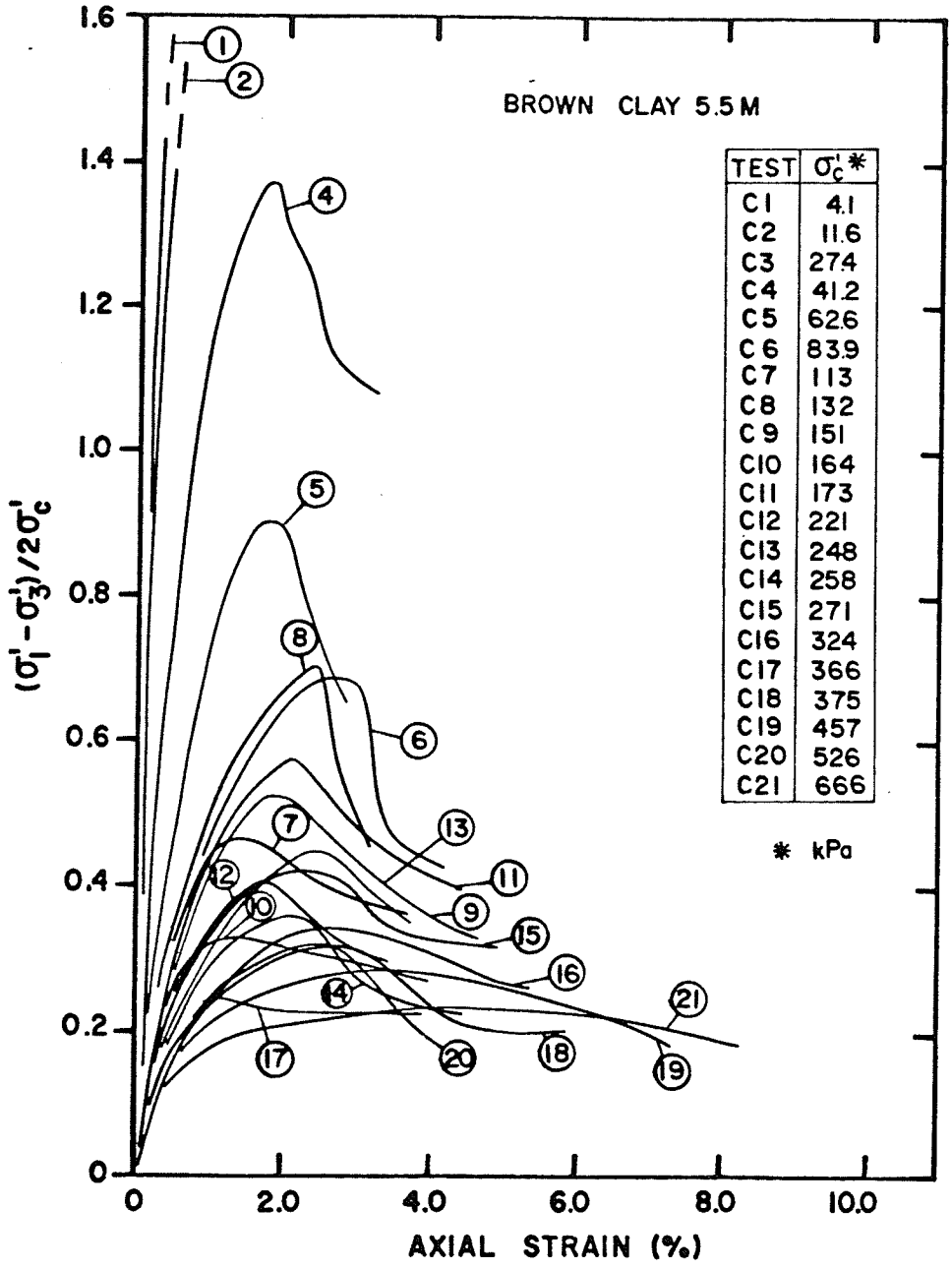

Figure 5.21 Normalized Deviator Stress versus Axial Strain at 5.5 m Depth

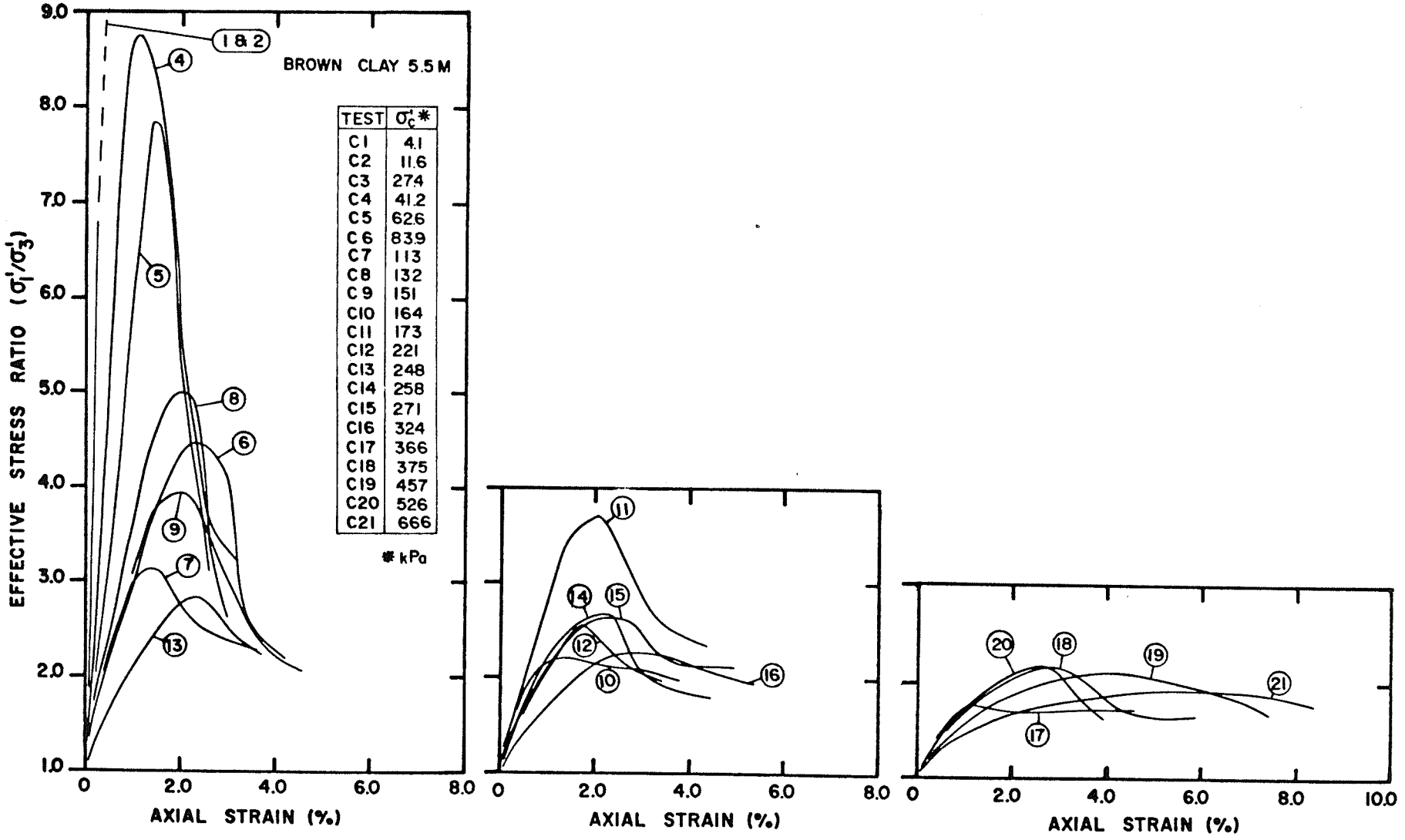

Figure 5.22 Effective Stress Ratio versus Axial Strain at 5.5 m Depth (Series C)

clear. Freeman and Sutherland (1974), using Winnipeg brown clay from a depth of 3.0 m, also reported a large scatter in CIŪ triaxial peak strengths. Their maximum strength envelope, c' = 42 kPa, ϕ ' = 19.1^{o} is also shown in Figure 5.18, and it fits the author's results quite well.

At low stresses the failure envelope is similar to that of the blue clay, and there is little scatter. This is surprising in view of the failure modes shown in Figure 5.19. Failed samples contained numerous external cracks, and formed multiple or jagged failure planes.

An overall comparison between the blue and brown clay failure envelopes, (Figure 5.12), shows that the brown clay has a higher upper bound strength in the range of normal stresses, p', from 50 kPa to 450 kPa. This is not really a surprise, considering that the brown clay has a higher value of p_c' and is thus more overconsolidated.

5.13 VALUES OF THE PORE-PRESSURE PARAMETER A_f

Skempton's pore-pressure parameter, A, describes the pore-pressure changes induced by an increase in deviator stress and is defined by the equation:

$$u = B\{\Delta\sigma_3 + A(\Delta\sigma_1 - \Delta\sigma_3)\} \qquad (5.8)$$

For triaxial compression, $\Delta\sigma_3 = 0$, and under saturated conditions B = 1.0 so that:

$$A = \Delta u/\Delta\sigma_1 \qquad (5.9)$$

The value of A at failure, A_f, is a function of the consolidation stress, or more specifically the overconsolidation ratio. Figure

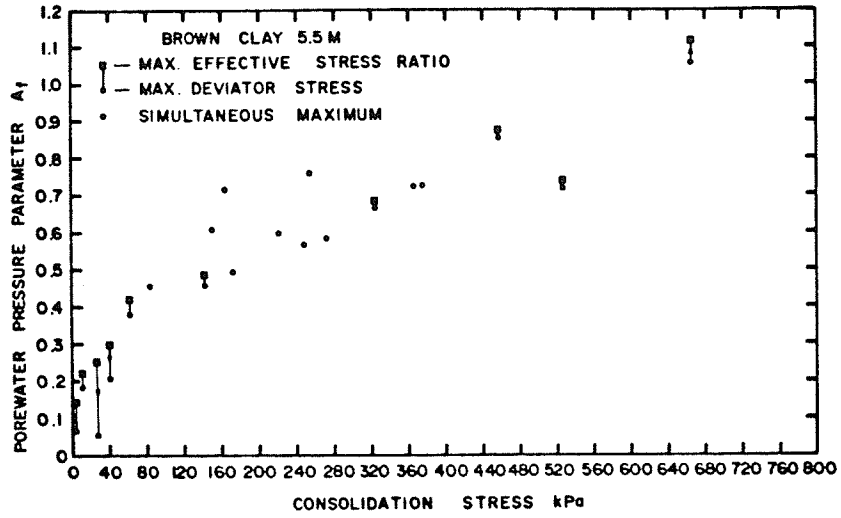

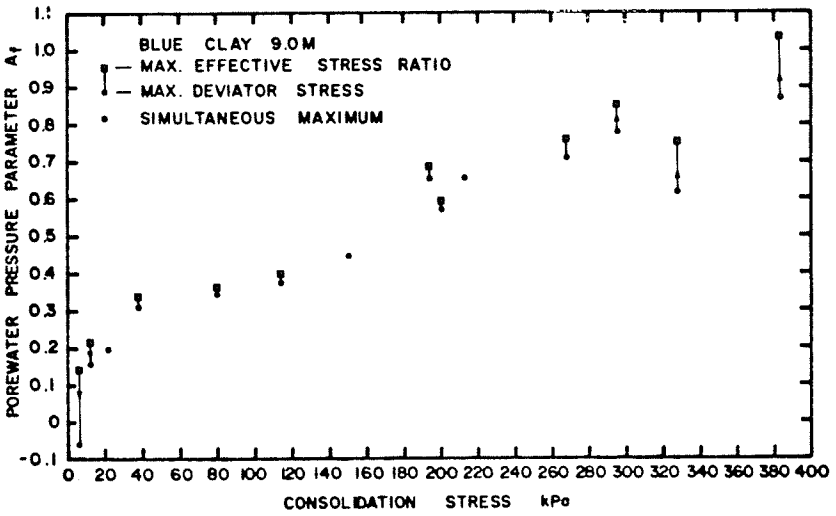

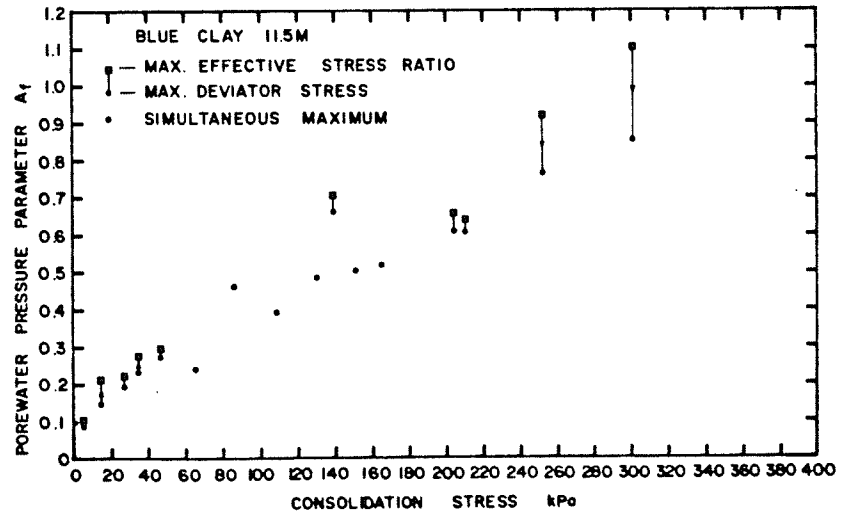

Figure 5.23 A_f versus Consolidation Stress from Triaxial Tests on Winnipeg Clay

5.23 shows that the behaviour is similar at each depth. Values of A_f varied from about 0.0 at very low stresses to above 1.0 at stresses higher than the preconsolidation pressure. This behaviour is typical of a lightly to moderately overconsolidated clay. A heavily overconsolidated deposit would be expected to give negative values of A_f, even at in-situ stresses.

5.14 VALUES OF YOUNG'S MODULUS, E_{50}

E_{50} is a secant value of Young's modulus, calculated from the axial strain at one half of the peak deviator stress.

$$E_{50} = \frac{(\Delta\sigma_1)_{50}}{\varepsilon_{1(50)}} = \frac{(\sigma_1-\sigma_3)_{50}}{\Delta\varepsilon_{1(50)}} \qquad (5.10)$$

where $(\sigma_1-\sigma_3)50$ = half peak deviator stress

and $\varepsilon_{1(50)}$ = axial strain at above stress

Values of E_{50} are shown plotted versus consolidation stress in Figure 5.24. There is a lot of scatter in results, but it is clearly shown that the value of E_{50} increases with consolidation stress, and that the values for the brown clay are generally higher than values for the blue clay. In the effective pressure range 50 to 100 kPa, values of E_{50} vary from about 5 to 15 MPa. This range is identical to the range of values of E computed from in-situ Menard pressuremeter tests at a North Winnipeg site, (Burgess, 1981).

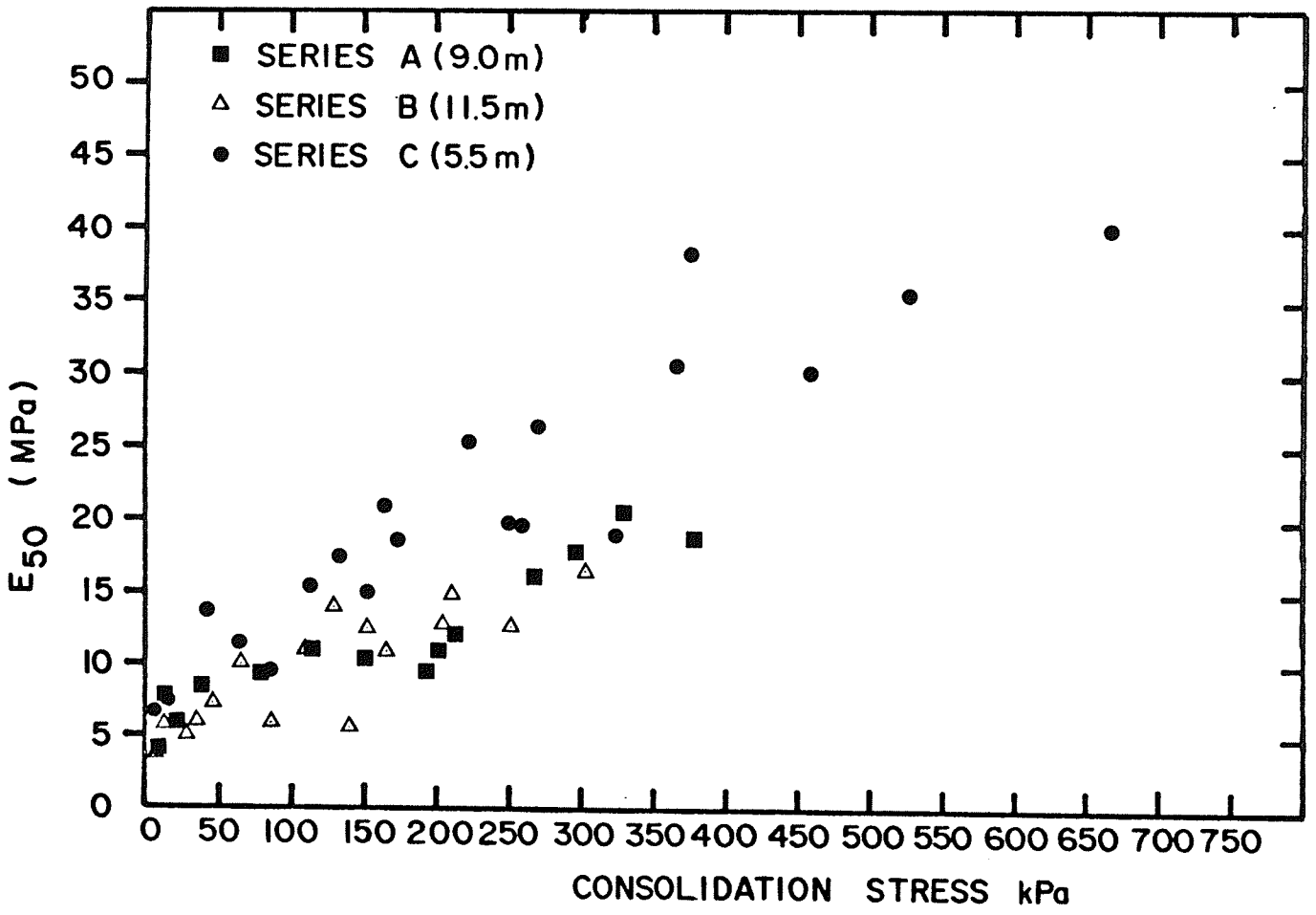

Figure 5.24 E_{50} versus Consolidation Stress from Triaxial Tests on Winnipeg Clay

5.15 GENERAL DISCUSSION AND SUMMARY

The program of triaxial tests on the Winnipeg blue clay at the 9.0 m and 11.5 m depths led to three important findings:

(a) That in the normally consolidated range of stresses, the peak friction angle, $\phi'_{n/c}$ decreases with increasing normal stress.

(b) That the overconsolidated section of the peak strength envelope curves at low normal stresses and appears to pass through the origin.

(c) That the curvature of the envelope at low stresses is due primarily to a softening of the clay microstructure, rather than due to the effects of fissuring. This softening can be correlated to the high swelling strains observed at low normal stresses.

It was also pointed out that the above behaviour is similar to that of the clay mineral calcium montmorillonite which is present in the natural clay. Research on artifically prepared samples of this mineral has shown that both normally and overconsolidated triaxial peak strength envelopes are highly curved, (Mesri, 1970).

These conclusions are of considerable practical importance in the evaluation of slopes and other stability problems in the Winnipeg area. In the design of slopes in an overconsolidated clay it is useful to know the equivalent normally consolidated peak strength at field values of effective normal stress. This can be estimated by testing in a range of high normal stresses, because $\phi_{n/c}$ is usually a constant. The difference between peak overconsolidated strength, and peak normally consolidated strength is an estimate of the reserve capacity due to

overconsolidation.

Softening mechanisms, however, may gradually destroy the reserve capacity. It has been suggested that in many overconsolidated clays the fully softened strength is approximately equal to the strength at large strains, and that the strength at large strains is similar to the normally consolidated strength, (Skempton, 1970). In the case of Winnipeg clays, if the normally consolidated envelope is curved, then the evaluation of long term strength becomes more difficult.

The suggestion of a curved overconsolidated envelope at low normal stresses, (b) above, is entirely compatible with the results obtained by Pietrzak (1979). The significant new finding, however, is that a general softening of the clay microstructure appears to occur, even within the 24 hours consolidation period. Larger consolidation times may lead to even more softening, with the lower limit of peak strength being the normally consolidated strength envelope, (see above).

In comparison with the blue clay, triaxial tests on the brown clay showed generally higher strengths in the intermediate overconsolidated stress range (100 kPa < p' < 250 kPa). However, there was a wide scatter of results, almost certainly due to fissuring, and a better evaluation of the field peak strength in this range could be obtained from large diameter samples. Surprisingly, the scatter in the low stress range was extremely low, even though fissures and cracks were clearly visible upon failure. A possible explanation, is that swelling reduces the strength of the intact material to that of the already softened fissures. As a result the overall strength is not highly dependent upon whether the failure plane forms through preferentially orientated fissures or intact material.

Finally, note should be taken of the high swelling pressures of 35 to 40 kPa recorded in triaxial consolidation. Note should be taken of this phenomenon whenever design prevents lateral movement of the clay, and there is a possibility of the supply of excess water.

CHAPTER 6

CONCLUSIONS AND SUGGESTIONS FOR FURTHER RESEARCH

6.1 CONCLUSIONS FROM OEDOMETER TESTS

(1) Significant insights into the behaviour of Winnipeg clay have been gained by the loading of oedometer samples with small equal increments, and by the use of arithmetic scale plots to interpret the compression versus pressure relationship.

(2) In the recompression range undisturbed Winnipeg clay is highly compressible, but the voids ratio versus pressure relationship is linear and can be defined by the slope a_{vo}. Average values of a_{vo} were:
(a) 3.7×10^{-4} kPa^{-1} at 5.5 m depth (brown clay)
(b) 3.6×10^{-4} kPa^{-1} at 9.0 m depth (blue clay)
(c) 6.7×10^{-4} kPa^{-1} at 11.5 m depth (blue clay)

(3) The linear recompression is followed by a yield, at the preconsolidation pressure, and then strain hardening. If the preconsolidation pressure is high this yield becomes less noticeable because there is less difference between the relative shapes of the recompression branch (linear), and the virgin compression branch (approx. logarithmic).

(4) There is a significant increase in the magnitude of the coefficient of secondary compression, C_α, in the region of the preconsolidation pressure. Peak values of C_α are

quite high even when the degree of yield is insignificant.

(5) Average values of the preconsolidation pressure, p'_c at the three depths were:

(a) 500-800 kPa at the 5.5 m depth

(b) 410 kPa at the 9.0 m depth

(c) 260 kPa at the 11.5 m depth

At the 11.5 m and 9.0 m depths, p'_c was evaluated from the yield. At 5.5 m, however, the yield was barely noticeable and of no practical significance. The estimated range of p'_c was based on both the very slight yields which did occur, and the accompanying peaks in C_α.

(6) The traditional compression versus log. pressure plotting technique is not appropriate for the Winnipeg clay, because:

(a) Even though the oedometer samples were undisturbed, the recompression was not even approximately linear on a semi-logarithmic scale.

(b) It was not possible to tell whether the preconsolidation pressure as defined by the Casagrande construction implied an increase in compressibility.

(7) Allowing the oedometer samples to swell under vertical pressures as low as 18 kPa had no significant effect on the magnitude of p'_c or of a_{vo}.

(8) The compression versus pressure curves for Winnipeg clay did not appear to be particularly strain-rate sensitive.

(9) During the equal load increment tests, the transition between type I and type III consolidation curves appeared

to occur at a load increment ratio of about 1.20-1.25. When a constant load increment ratio of 1.6 was used, only type I curves were produced.

6.2 CONCLUSIONS FROM TRIAXIAL TESTS

(1) The recompression and yield behaviour of the Winnipeg clay in triaxial consolidation was very similar to the behaviour in oedometer consolidation, except that $p'_{c(iso)}$ was lower than p'_c. In addition, swelling strains of up to 4% occurred at low stresses in samples from all three depths; 11.5 m, 9.0 m and 5.5 m.

(2) Effective stress shear strength envelopes were defined for the 5.5 m, 9.0 m and 11.5 m depths. Tests were performed over a wide range of normal stresses, so as to include normally consolidated behaviour, intermediate overconsolidated behaviour, and low stress overconsolidated behaviour, at each depth.

(3) The strength envelopes for the blue clay at 9.0 m and 11.5 m were unusual because:

   (a) In the low stress overconsolidated region the envelopes were highly curved and appeared to pass through the origin.

   (b) The normally consolidated envelopes appeared to have a substantial c' intercept, and there was no distinct discontinuity in slope between the intermediate overconsolidated envelopes and the normally consolidated envelopes.

(4) Failure modes and stress-strain curves for the blue clay samples indicated a distinct contrast between overconsolidated (brittle) failure and normally consolidated (ductile) failure. Also, the reduction in strength (curvature of the envelope) in the low stress overconsolidated range was not caused by fissures, as had previously been suggested (Baracos et. al., 1980). Failure planes formed through the microstructure which appeared to be considerably softened due to swelling.

(5) The intact Winnipeg clay may have a curved normally consolidated envelope as well as a curved overconsolidated envelope. The behaviour of the natural clay would thus be similar to the behaviour of one of its constituent minerals, calcium montmorillonite. The latter is a swelling clay mineral tested by Mesri and Olson, (1970). The existence of a curved normally consolidated envelope would explain the c' intercept (above), and the lack of a transition between overconsolidated and normally consolidated envelopes.

(6) The unusual shape of the strength envelopes for the blue clay is an explanation for the wide variety in c' and ϕ' parameters cited by previous researchers. In the low stress and overconsolidated stress ranges, the author's test results are compatible with those of Pietrzak (1979), Mishtak (1964) and Freeman and Sutherland (1974). In the normally consolidated stress range, the author's results are compatible with those of Mishtak (1964) and

Crawford (1964).

(7) The shape of the strength envelope for the brown clay at 5.5 m depth was similar to the shape of the envelopes for the blue clay at 9.0 m and 11.5 m. However, in the intermediate overconsolidated stress range the upper bound strength was considerably higher than the strength of the blue clay. There was considerable scatter in this stress range, and this was most likely caused by the numerous fissures present in the brown clay. In the field, or in large diameter samples, the higher strength would not be realized. In the low stress overconsolidated range, the envelope for the brown clay merged with that for the blue clay, and there was very little scatter in test results, even though numerous fissures and cracks were clearly visible upon failure. It is suggested that swelling softens the clay, so that there is very little difference between the microstructure strength, and the strength along fissures.

6.3 SUGGESTIONS FOR FURTHER RESEARCH

(1) Constant rate of strain oedometer tests with pore-pressure measurement would give a much better evaluation of strain rate effects.

(2) The high C_α values and low sensitivity of the Winnipeg clay make it an excellent material for an experimental study on the direct effect of thickness on consolidation.

(3) It has been suggested that the normally consolidated

envelope for Winnipeg clay is curved, particularly at low stresses. An approximation to normally consolidated strength could be obtained from samples which have been remoulded with the addition of water to increase the void ratio.

(4) Stress-strain curves from triaxial consolidation of individual samples would lead to a better definition of $a_{v(iso)}$ and $p'_{c(iso)}$. Loads could be applied either incrementally as in the oedometer test, or continually at a constant rate of loading. The latter could easily be achieved by motorizing the winch which adjusts the mercury pot pressure supply.

(5) No axial extension tests have yet been performed on the Winnipeg clay. Comparison of the failure envelopes for such tests with the author's envelopes would give an indication of strength anisotropy.

LIST OF REFERENCES

Aboshi, H. 1973. "An Experimental Investigation on the Similitude in the Consolidation of a Soft Clay, Including the Secondary Creep Settlement". Proc., 8th Int. Conf. on Soil Mechanics and Foundation Engineering, Vol. 4.3, pp. 88.

Au, V. 1982. M.Sc. Thesis in Preparation, University of Manitoba, Winnipeg, Manitoba.

Baracos, A. 1977. "Compositional and Structural Anisotropy of Winnipeg Soils - A Study Based on Scanning Electron Microscopy and X-Ray Diffraction Analyses". Canadian Geotechnical Journal, Vol. 14, No. 1, pp. 125-137.

Baracos, A., Graham, J., and Domaschuk, L. 1980. "Yielding and Rupture in a Lacustrine Clay". Canadian Geotechnical Journal, Vol. 17, No. 4, pp. 559-573.

Baracos, A., and Graham, J. 1981. "Landslide Problems in Winnipeg". Canadian Geotechnical Journal, Vol. 18, No. 3, pp. 390-401.

Barden, L. 1965. "Consolidation of Clay with Non-Linear Viscosity". Geotechnique, Vol. 15, No. 4, pp. 345-362.

Berre, T., and Iverson, K. 1972. "Oedometer Tests with Different Specimen Heights on a Clay Exhibiting Large Secondary Compression". Geotechnique Vol. 17, No. 2, pp. 82-118.

Bishop, A.W., and Henkel, D.J. 1962. "The Measurement of Soil Properties in the Triaxial Test". London: Edward Arnold. 2nd Edition.

Bjerrum, L. 1967. "Engineering Geology of Norwegian Normally-Consolidated Marine Clays as Related to Settlements of Buildings". 7th Rankine Lecture, Geotechnique, Vol. 17, No. 2, pp. 81-118.

Burgess, N.C. 1981. "Tunnel Instrumentation Project, Year I Report". City of Winnipeg, Waterworks, Waste, and Disposal Department, Winnipeg, Manitoba.

Burland, J.B., Broms, B.B., and De Mello, V.F.B. 1977. Proc. 9th Int. Conf. on Soil Mechanics and Foundation Eng., Tokyo, Japan, Vol. 2, pp. 495-546.

Crawford, C.B. 1964(a). "Some Characteristics of Winnipeg Clay". Canadian Geotechnical Journal, Vol. 1, pp. 227-235.

Crawford, C.B. 1964(b). "Interpretation of the Consolidation Test". A.S.C.E. Journal of the Soil Mechanics and Foundation Engineering Division, Vol. 90, No. SM5, pp. 87-102.

Crawford, C.B. 1965. "The Resistance of Soil Structure to Consolidation". Canadian Geotechnical Journal, Vol. 2, pp. 90-97.

Day, M.J. 1977. "Analysis of Movement and Hydrochemistry of Groundwater in the Fractured Clay and Till Deposits of the Winnipeg Area, Manitoba". M.Sc. Thesis, University of Waterloo, Ontario.

De Mello, V.F.B. 1977. "Reflections on Design Decisions of Practical Significance to Embankment Dams". 17th Rankine Lecture, Geotechnique, Vol. 27, pp. 281-355.

Domaschuk, L. 1977. "Soil Block Sampler". Canadian Geotechnical Journal, Vol. 14, pp. 262-265.

Elson, J.A. 1961. "Soils of the Lake Agassiz Region". in soils of Canada: Geological, Pedological, and Engineering Studies. Edited by R.F. Legget. R. Soc. Canada Special Publ. No. 3, University of Toronto Press, Toronto, Ontario, pp. 51-79.

Elson, J.A. 1967. "Geology of Glacial Lake Agassiz". in Life, Land and Water, Edited by W.J. Mayer-Oakes, University of Manitoba Press, No. 1, pp. 37-96.

Freeman, W.S., and Sutherland, H.B. 1974. "Slope Stability Analysis in Anisotropic Winnipeg Clays". Canadian Geotechnical Journal, Vol. 11, pp. 59-71.

Garlanger, J.E. 1972. "The Consolidation of Soils Exhibiting Creep under Constant Effective Stress". Geotechnique, Vol. 22, No. 1, pp. 71-78.

Gibson, R.E., and Lo, K.-Y. 1961. "A Theory of Consolidation for Soils Exhibiting Secondary Compression". Publication 41, Norwegian Geotechnical Institute, Oslo, pp. 1-16.

Gibson, R.E. 1974. "The Analytical Method in Soil Mechanics". 14th Rankine Lecture, Geotechnique, Vol. 24, No. 2, pp. 115-140.

Graham, J., Pinkney, R.B., Lew, K.V., and Trainor, P.G.S. 1982. "On Curve Fitting and Laboratory Data". Accepted for Publication in the Canadian Geotechnical Journal.

Hawley, J.G., and Borin,D.L. 1973. "A Unified Theory for the Consolidation of Clays". Proc. 8th Int. Conf. on Soil Mechanics and Foundation Eng., Moscow, Vol. 1, No. 3, Section 2/18, pp. 107-119.

Last, W. 1974. "Clay Mineralogy and Stratigraphy of Offshore Lake Agassiz Sediments in Southern Manitoba". M.Sc. Thesis, University of Manitoba, Winnipeg, Manitoba.

Leonards, G.A., and Girault, P. 1961. "A study of the One-Dimensional Consolidation Test". Proc. 5th Int. Conf. on Soil Mechanics and Foundation Eng., Paris, Vol. 1, pp. 213-218.

Leonards, G.A. 1962. "Engineering Properties of Soils". Chapter 2 in Foundation Engineering, Edited by G.A. Leonards, New York: McGraw Hill Book Company.

Leonards, G.A., and Altschaeffl, A.G. 1964. "Compressibility of Clay". A.S.C.E., Journal of the Soil Mechanics and Foundations Division, Vol. 90, No. SM5, pp. 133-155.

Leonards, G.A. 1967. "Behaviour of Foundations and Structures". Discussion in Session II, Proc. 9th Int. Conf. on Soil Mechanics and Foundation Engineering, Tokyo, Japan, Vol. 3, pp. 384-386.

Lew, K.V. 1981. "Yielding Criteria and Limit-State in a Winnipeg Clay". M.Sc. Thesis, University of Manitoba, Winnipeg, Manitoba.

Martin, R.T. 1961. "Some Aspects of Consolidation for a Varved Lake Agassiz Clay". M.Sc. Thesis, University of Manitoba, Winnipeg, Manitoba.

Mesri, G., and Olson, R.E. 1970. "Shear Strength of Montmorillonite". Geotechnique Vol. 20, No. 3, pp. 261-270.

Mesri, G., and Godlewski, P.M. 1977. "Time-and stress-Compressibility Interrelationship". A.S.C.E., Journal of the Geotechnical Engineering Division, Vol. 103, No. GT5, pp. 417-430.

Mishtak, J. 1964. "Soil Mechanics Aspects of the Red River Floodway". Canadian Geotechnical Journal, Vol. 1, pp. 133-146.

Noonan, M.L. 1980. "Limit-State Studies in Winnipeg Clays". M.Sc. Thesis, University of Manitoba, Winnipeg, Manitoba.

Olson, R.E. 1962. "Shear Strength Properties of Calcium Illite". Geotechnique, Vol. 12, No. 1, pp. 23-43.

Pietrzak, A.P. 1979. "Geotechnical Properties of Winnipeg Clay". M. Eng. Thesis, University of Manitoba, Winnipeg, Manitoba.

Render, F.W. 1970. "Geohydrology of the Metropolitan Winnipeg Area as Related to Groundwater Supply and Construction". Canadian Geotechnical Journal, Vol. 7, pp. 243-274.

Skempton, A.W. 1970. "First-Time Slides in Over-Consolidated Clays". Geotechnique, Vol. 20, pp. 320-324.

Sulkje, L. 1969. "Rheological Aspects of Soil Mechanics". New York: John Wiley and Sons.

Symons, I.F. 1967. "Shear Strength of Stiff Clay". Proc. of the Geotechnical Conference, Olso, Norway, Session 2, pp. 175-177.

Teller, J.T. 1976. "Lake Agassiz Deposits in the Main Offshore Basin of Southern Manitoba". Canadian Journal of Earth Sciences, Vol. 13, No.1, pp. 27-43.

Wahls, H.E. 1962. "Analysis of Primary and Secondary Consolidation". A.S.C.E., Journal of the Soil Mechanics and Foundations Division, Vol. 88, No. SM6, pp. 207-231.

Walker, L.K., and Raymond, G.P. 1968. "The Prediction of Consolidation Rates in a Cemented Clay". Canadian Geotechnical Journal, Vol. 5, No. 4, pp. 192-216.

Wicks, F.J. 1965. "Differential Thermal Analysis of the Sediments of the Lake Agassiz Basin in Metropolitan Winnipeg, Manitoba. M.Sc. Thesis, University of Manitoba, Winnipeg, Manitoba.

APPENDIX A

TECHNICAL NOTE "ON CURVE FITTING AND LABORATORY DATA"

ON CURVE-FITTING, AND LABORATORY DATA

by

J.Graham[1], R.B.Pinkney[1], K.V.Lew[2] and P.G.S.Trainor[2].

SUMMARY

Evaluation of soil properties from laboratory tests requires the use of empirical procedures. It has proved difficult to establish procedures for identifying yield stresses that are independent of stress path and the method of plotting. Mini-computers and automatic curve-fitting techniques have been proposed for rational, repeatable, inexpensive results. However conclusions drawn from the tests still depend strongly on the curve-fitting procedures. Care and judgement are necessary.

[1]Associate Professor, [2]Graduate Student, Civil Engineering Department, University of Manitoba, Winnipeg, Manitoba.

INTRODUCTION

Figures 1a, b, c show results from drained stress-controlled triaxial tests on carefully trimmed samples of three different soils that were consolidated anisotropically to in-situ stresses. Figure 1a shows σ'_{oct} versus $\Delta V/V$ results from a soft marine clay from Northern Ireland that was tested at constant shear stress (Crooks and Graham, 1976). In Figure 1b the results are from a triaxial test at approximately K_o- conditions on plastic lacustrine clay from Manitoba (Lew, 1981). Figure 1c shows the strain energy W absorbed during undrained shearing versus stress vector length LSSV from a sample of highly sensitive marine clay from Norway (Graham, 1969). If results of this general shape are obtained in many branches of materials science, they are interpreted as showing evidence of yielding.

In solid mechanics, yielding is defined as the state when non-reversible plastic straining commences. Initial linearity is not prerequisite. A clay soil is not a continuum, but a particulate material, and the classical definition of yielding is not appropriate. Clays experience some non-recoverable straining, even at low stresses.

However, the concept of yielding in clays is now commonly accepted (Crooks and Graham, 1976; Tavenas et al., 1979) to be the limit-state when soils reach a well-defined boundary in p',q,e-space. At stresses lower than yield, the clay is relatively incompressible, creep rates are slow, porewater pressure generation small, and porewater pressure dissipation rapid. At stresses above yield, the clay is more compressible, creep rates are faster, larger porewater pressures are generated, and their dissipation is slower. Questions then arise regarding the empirical procedures to be

used for determining the stresses at yielding. Bilinear curve-fitting has frequently been used for data similar to those in Figures 1a,c (Crooks and Graham, 1976) but mostly with lean, sensitive, kaolin-illite clays. In contrast, the clay in Figure 1b is plastic, insensitive illite-montmorillonite (Baracos et al., 1980).

The procedures used to define yielding should be rational and repeatable; and should minimise personal influences. Mini-computers and automatic curve-fitting techniques might appear useful for this purpose. This Note suggests that they must be used with discretion.

EXAMPLES

Test data like those in Figure 2a from Lake Agassiz clay (Lew, 1981) can be represented by two reasonably linear sections separated by a curved transitional section. During review of these data, it was suggested that yielding could be associated with the point of minimum radius of curvature, $\frac{\partial R}{\partial s} = 0$. A computer program for fitting stress-strain data from metals was adapted to superimpose a best-fit Ramberg-Osgood function

(1) $$x/x_0 = (y/y_0)(1 + |y/y_0|^{r-1})$$

through the test data using least squares (Popov and Pinkney, 1969). This was differentiated numerically for the point of minimum radius. The process was essentially automatic, once the data had been read to the computer. However on visual examination, the Ramberg-Osgood function was a relatively poor representation for clay, although it had worked well for metals. Attempts were then made to fit the data by simple polynomial functions. Good agreement was obtained using 4th order and higher polynomials. However, there was no obvious agreement between limit-states obtained from

differentiation of the polynomial, and values selected on the basis of judgement.

It then seemed appropriate to return to bilinear fitting of the data, and to interpret yielding as the intersection of initial and final linear sections. This was done using a bilinear function with a slope discontinuity at $x = c$ represented by

(2) $$y = y_o + ax + (b - a)\,[x - c]^1,$$

where $[x - c]^1 \equiv x - c$, when $x \geq c$,

$\equiv 0$, when $x < c$

and a,b are the slopes of the function for $x < c$,

and $x \geq c$ respectively.

If (x_i, y_i) represents the i-th observation of the independent and dependent variables, then the "error" between the observed and predicted values of y is

(3) $$e_i = y_o + ax_i + (b - a)\,[x_i - c]^1 - y_i$$

The method of least squares was used to determine y_o, a, b and c over N observations. The program was applied to a variety of tests like those in Figures 1 and 2, and worked well for most tests. It appeared that a reliable, impersonal procedure had been developed. It was possible (but inadvisable) to proceed from tabulated data to predictions of yield stresses without inspecting the stress-strain curves. We advise against this automatic process. Recent studies have shown that only 6 out of 43 tests could be handled without discretionary judgement.

Two examples will show why this is important. In Figure 2, data points have been shown as open circles in the initial and final linear sections, and as solid circles in the transition section. The computer has not been programmed to identify the transition section, and fits two straight lines

through all data points, as shown by dashed lines in Figure 2a. If judgement is permitted and the solid points ignored, then the bilinear curve-fitting is shown by the solid lines. The differences in yield stresses can be significant. Figure 2b shows an undrained extension test on sensitive clay after anisotropic consolidation to in-situ stresses. It gave out energy in the early stages of the test. As failure approached however, the behavior changed and it began absorbing energy at a high rate. It is unreasonable to interpret the yield stress as the intersection of the two straight lines in Figure 2b.

In contrast with these examples where yielding is self-evident and the difficulty lies in establishing consistent evaluation procedures, Figure 3a shows oedometer results from two samples of brown, fissured, plastic Lake Agassiz clay which have not yielded (Trainor, 1981). However, if the same data are plotted on a traditional e-log p' curve, Figure 3b shows what might be considered acceptable results for many swelling clays. Unthinking application of the Casagrande construction can apparently produce values for p'_c, even though the samples do not yield (Figure 3a) in the sense that the compressibility increases at some identifiable limit stress. Care should be taken that the plotting technique - in this case semi-logarithmic plotting - does not imply behavior which is absent from the original data.

This point is developed further in Figure 4. Figure 4a shows some non-yielding test data, and three straight lines representative of this type of behavior. The same data and lines are plotted in e,log p'-space in Figure 4b. Not only may there be a temptation to infer p'_c values from non-yielding data, but the inferred values depend on the slopes of the lines. They also depend on the relative dimensional scales used for the void ratio and log p' axes.

The semi-logarithmic construction for p_c' requires the identification of the point of maximum curvature. If a straight line

(4) $e = a - bp'$

in e, p'-space is transformed into e, log p'-space, then

(5) $P' = K \log_{10}(p')$, and therefore

(6) $e = a - b \exp(P'/0.434\ K)$, where

(7) (dimension of one log cycle of p') = K x (dimension of $\Delta e = 1.0$)

The curvature of (6) is given by

(8) $C(P') = \{1 + (de/dP')^2\}^{-1.5} \times d^2e/d(P')^2$

This is maximum when

(9) $p' = 0.434\ K/\sqrt{2}\ b$

Thus the points of maximum curvature, and therefore by implication the values of p_c', depend directly on the physical scales which are used for plotting. It should be noted of course that when yielding does occur, the maximum curvature is usually clear on a semi-logarithmic plot, and the virgin consolidation line is fairly straight.

Finally, attention is drawn to the common use of engineering strain in soil mechanics, despite the large strains which are measured. Other branches of engineering commonly limit the use of engineering strain to only a few percent. Oedometer tests often measure vertical compression of 20 percent, and after p_c' is exceeded, the virgin consolidation line may appear concave upwards. In sensitive marine clays, this has been attributed to changes in porewater chemistry since deposition. However, some of the concavity may depend simply on processing and plotting procedures, and may be reduced by calculating "natural" strains as

(10) $\epsilon_v = \Sigma \{(H_i - H_{i-1})/0.5 \times (H_i + H_{i-1})\}$

DISCUSSION AND CONCLUSIONS

Previous paragraphs discuss curve-fitting techniques which have in some cases failed to identify yield points that are clearly present in the data; and in others have implied yields for which there is no justification. Similar problems exist in mechanical and electrical engineering. Little has been written on the influence of empirical data-handling methods on the conclusions drawn from the data. The interaction of measuring systems with observations is well known. Influences at the interpretive stage of reducing laboratory data appear to be less generally appreciated.

Impersonal treatment of data by automatic computation produces consistent and rational results with less effort and cost, but the results may not in fact be more relevant to practical applications. Despite the convenience and efficiency of computers, engineers must still exercise judgement, experience and common sense.

ACKNOWLEDGEMENTS

Funding support was provided by the Natural Sciences and Engineering Research Council of Canada under Grant Number A3712, and a Graduate Fellowship from the University of Manitoba.

REFERENCES

Baracos, A., Graham, J., and Domaschuk, L. 1980. "Yielding and Ruture in a Lacustrine Clay". Canadian Geotechnical Journal, 17, pp. 559-573.

Crooks, J.H.A., and Graham, J. 1976. "Geotechnical properties of the Belfast Estuarine Deposits". Geotechnique 26, pp. 293-315.

Graham, J. 1969. "Laboratory Results from Mastemyr Quick Clay After Reconsolidaion to the In-situ Stresses". Norwegian Geotechnical Institute, Oslo, Norway, Internal Report F372-5.

Lew, K.V. 1981. "Yielding Criteria and Limit-State in a Winnipeg Clay". M.Sc. Thesis, University of Manitoba, Winnipeg, Manitoba, 197p.

Popov, E.P., and Pinkney, R.B. 1969. "Cyclic Yield Reversal in Steel Building Connections". A.S.C.E. Journal of the Structural Division, 95, ST3, pp. 327-353.

Tavenas, P., Des Rosiers, J.P., Leroueil, S., La Rochelle, P. and Roy, M. 1979. "The Use of Strain Energy as a Yield and Creep Criterion for Lightly Overconsolidated Clays". Geotechnique, 29, pp. 285-304.

Trainor, P.G.S. 1981. M.Sc. Thesis, University of Manitoba, Winnipeg, In preparation.

NOTATION

b	= slope of linear data in e, p'-space
e	= void ratio, error
H	= sample height
K	= ratio of scale dimensions in e, log p'-space (Eqn. 6)
K_o	= ratio of horizontal to vertical effective stresses under conditions of zero lateral strain
LSSV	= length of stress vector in p', q-space
q	= deviator stress $(\sigma_1 - \sigma_3)$
p'	= mean principal effective stress $(\sigma_1' + 2\sigma_3')/3$
$\Delta V/V$	= volumetric strain
W	= energy absorbed/unit volume
ε_v	= vertical strain
σ'_{oct}	= effective normal octahedral stress = p'

LIST OF FIGURES

GRAHAM, PINKNEY LEW TRAINOR, FIG1

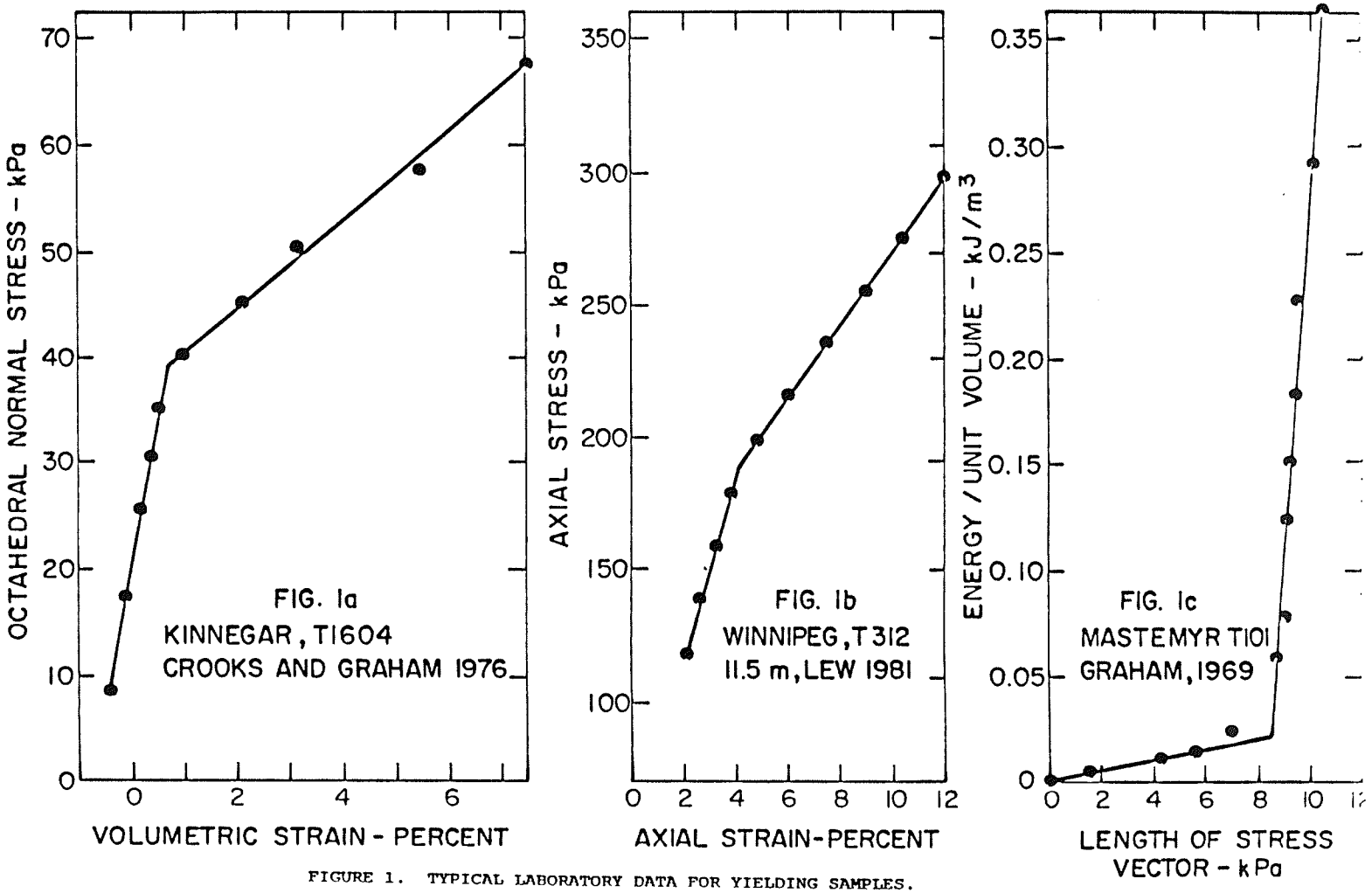

FIGURE 1. TYPICAL LABORATORY DATA FOR YIELDING SAMPLES.

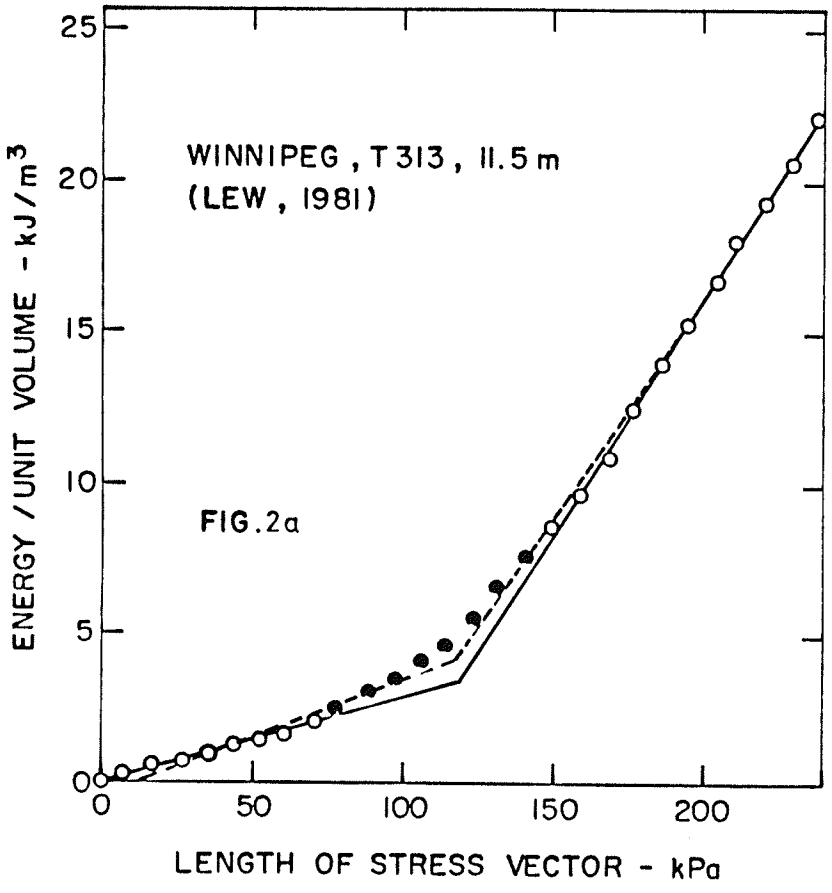

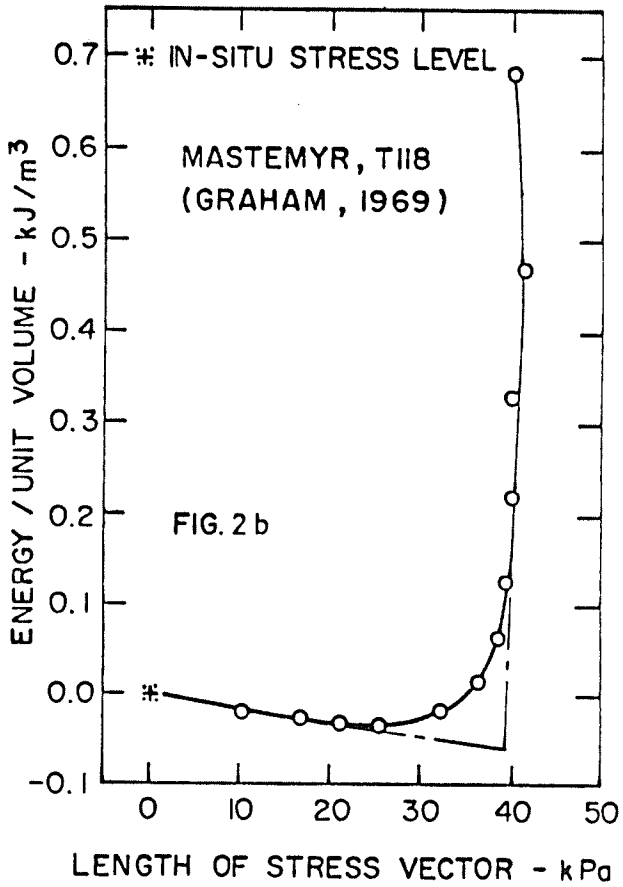

FIGURE 2. AUTOMATIC CURVE-FITTING OF EXPERIMENTAL DATA

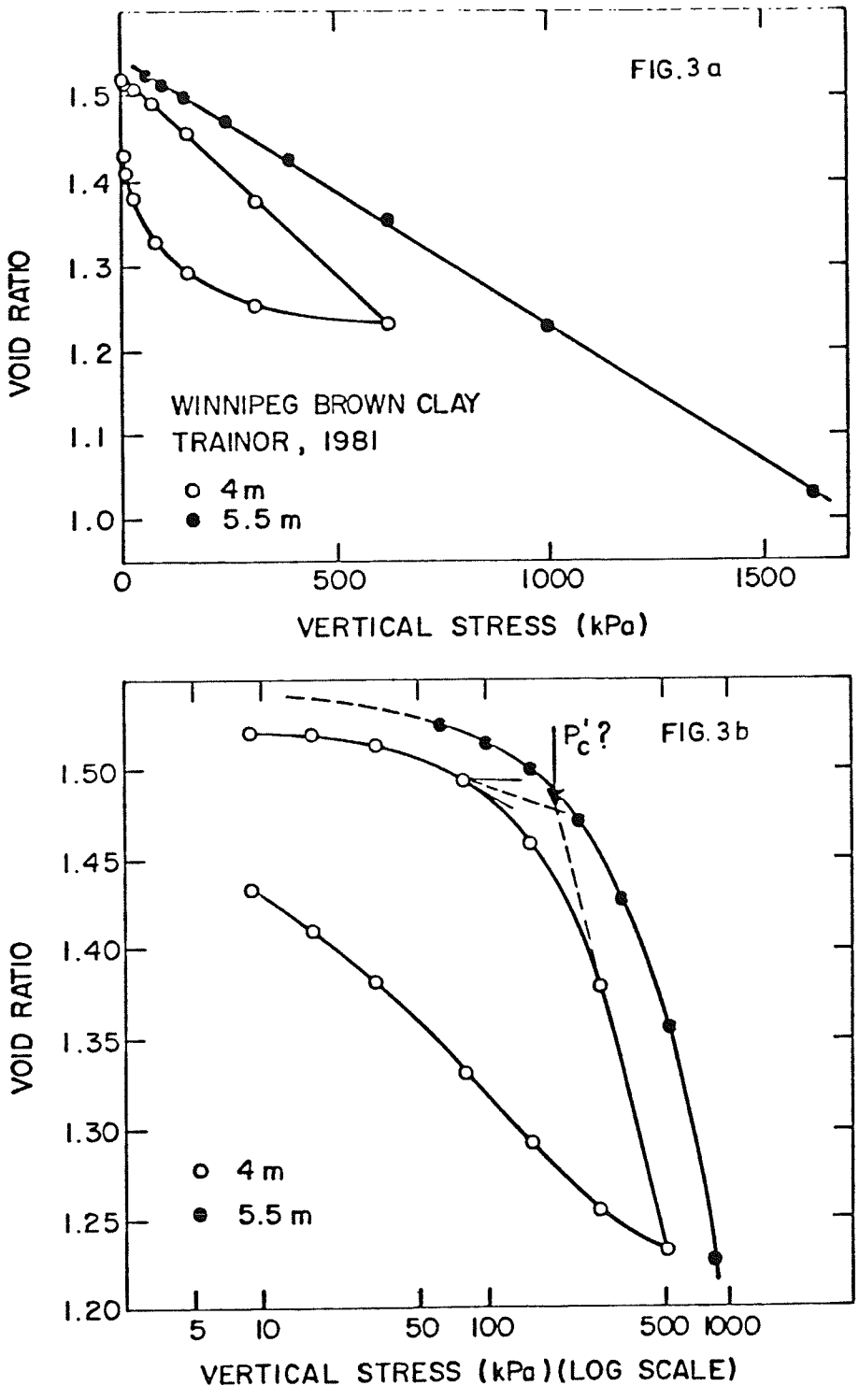

FIGURE 3. OEDOMETER RESULTS IN ARITHMETIC AND SEMI-LOGARITHMIC PLOTS.

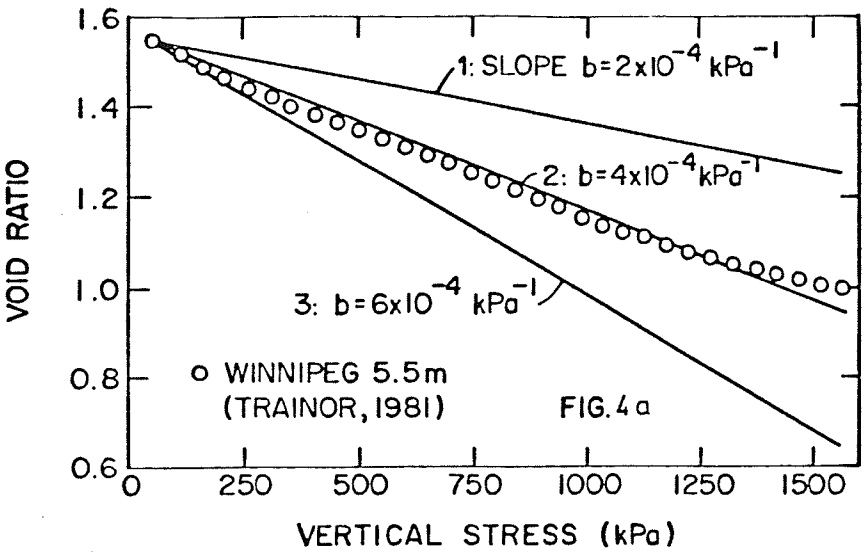

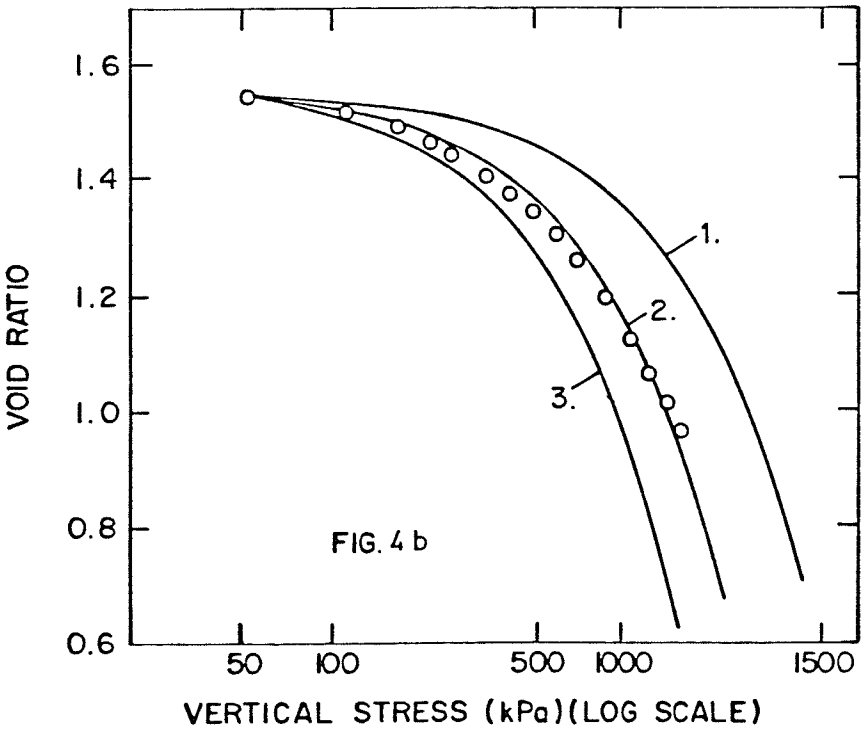

FIGURE 4. IMPLICATIONS OF SEMI-LOGARITHMIC PLOTTING.

APPENDIX B

THE INSTALLATION OF TRIAXIAL SAMPLES:

CHECKLIST AND TIPS

APPENDIX B

THE INSTALLATION OF TRIAXIAL SAMPLES: CHECKLIST AND TIPS

PRELIMINARY EQUIPMENT CHECKS AND OPERATIONS

(1) Check the calibration of the pressure transducers and the L.V.D.T; adjust if necessary.

(2) Restore maximum reserve levels in the self-compensating mercury-pot pressure supply systems.

(3) Adjust the mercury-wheel burette to read zero volume change, and make sure that output valve is closed.

(4) Ensure that drainage lines are clean, and flush them with de-aired distilled water. Remove any air bubbles.

(5) Grease the pedestal with water-repellant silicon grease.

(6) Trim a sample to correct height, weigh it, measure it, and wrap in plastic film to retain moisture.

ASSEMBLE ACCESSORY EQUIPMENT AND MATERIALS

(1) Porous stone and filter paper strips, soaked in de-aired distilled water. Before soaking, the filter strips should be cut to a length equal to the sample height plus the thickness of the porous stone.

(2) Water bottle containing fresh distilled de-aired water.

(3) Silicon oil.

(4) Thick oil to seal loading piston bushing.

(5) Resevoir cylinder full of clean tap water for use in cell.

(6) One greased loading cap.

(7) Two or three small pieces of flexible capillary tube; these are inserted between the membrane and the loading cap to facilitate the de-airing of the sample.

(8) Two membranes, cut to the correct height, one already stretched on a cylindrical former.

(9) At least four rubber O-ring seals, clean and free from oil.

(10) Cleaned triaxial cell casing, with loading piston and two ball bearings.

(11) An appropriate number of weights to counterbalance the piston upthrust.

(12) A hypodermic syringe containing distilled, de-aired water; this is useful for removing small air bubbles trapped in the pedestal grooves.

TIPS ON INSTALLATION

(1) To expell air bubbles from between the two rubber membranes, it may be necessary to introduce excess silicone oil by means of a hypodermic syringe, the tip of which is guarded by means of a piece of capilliary tubing.

(2) Open one drainage line valve (to burette) slightly to create slight upward seepage through the pedestal just before placing the sample, porous stone and inner membrane. This prevents air bubbles from becoming trapped in the pedestal drainage grooves underneath the porous stone.

(3) Introduce the thick oil into the cell by displacement of water not by excessive pressure. Completely fill the cell with water, connect oil hose to top valve, and then open the bottom drainage valve so that as water flows out through the cell base, oil flows in through the top.

(4) Pressurise the water in the cell by use of an air pressure line before connecting the mercury-pot system.

APPENDIX C

CORRECTIONS FOR THE STRENGTH OF MEMBRANES AND FILTER DRAINS

APPENDIX C

CORRECTIONS FOR THE STRENGTH OF MEMBRANES AND FILTER DRAINS

An accurate estimation of the portion of the deviator stress $(\sigma_1-\sigma_3)$ carried by the membranes and filter paper drains is very difficult. Control tests should ideally be run, with and without membranes and drains, using dummy samples of known strength. As a general guide, the results obtained by Bishop and Henkel, (1962), are often used, and their conclusions are summarized below:

(1) An average correction to peak $(\sigma_1-\sigma_3)$ of about 14 kPa was suggested to take account of both the membrane and the drains.

(2) For a sample without drains, the correction can be estimated from the following equation:

$$\sigma_r = \frac{\pi\ D\ M\ \varepsilon_1(1-\varepsilon_1)}{a_o}$$

where M is the extension modulus for the membrane

D = Diameter of sample

a_o = Initial area

ε_1 = Axial strain

(3) For a "standard" membrane of thickness 0.2 mm, the correction is approximately 4 kPa at 15% axial strain.

(4) When the strains are small, the sample, the rubber membranes, and the drains, act as an unit, but buckling occurs in the drains at strains greater than 2-3%.

(5) For cell pressures below about 35 kPa, shippage occurs between the drains and the sample, and the combined correction falls below 14 kPa.

In the present research, very thin membranes were used, with an extension modulus, M, of only 0.08 N/mm. Thus the correction to $(\sigma_1-\sigma_3)$ at typical failure strains of 4% would only be 0.4 kPa, a negligible amount. Also, the filter drains used were individual strips cut from very thin filter paper (Whatman 541), whereas in the tests run by Bishop and Henkel the drains were a single unit cut out of one piece of filter paper. It is thus reasonable to assume that the correction applicable to the author's results should be considerably less than that suggested by Bishop and Henkel; perhaps half, or 7 kPa. Thus the correction to the peak value of $q = (\sigma_1-\sigma_3)/2$ on the q versus p' stress path would be 3.5 kPa, a negligible amount.

It was decided on the basis of the above that for measurement of peak strength, no correction was necessary. It should be noted, however, that to measure post-peak strength after a failure plane has formed, the correction is much larger, (Symons, 1967). It was not a requirement of this research to measure post-peak strength.

APPENDIX D

YIELD ENVELOPES FOR WINNIPEG CLAY

APPENDIX D

YIELD ENVELOPES FOR WINNIPEG CLAY

The yield envelopes shown in Figure D.1 were originally plotted in $(\sigma_1-\sigma_3)$ versus σ'_{oct} stress space, (Baracos et. al., 1980, Noonan, 1980, and Lew, 1981). The author has transferred the envelopes to the q versus p' space used in this thesis. It can be seen that sample A15, a triaxial sample from 9.0 m depth, was consolidated to an anisotropic stress well inside the yield envelopes for this depth. As discussed in Chapter 5, the stress path of A15 in undrained shear followed exactly that of A10 which was consolidated isotropically, and both samples failed as normally consolidated samples.

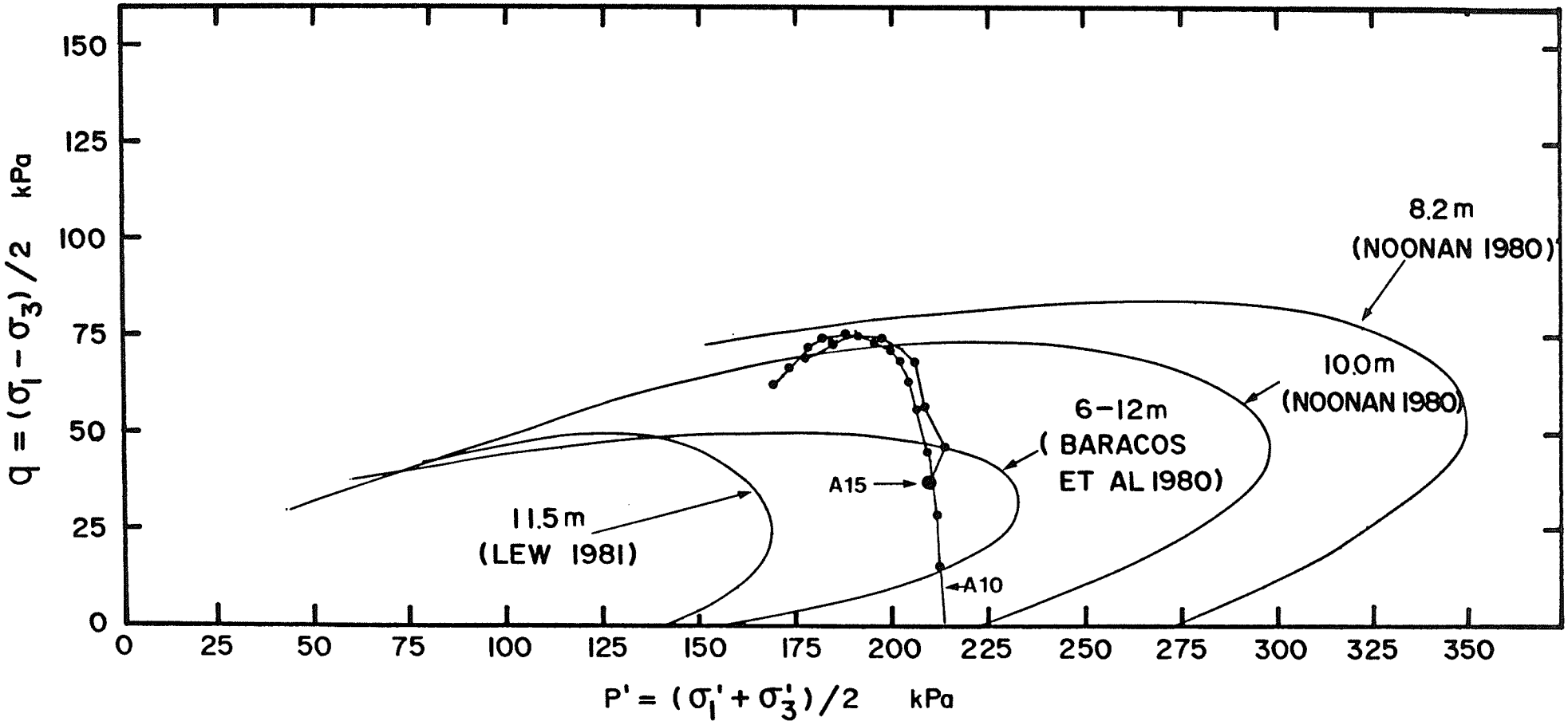

Figure D.1 Yield Envelopes for Winnipeg Clay in q versus p' Stress Space (Transformed from Lew, 1981, Fig. 6.1)